Conditioning fast-twitch skeletal muscles for fatigue resistance: early changes with low frequency stimulation

Thesis submitted in accordance with the requirements of the University of Liverpool for the degree of the Doctor of Philosophy by Joanne Hazel Christina McDonald B.A. (Mod), MSc

June 2001

Abstract

Conditioning fast-twitch skeletal muscles for fatigue resistance: early change with low frequency stimulation

Mc Donald J. H. C.

The stimulation protocols employed to increase the fatigue resistance of fast-twitch skeletal muscle may also damage it. It has been demonstrated, using a two-stage stimulation protocol, that the potential for stimulation-induced damage may be minimised by subjecting the muscle to a progressively increasing amount of stimulation **(Jones *et al.*, 1997)**.

I investigated the effect of low frequency pre-stimulation at 2.5 Hz for 7, 10 or 14 days, either alone or followed by stimulation at 10 Hz (a potentially damaging pattern) for 9 days on stimulation-induced damage, capillarization, fibre type composition, myosin isoform content and contractile characteristics in rabbit *tibialis anterior* (TA) muscle.

Muscles stimulated at 10 Hz for 9 days showed a significantly higher level of damage ($P<0.001$) and significantly reduced maximum tetanic tension ($P<0.001$) and contractile speeds ($P<0.001$) with respect to control fast twitch muscles. The damage resulting from stimulation at 10 Hz was significantly lower in muscles that were first pre-stimulated at 2.5 Hz for 14 days ($P<0.05$). The force deficits incurred after the 10 Hz challenge did not show substantive changes in muscles that were first pre-stimulated at 2.5 Hz for 14 days. Pre-stimulation prior to the 10 Hz stimulation significantly decreased the time to relax ($P<0.01$) but evoked no substantive changes in the time to contract.

Pre-stimulation has a significant protective effect on muscles subjected to a metabolically challenging pattern. Results suggest that this is not attributable to capillary development, fibre type composition and/or myosin isoform expression alone. Pre-stimulation prior to the 10 Hz stimulation did evoke faster trafficking of calcium into the lumen of the SR and this may be a contributory factor in the pre-stimulation-induced protective effect.

There are two distinct modes of force transmission within skeletal muscle namely myotendinous (longitudinal) and myofascial (lateral) force transmission **(Monti *et al.*, 1999; Huijing, 1999)**. It has been demonstrated that there are length dependent disparities between forces exerted at the proximal and distal tendons of the *extensor digitorium longus* (EDL) muscle i.e. intra-muscular myofascial force transmission. Subsequent studies have shown that forces exerted at either end of the EDL muscle and at the distal tendons of TA and *extensor hallicus longus* (EHL) muscles may be effected by the muscle tendon lengths of both muscles **(Huijing, 1999; Huijing & Baan, 2000)**. This lead to the proposal that inter-muscular myofascial force transmission may occur between these muscles in the anterior compartment **(Huijing & Baan, 2000)**.

I investigated the effect of passive proximal EDL tendon lengthening on forces exerted at the proximal and distal tendons of rat EDL muscle and at the distal tendons of TA and EHL muscles before and after a fatiguing isometric stimulation regime (3 hr at 30 Hz) and after a 10 min 'rest' period upon completion of the regime.

Disparities between maximal proximal and distal EDL forces were dependent on proximal EDL tendon length with the magnitude of the disparity dependent on the fatigue status of the muscle.

In non-fatigued TA-EHL muscles the peak forces were recorded at low proximal EDL tendon lengths. In the presence of force fatigue the distal TA-EHL forces increased with increasing proximal EDL tendon length reaching peak forces at the longest length tested. 'Rested' TA-EHL muscles exhibited peak distal TA-EHL forces, above those recorded before commencement of the regime, over the entire proximal EDL tendon length range tested (i.e. low and high lengths).

It is conceivable that there is myofascial force transmission from the EDL muscle to the TA-EHL muscle complex however the complexity of the length-force relationship between these neighbouring muscles warrants further investigation.

Acknowledgements

I would like to acknowledge the funding body, TMR Neuros, for their financial support during this project.

I would like to thank all the staff in the department of Human Anatomy and Cell Biology and in the animal surgery unit in the Duncan building for their help and encouragement over the last four years.

More specifically I wish to thank all the members of the Muscle Research Group. In particular I am indebted to Dr Jonathan Jarvis and Professor Stanley Salmons for the opportunity to undertake this piece of work.

I also want to extend my thanks to Professor Peter Veltink, at the University of Twente, and Professor Peter Huijing, at the Vrije University of Amsterdam, and the staff at both Universities, particularly Guus Baan, whose combined knowledge, patience and humour made my time in Holland a thoroughly rewarding experience.

I want to wish all the best to the great friends I made in both Liverpool and Enschede who are great craic and brillant people, thanks a million.

Finally and most importantly I want to express my gratitude to my family, especially my mum, for their support and love.

Abbreviation	Non Abbreviation
ATP	adenosine triphosphate
ADP	adenosine diphosphate
AMPS	ammonium persulphate
BIS	N-N-methylene bis-acrylamide
CAT	catalase
Ca^{2+}	calcium
Ca^{2+} ATPase	calcium adenosine triphosphatase
$CaCl_2$	calcium chloride
Cl^-	chloride
CPK	creatine phosphokinase
Cr	creatine
CS	citrate synthase
CSA	cross sectional area
C_t	contraction time
DOMS	delayed onset muscle soreness
DHPR	dihydropyridine receptor
DNA	deoxyribonucleic acid
E-C	excitation contraction coupling
EDL	*extensor digitorium longus*
EDTA	ethylene diamine tetra acetic acid
EMG	electromyography

EHL	*extensor hallicus longus*
F-actin	filament of actin
FES	functional electrical stimulation
GADPH	glyceraldehydephosphate dehydrogenase
GP	glycogen phosphate
GSH	reduced glutathione
GPX	glutathione peroxidase
HAD	β-hydroxyacyl-CoA dehydrogenase
H&E	haematoxylin and eosin
H_2O_2	hydrogen peroxide
HK	hexokinase
HSP	heat shock proteins
HOCl	hypochlorous acid
Hz	hertz
IMP	inosine monophosphate
JSR	junctional sarcoplasmic reticulum
K^+	potassium
KCl	potassium chloride
KACAT	3-keto-acyl CoA transferase
LDH	lactate dehydrogenase
L_o	optimum length

$MgCl_2$	magnesium chloride
MHC	myosin heavy chains
MLC	myosin light chains
MPO	myeloperoxidase
MTJ	myotendinous junction
M-wave	compound muscle action potential amplitude
mRNA	messenger ribonucleic acid
Na^+	sodium
NaCl	sodium chloride
NO	nitric oxide
e-NOS	endothelial nitric oxide synthase
n-NOS	neuronal nitric oxide synthase
PAGE	polyacrylamide gel electrphoresis
PCr	phosphocreatine
P_o	maximum tetanic tension
P_t	twitch force
rpm	rotations per minute
R_t	relaxation time
RyR	ryanodine receptor
SDH	succinate dehydrogenase
SDS	sodium dodecyl sulphate

SEM	standard error mean
SERCA	SR Ca^{2+}-ATPase
SMV	skeletal muscle ventricles
SOD	superoxide dismutase
SR	sarcoplasmic reticulum
TA	*tibialis anterior*
TCA cycle	tricarboxylic acid cycle
TEMED	tetramethylethylene diamine
Tn	troponin
T-tubule	transverse tubule
V_{max}	maximum velocity of shortening

List of Appendices

List of Figures

Chapter 5

Chapter 1

Introduction

By way of introduction to my research I will briefly explain how skeletal muscles are classified and describe the mechanical and metabolic characteristics of the different fibre types, which comprise skeletal muscle. This will be followed by a general overview of the main proteins in the contractile, calcium (Ca^{2+}) trafficking and excitation-contraction (E-C) coupling structures. I will discuss the inherent adaptive capacity of skeletal muscle and the evolution of neuromuscular electrical stimulation and review the many changes incurred by skeletal muscle during stimulation-induced transformation, from a fast to slow muscle phenotype. The stimulation regimes employed to reversibly transform muscle fibre types may cause skeletal muscle damage. However, damage is not an inevitable consequence of stimulation and/or transformation. There are many different schools of thought on the primary factors involved in the damage process and I will discuss and appraise the main ones in this introduction. In addition, there is a growing body of evidence, which show that specific training regimes can induce protective mechanisms' against the potential for stimulation-induced damage. I will review some of the literature pertaining to the induction of cytoprotection in skeletal muscle. In conclusion I will briefly describe the clinical applications for conditioned skeletal muscle and will outline my research objectives, which are primarily concerned with ascertaining the effects of low frequency stimulation on: (a) the induction of cytoprotection against the potential for stimulation-induced damage in rabbit, fast twitch, TA muscle and (b) on the length-force relationships at the distal and proximal tendons of the EDL muscle and at the distal tendons of TA and EHL muscles.

1.1 Classification of skeletal muscle

Skeletal muscle is comprised of muscle fibres (muscle cells), see Figure. 1.1. Fibre types can be classified on the basis of their physiological and biochemical characteristics **(Pette & Staron, 1990)**. The two main fibre types that constitute skeletal muscle are defined as type 1('slow') and type 2 ('fast'): type 2 can be sub-divided into 2A, 2D and 2B **(Brooke & Kaiser 1970, Gorza, 1990; Pette & Staron, 1990)**. The classification of individual skeletal muscles as fast or slow depends on the percentage of each fibre type present.

1.1.1 Type 2 fibres

Type 2, fast-twitch, fibres are involved in phasic movements for example, sprinting, and exhibit a fast phenotype. These fibres display fast twitch contraction times, and are capable of producing high levels of power. These fibre types are innervated by large diameter axons with high thresholds and they receive intermittent bursts of impulses at frequencies typically above 50 Hz from the motorneurones **(Eccles *et al.*, 1958).**

Type 2 fibres have a low capillary density and contain a low number of mitochondria **(Eisenberg & Salmons, 1981)**. Within the sarcomeres of type 2 fibres the Z-disc is a thin structure while the sarcoplasmic reticulum (SR) and transverse tubule (T-tubule) infrastructures are extensive. The Ca^{2+} ATPase enzyme, which functions to pump Ca^{2+} ions from the cytosol into the SR, is present in the fast high activity SERCA 1a isoform. **(Brandl *et al.*, 1986)**. Phospholamban, the regulatory protein of SR ATPase, is not present in type 2 fibres **(Pette & Staron, 1990)**. Troponin (Tn) and tropomyosin

are associated with the actin filament where they regulate the binding of actin to myosin. Tropomyosin is composed of a two chain α-helical coiled molecule and Tn is comprised of three different subunits, namely TnT (tropomyosin binding), TnC (Ca^{2+} binding) and TnI (inhibitory). Tropomyosin and the Tn subunits exist as fast and slow isoforms. Collectively these two protein complexes comprise a Ca^{2+} sensitive switch, which controls muscle contraction. In a relaxed muscle the positioning of the tropomyosin molecule prevents actin from interacting with myosin. Upon contraction there is an increase in free Ca^{2+} in the cytoplasm. TnC binds to these Ca^{2+} ions and induces a conformational change which allows tropomyosin to move further into the two helical rows of actin monomers thus permitting actin and myosin to interact and muscle contraction to take place **(Pette & Vrbová, 1992)**.

In type 2 fibres Tn is present in the high affinity fast form and the α-tropomyosin isoform is more abundant then the β-tropomyosin isoform. Type 2 fibres contain large amounts of calsequestrin, a major SR Ca^{2+} binding protein, and parvalbumin, a cytosolic binding protein. These proteins speed up the relaxation of muscle by assisting in the transport of Ca^{2+} between TnC and the SR **(Pette & Staron, 1990; Moss *et al.*, 1995)**.

Each sub-group, of which there are three (2A, 2D and 2B), within this fibre type confer different physiological and biochemical properties on the muscle.

2D and 2B fibres, fast-glycolytic (FG) fibres, exhibit fast contractile speed, though type 2B fibres contract faster than 2D fibres **(Bottinelli *et al.*, 1991)**. Type 2D fibres contain fast isomyosins and the myosin ATPase has a high activity thus the

crossbridge cycling rate is high. These fibre types utilise an anaerobic metabolism, where glycolytic and glycogenolytic enzyme activity is high. These fibre types are susceptible to fatigue **(Romanul, 1965; Peter *et al.*, 1972)**

2A fibre types, fast-oxidative-glycolytic (FOG) fibres, display a fast contractile speed yet have the capacity to employ both an aerobic and an anaerobic metabolism. Type 2A fibres contain fast isomyosins and the myosin ATPase has an intermediate activity **(Romanul, 1965)**. They contract at a slightly slower speed than type 2D fibres but due to their ability to utilise an aerobic metabolism they are resistant to fatigue **(Burke *et al.*, 1973; Salmons & Sréter, 1976).**

1.1.2 Type 1 fibres

In direct contrast to fast type 2 fibres, type 1 slow-twitch fibres are employed in the maintenance of posture and display a slow phenotype. They exhibit slow contraction times and are capable of producing only low levels of power.

Slow fibres are innervated by small diameter axons with low firing thresholds. They receive impulses from the motoneurones at an average rate of 10 to 20 per second, that is 10 Hz to 20 Hz **(Eccles *et al.*, 1958)**.

Type 1 fibres have a high capillary density and a high number of mitochondria **(Eisenberg & Salmons, 1981a)**. The Z-disc is thicker than that found in type 2 fibres. The SR of these fibre types is not extensive and the T-tubule is poorly developed **(Sréter, 1969)**. The Ca^{2+} ATPase isoenzyme is present in the low activity SERCA 2a form **(Jorgensen *et al.*, 1988)**. In type 1 fibres the SR contains a regulatory protein of

the SR ATPase, phospholamban. Within the sarcomere, the Tn subunits are present in their slow isoforms and there is a reduction in the α to β tropomyosin ratio. Thus slow fibres are both slow to contract and slow to relax.

Type 1 fibres contain slow myosin isoforms and the myosin ATPase enzyme has a low activity thus the crossbridge cycling is low. These fibres employ oxidative pathways; ATP is provided for contraction at a low but constant rate by the tricarboxylic acid (TCA) cycle and oxidative phosphorylation. These processes require substrates, which are provided for by the breakdown of fatty acids and carbohydrates. Type 1 fibres exhibit a resistance to fatigue **(Romanul, 1965)**.

Metabolic studies have demonstrated that there is variation within fibres of the same type **(Reichmann & Pette, 1982)**. Single fibre analysis of myosin heavy chains (MHC) showed that a large number of fibres that stain as a specific fibre type contain more than one MHC isoform **(Staron & Johnson, 1993)**. Histochemical staining and myosin heavy chain probing have identified up to nine sub-divisions of the four main fibre types. These sub-divisions include hybrid fibre types, which contain two types of heavy isomyosins that can be present in differing amounts. **(Aigner *et al.*, 1993)**. A gradient of fibre types has been identified with decreasing rates of contraction and relaxation: 2B 2BD 2DB 2D 2DA 2AD 2A 2C 1C 1.

1.2 Contractile machinery

In skeletal muscle actin and myosin (Figure 1.2), are the two main components of the contractile apparatus. These two molecules form filaments, which are capable of

binding to and sliding past each other converting chemical energy into mechanical energy and producing muscle contraction.

1.2.1 Actin

The actin filaments are composed of a double helical strand of F-actin and two regulatory proteins, tropomyosin and Tn. Tropomyosin serves to block the myosin-binding site; a block that can be removed by Ca^{2+} activated Tn **(Ebashi *et al.*, 1969)**.

1.2.2 Myosin

The myosin molecules comprise two heavy chains and four light chains. The heavy chain forms a two-stranded α-helical rod at the end of which there is a double headed globular region. It is in the globular head region that the ATPase and actin binding sites are found. At each head (S1) of the heavy chain two different light chains are bound **(Rayment *et al.*, 1993)**. There are four main MHC groups namely type 1, type 2A, type 2D and type 2B found in type 1, 2A, 2D and 2B fibres, respectively. Each of these groups may exist as fast, slow, developmental and transitional isoforms **(Pette & Staron, 1990)**. There are two classes of myosin light chain (MLC) which may exist as fast or slow isoforms. The fast MLC isoforms are the phosphorylatable LC2f (regulatory) and, the alkali LC1f and LC3f (essential). The slow MLC isoforms are the phosphorylatable LC2s (regulatory) and, the alkali LC1s and LC1s' (essential) **(Pette & Vrbová, 1992)**. Each heavy chain is associated with two light chains, which always express an equal ratio of alkali to phosphorylatable isoforms.

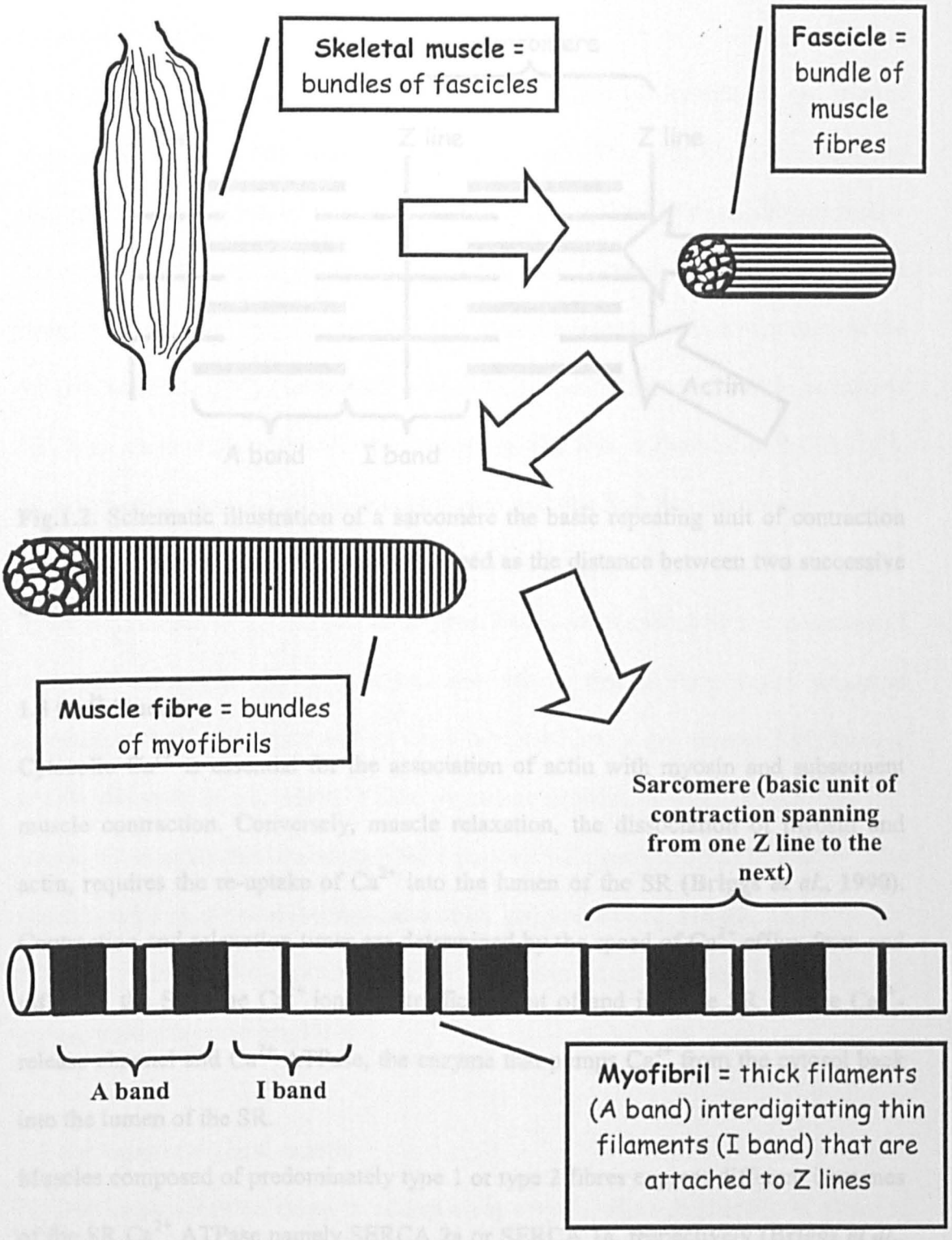

Fig.1.1. Schematic illustration of the structure of a skeletal muscle adapted from Skeletal muscle: Form and Function; A.J. McComas, Figure 1.1.

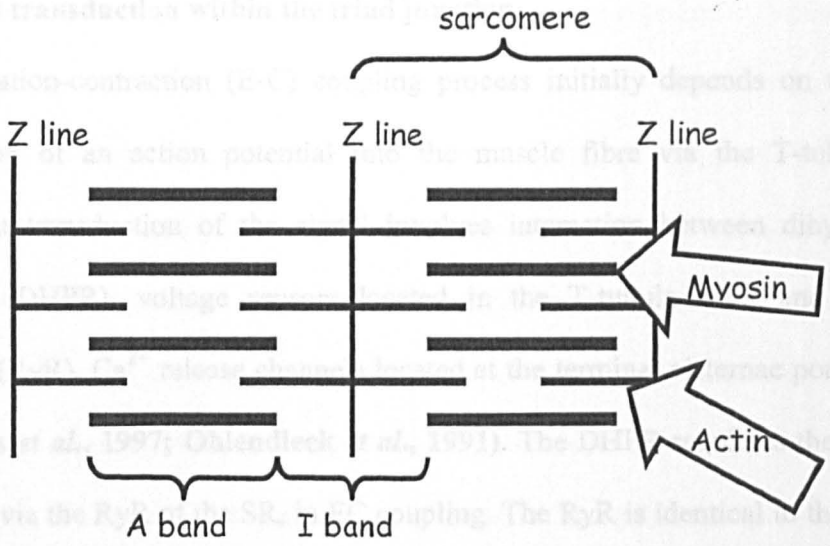

Fig.1.2. Schematic illustration of a sarcomere the basic repeating unit of contraction along the myofibril. One sarcomere is defined as the distance between two successive Z lines.

1.3 Ca^{2+} kinetics

Cytosolic Ca^{2+} is essential for the association of actin with myosin and subsequent muscle contraction. Conversely, muscle relaxation, the dissociation of myosin and actin, requires the re-uptake of Ca^{2+} into the lumen of the SR **(Briggs *et al.*, 1990)**. Contraction and relaxation times are determined by the speed of Ca^{2+} efflux from and influx to the SR. The Ca^{2+} ions are trafficked out of and into the SR via the Ca^{2+}-release channel and Ca^{2+} ATPase, the enzyme that pumps Ca^{2+} from the cytosol back into the lumen of the SR.

Muscles composed of predominately type 1 or type 2 fibres express different isozymes of the SR Ca^{2+} ATPase namely SERCA 2a or SERCA 1a, respectively **(Briggs *et al.*, 1990)**.

1.4 Signal transduction within the triad junction

The excitation-contraction (E-C) coupling process initially depends on the inward propagation of an action potential into the muscle fibre via the T-tubules. The subsequent transduction of the signal involves interaction between dihyropyridine receptors (DHPR), voltage sensors located in the T-tubule wall, and ryanodine receptors (RyR), Ca^{2+} release channels located at the terminal cisternae portion of the SR (**Hicks *et al.*, 1997; Ohlendieck *et al.*, 1991**). The DHPR regulates the release of Ca^{2+} ions via the RyR of the SR, in EC coupling. The RyR is identical to the SR Ca^{2+}-release channel. How the DHPR communicates with the RyR has not been elucidated. A detailed description of the structure of the triad region, where the T-tubules and terminal cisternae of the SR face each other, has been hampered by the closeness of these two structures. However, it has been shown that electron dense structures comprising the RyR project out to the T-tubule where, every second RyR faces a DHPR (**Bruton *et al.*, 1998**). Other important proteins in the T-tubule are the junctional sarcoplasmic reticulum (JSR) proteins of apparent 90 kDa and 94 kDa which may be involved in the regulation of EC coupling or Ca^{2+} release. The RyR, 94-kDa JSR protein and α-subunit of DHPR are present at lower levels in slow twitch muscle (**Ohlendieck *et al.*, 1991**)

1.5 Plasticity of skeletal muscle

Skeletal muscle has an inherent adaptive capacity to adjust to functional changes imposed on it. The plasticity of muscle was first demonstrated by cross re-innervation experiments described by Buller *et al.*, 1960. Fast and slow muscles of the cat hind

limb were cross re-innervated so that the slow muscle was supplied by a fast nerve and vice versa. The fast muscles became slower and the slow muscles became faster (**Buller *et al.*, 1960**). Numerous hypotheses were debated to explain the nature of the stimulus causing the change in muscle phenotype. Initially, the transformation from a fast to slow phenotype was attributed to chemical trophic substances transported by the respective nerves (**Buller *et al.*, 1960**). The development of miniature implantable stimulators (**Salmons, 1967**) enabled *in vivo* indirect electrical stimulation of a muscle via its nerve. Neuromuscular stimulation is based on the principle that a muscle will recognise an action potential received at its neuromuscular junction whether it has been generated by events at its motor neurone or artificially by depolarisation of a segment of the motor nerve (**Salmons, 1994**). Salmons and Vrbova, 1969 demonstrated that transformation from a fast to a stable slow phenotype can be achieved by subjecting the muscle to chronic low frequency activity by indirect stimulation of its motor nerve but with no disturbance of that nerve (**Salmons & Vrbová, 1969**). Salmons and Sréter, 1976 showed that following cross-re-innervation, where a slow nerve supply was imposed on a fast muscle and vice versa, chronic low-frequency stimulation could block the expected changes in muscle phenotypes (**Salmons & Sréter, 1976**). These experiments rendered the chemotrophic theory redundant and illustrated that the primary influence of the motor nerve during transformation is in the pattern of the impulse activity it delivers to the muscle (**Salmons, 1980**).

1.6 Neuromuscular stimulation

Neuromuscular electrical stimulation exploits the plasticity of skeletal muscle by imposing an altered muscle activity and causing a series of physiological, biochemical and morphological changes to meet the altered functional demands.

It has been extensively documented that chronic low frequency neuromuscular stimulation reversibly transforms, in a sequential manner, fast fatigue susceptible type 2 fibres into slow fatigue resistant type 1 muscle fibres **(Salmons & Sréter, 1976; Salmons & Henrikkson, 1981; Jarvis, 1993)**. The stable expression of a slow phenotype by a stimulated muscle (originally fast-twitch) is reversible. Stopping stimulation so that the muscle receives only its normal endogenous pattern of motor activity results in the muscle recovering its fast properties **(Eisenberg *et al.*, 1984; Brownson *et al.* 1992; Brown *et al.*, 1989; Salmons, 1990)**

1.7 Neuromuscular stimulation-induced transformation

Conditioning or increasing the fatigue resistance of fast twitch skeletal muscle involves many changes in the properties of the muscle. These alterations include changes in the ultra-structure, mitochondrial volume, capillary density, Ca^{2+} transport kinetics, metabolism, and myosin isoform content **(Pette & Vrbová, 1992)**.

1.7.1 Ultra-structural changes

After 2 weeks of 10 Hz stimulation the volumes of the terminal cisternae, the T tubules, the SR and the Z disc decrease to levels similar to those observed in control slow muscle **(Salmons *et al.*, 1978; Eisenberg & Salmons, 1981; Sreter *et al*, 1974;**

Heilmann & Pette, 1979). However, the volume of the transforming fibres has been shown to be higher than the volume of the control slow fibres. The mitochondrial volume was reported to increase between days 5 and 12 of stimulation. Upon cessation of stimulation the mitochondrial volume was reported, after 7 weeks, to have decreased but remained elevated above control fast and slow values (**Eisenberg & Salmons, 1981**).

1.7.2 Changes in the contractile apparatus

During the transition from a fast to slow phenotype, and vice versa, the muscle exhibits a heterogeneous isomyosin population owing to the multiple combinations possible within and between the fast and slow myosin heavy and light chain isoforms. (**Pette & Staron, 1990; Staron & Johnson, 1993; Pette & Vrbová, 1992**). Stimulation of fast-twitch muscle induces the sequential replacement of fast MHC and MLC with their slow isoforms. This induction is initiated after 2 weeks and the transition to a slow phenotype is complete after 6 weeks of 10 Hz stimulation. The myosin isoform profile is the last parameter to change in the transformation process (**Brown *et al.*, 1983**). Induction of slow myosin isoforms in rat fast-twitch muscles occurred over a more extended stimulation time period than that recorded for rabbit muscles. This may be due to the fact that the rat is a more active species and the slow motor units in rat muscles fire at higher frequencies (**Mayne *et al.*, 1993**).

Immunoaffinity experiments, using immuno-gold labelled antibodies against fast and slow MHC, demonstrated that during transformation of fibre type individual heavy

chains are replaced within the sarcomere, rather than replacement of the whole fibre or myofibril (**Franchi *et al.*, 1990; Brown *et al.*, 1985; Brown *et al.*, 1983**).

1.7.3 Changes in Ca^{2+} kinetics

The rate of muscle contraction and relaxation is determined by the speed of Ca^{2+} efflux from and influx into the SR. Relaxation and contraction times increased after 4-10 days of stimulation at 10 Hz, although at this early stage of the transformation process no changes in the contractile proteins had occurred (**Pette *et al.*, 1973**). Longer stimulation periods, 20 weeks, demonstrated that the contraction times for fast muscle continued to increase, stabilising after 10 weeks, and exceeded the contractile speed recorded for control soleus muscles (**Salmons & Sréter, 1976**).

Changes in the rate of contraction and relaxation are the result of alterations in the SR. Eisenberg and Salmons, 1981 described the sarcotubular changes as diphasic. Phase one occurs within the first 2 weeks of stimulation where there is a dramatic reduction in the amount of Ca^{2+} transporting membrane. This reduction in the capacity for Ca^{2+} release and re-uptake is reflected physiologically by the slowing of the contraction and relaxation times. The second phase occurs with continued stimulation and includes ultra-structural adaptations, which alter Ca^{2+} transport characteristics incurring further slowing of contractile speed. (**Salmons & Vrbová, 1969; Pette *et al.*, 1976; Heilmann & Pette, 1979; Eisenberg & Salmons, 1981**).

Species; Muscle	Stimulation Times	Results	Authors
Rabbit; EDL	4-10 days at 10 Hz for 12 hr on - 12 hr off/day	Increased R_t and C_t, with no change in contractile proteins	Pette et al., 1973
Rabbit; EDL	20 weeks at 10 Hz for 24 hr/day	Increased R_t and C_t	Salmons & Sréter, 1976
Rabbit; TA	24 weeks at 10 Hz for 24 hr/day		Eisenberg & Salmons, 1981
	Within 1 week	Decreased amount of SR membrane and increased R_t and C_t	
	After 2 week	Further increases in R_t and C_t	
Dog; *Latissimus Dorsi*	6 - 8 weeks at 2 Hz for 24 hr/day	Decreased Ca^{2+} uptake and Ca^{2+} ATPase activity Increased expression of SERCA 2a Ca^{2+} ATPase slow isoform & suppression of SERCA 1a fast Ca^{2+} ATPase isoform	Briggs et al., 1990
Rabbit; TA	1-20 days at 10 Hz for 24hr/day	After 1 day decreased fast type II Ca^{2+} ATPase activity and increased R_t and C_t. No decrease in SERCA 1a fast isoform.	Hicks *et al.*, 1997
Rabbit; EDL	117 days at 10 Hz for 12 hr on - 12 hr off/day	After 35 - 50 days induction, which was complete after 72 days, of fast to slow transcription of SERCA Ca^{2+} ATPase mRNA and phospholamban mRNA	Leberer *et al.*, 1989
Rat; *Gastrocnemius*	1-6 weeks at 10 Hz for 24hr/day	No decrease in SR Ca^{2+} uptake or SR Ca^{2+} ATPase activity	Chin *et al.*, 1995

Table 1.1 Changes in Ca^{2+} kinetics; A list of the investigations into changes in Ca^{2+} kinetics as discussed in section 1.7.3 of Chapter 1.

Briggs *et al.*, 1989 demonstrated, using immunofluorescence and immunoblotting analysis, that chronic stimulation of canine skeletal muscle increased expression of the slow type 1 and decreased the expression of the fast SR Ca^{2+} ATPase isozyme (SERCA 1a). In addition stimulated muscle homogenates and SR fractions showed depressed levels of Ca^{2+} uptake and Ca^{2+} ATPase activities **(Briggs *et al.*, 1990)**.

In a more recent study Hicks *et al.*, 1997 showed that chronic stimulation of rabbit TA caused a rapid decrease in Ca^{2+}ATPase activity (50%). The activity of this enzyme decreased further but at a slower rate with continued stimulation (65% by 20d). After 10d of stimulation the SERCA 1a fast isoform of SR Ca^{2+}ATPase was found to decrease in a time-dependent manner. They also reported that after 1 day of stimulation the contraction and relaxation times had increased by 56 and 158%, respectively, compared to controls. Continued stimulation showed further increases in the relaxation times. Comparison of the time courses suggests that the decrease in SR Ca^{2+}ATPase activity and not a decrease in expression of the SERCA 1a fast isoform may account for the rapid slowing of contraction and relaxation times throughout the stimulation regime **(Hicks *et al.*, 1997)**. Leberer *et al.*, 1989 reported that chronic stimulation induced the fast to slow transcription of Ca^{2+} ATPase mRNA and phospholamban mRNA. The phospholamban protein (regulatory protein of slow Ca^{2+} ATPase) is present in slow but not present in fast muscles. The time course for the induction of these two mRNAs is similar. Slow Ca^{2+} ATPase mRNA showed initial induction after 35 days of stimulation and peak levels of expression were recorded after 50 days. Coincident decreases in total Ca^{2+} ATPase protein and calsequestrin content reflect the transition from a fast to slow SR. The fast to slow transition of the

SR Ca^{2+} ATPase isoforms and the induction of phospholamban appear to be late events in the transformation process. Conversion of these SR proteins is coincident with the fast to slow transition of the myofibrillar Ca^{2+}-binding protein Tn C **(Leberer *et al.*, 1989; Leberer *et al.*, 1987)**.

In contrast, Chin *et al.*, 1995 found that low frequency stimulated rat muscle homogenates showed no decrease in SR Ca^{2+} uptake or in SR Ca^{2+} ATPase activity **(Chin *et al.*, 1995)**. This discrepancy with the aforementioned studies may be due to the different animal models employed in these studies.

1.7.4 Changes in proteins involved in signal transduction

Immunoblot analysis has revealed that chronic stimulation of canine *latissimus dorsi* muscle (fast twitch muscle) reduces expression of the RyR and the α-subunit of the DHPR proteins demonstrating more specific stimulation-induced reductions in the SR volume **(Ohlendieck *et al.*, 1991)**. Hicks *et al.*, 1997 showed that after 10 days of chronic stimulation, rabbit TA exhibited a pronounced decline in the expression of the RyR and the α-subunit of the DHPR. After 20 days of stimulation the decreased expression and apparent levelling off of the time-dependent decline of the E-C coupling proteins suggests that these proteins were in the final stage of the transformation process. This indicates that stimulated-induced changes in proteins involved in E-C coupling precede changes in the myosin isoforms **(Hicks *et al.*, 1997)**.

1.7.5 Changes in capillary density

Capillary density increases early in the transformation process. After 4 days of low frequency stimulation an increase of 20% was found with further increases to 50% and 100% by days 14 and 28 respectively **(Brown *et al*, 1976; Cotter *et al*., 1973)**.

Skorjanc *et al*., 1998 found that capillary density and capillary to fibre ratio increased after 2 days and stabilised after 14 days of stimulation. The increases in capillarization were shown to occur in a fibre specific manner, affecting type 2D before types 2A and 1 fibres. Increases in citrate synthase (CS) and succinate dehydrogenase (SDH), mitochondrial enzymes, were not recorded until after 8 days of stimulation, which suggests that an improved oxygen supply may precede mitochondrial induction. An improvement in the local oxygen supply may be a result of angiogenesis and decreased fibre cross sectional area, both of which were completed after 2-3 weeks of stimulation. It has been suggested that an increase in capillarization, i.e. local oxygen supply, may be a contributory factor in the qualitative switch of energy metabolism **(Skorjanc *et al*., 1998)**. Others have proposed that local increases in blood pressure, endothelial injury and increased expression of an endothelial cell-stimulating angiogenic factor are the primary iniation factors in capillarization **(Brown *et al*., 1995)**.

1.7.6 Metabolic changes

Metabolic changes also occur early in the transformation process. After 4 days of stimulation increased activities for the enzymes involved in glucose phosphorylation (hexokinase [HK]) and fatty acid oxidation (palmitoyl-CoA synthetase) have been

reported. The activity of these enzymes continued to increase up until week 3-5 of stimulation. Concurrent decreases in the activities of enzymes involved in glycogenolysis (glycogen phosphate [GP]) and glycolysis (lactate dehydrogenase [LDH]) up until week 4 of simulation were observed. (**Pette *et al.*, 1973; Heilig & Pette, 1980; Pette & Vrbová, 1992**)

Mitochondrial enzymes involved in the TCA cycle (CS, SDH, fatty acid oxidation (β-hydroxy-acyl-CoA dehydrogenase [HAD]) and ketone body utilisation (3-keto-acyl-CoA transferase [KACAT]) showed increased activities up to 28 days of stimulation **(Pette *et al.*, 1973; Heilig & Pette, 1980; Pette & Vrbová, 1992)**. These increases in mitochondrial enzyme activity are consistent with the early increases seen in mitochondrial volume after 11 days of stimulation **(Salmons & Eisenberg, 1981)**.

Prolonged periods of stimulation (10 weeks) showed that the activity of enzymes involved in the anaerobic metabolism (LDH, GP) were markedly reduced, falling to levels reported for control slow muscles after 8 weeks of stimulation. Coincident decreases in the activities of enzymes employed in high-energy phosphate transfer namely, creatine phosphokinase (CPK), adenylate kinase and adenylate acid deaminase, have been described **(Pette *et al.*, 1973; Heilig & Pette, 1980; Pette & Vrbová, 1992)**. Changes in the enzymatic activity of the aerobic metabolism were found to be diphasic. Phase one occurs within 3-5 weeks of stimulation and involves dramatic increases in the activities of oxidative enzymes. Phase two occurs with continued stimulation, 5 weeks and more, when oxidative enzyme activities were seen to decrease **(Henrikkson *et al.*, 1986)**. The observed decrease in enzyme activity has been shown to coincide with the replacement of fast myosin with slow isoforms

(Brown *et al.*, 1983). Fast myosin isoforms have a higher associated ATPase activity than their slow isoforms. Upon transformation to the slow isoform the requirement for ATP decreases which is consistent with the reduction in the oxidative metabolism **(Henrikkson *et al.*, 1986)**.

1.7.7 Changes in fibre type composition

Histochemical staining has described the fibre type composition of, rabbit TA and EDL muscles, typical fast-twitch muscles as being composed of 60% and 40% type 2D and 2A fibres, respectively, depending on the number of type 1 fibres, which varies from 1 to 5 %. EDL has a higher proportion of type 1 fibres (3%) than TA, which are found mainly towards the distal end of the muscle **(Lexell** et al., **1994a; Mayne *et al.*, 1996)**. Aigner *et al.*, 1993 reported that approximately 1% of the type 2D fibres contain the type 2B myosin heavy chain **(Aigner *et al.*, 1993)**. After 30 days of stimulation 60% of the fibres show transformation to type 2C fibres, an intermediate fibre type between type 2A and type 1 **(Staron *et al.*, 1987a)**. After 60 days of stimulation, complete transformation to type one has been reported **(Pette *et al.*, 1976; Jarvis 1993)**.

1.8 Fibre type specificity of transformation

1.8.1 Specific fibre types may be involved in the rapid force depression recorded with the onset of stimulation

There is a growing body of indirect evidence, which suggests that heterogeneous fast-twitch fibre populations respond or adapt to low frequency stimulation in a non-uniform manner i.e. there is a fibre-type-specific response. With the onset of stimulation rabbit TA, fast-twitch muscle, does not show uniform contractile activity and exhibits a rapid and profound decrease in force output (40-60%) which does not recover until after 6 days of stimulation (**Cadefau *et al.*, 1993**). Rabbit TA is composed of 60% fast fatiguable-glycolytic 2D fibres, 40% fast fatigue resistant oxidative 2A fibres, and 1-5% slow fatigue resistant oxidative fibres (**Lexell *et al.*, 1994a; Mayne *et al.*, 1996**). It has been suggested that the decline in tension with the onset of stimulation may be due to a rapid decline in the number of fibres contributing to the contractile activity. This may imply that only a sub-population of fibres, most likely type 1 and 2A fibres, are able to meet the mechanical and metabolic demand during the initial stimulation period (**Cadefau *et al.*, 1993; Maier & Pette, 1997**).

The time course of changes in the metabolites at the onset of continuous stimulation is consistent with this hypothesis. High-energy phosphates (ATP and phosphocreatine) and glycogen concentrations fall 50-80% within the first 15 min of stimulation. These changes are characteristic of muscle with a high percentage of type 2D fibres and coincide with a rapid fall in force output (**Cadefau *et al.*, 1993**). Levels of ATP, phosphocreatine and glycogen start to recover after 1hr and are nearly completely

restored to control levels after 24hr. This apparent metabolic recovery occurs without any restoration in force output (**Cadefau *et al.*, 1993**). Mayne *et al.*, 1991 showed that after 2 min of stimulation there was a reduction in ATP and PCr and within 5 min there was an increase in Cr, ADP and IMP. After 15 min of stimulation all the metabolites showed signs of recovery which reached control levels after 2h of stimulation. With continued stimulation the metabolites showed no decreases and remained at control values up to 24 hours (length of experiment). The phasic metabolic responses were concurrent with an initial rapid decrease in force production and EMG recordings, which showed more gradual depressions after 4 min finally levelling off at very low levels after 2h of stimulation (**Mayne *et al.*, 1991**). Numerous studies have demonstrated metabolic recovery in the presence of force fatigue which suggests that the persistency of this force deficient may not be attributable to a decrease in high energy metabolites (**Cadefau *et al.*, 1993; Mayne *et al.*, 1991; Green *et al.*, 1992; Green *et al.*, 1997**).

Hicks *et al.*, 1997 showed that continuous low frequency stimulation (10Hz) of rabbit TA for 1 day decreased tetanic tension to 24 % of control, with subsequent slow recovery of tetanic tension to 61% after 20 days of stimulation. The persistency of these low levels may be attributable to decreases in cross sectional fibre area and muscle mass. The M wave, the propagated transient change in electrical potential along the muscle membrane which has an ionic basis (movement of K^+ and Na^+ ions), showed dramatic decreases with a decline of 98% after 1 day and it remained depressed (at 86% of control) after 20 days of stimulation. An increase in connective tissue could exert a dampening effect on the M wave but can not wholly explain the

early and persistent decrease. There was an increase in N^+-K^+-ATPase content in 6 day and 20 day stimulated muscle. A positive correlation was reported between the upregulation of N^+-K^+-ATPase content and the recovery of the M-wave in the stimulated muscles. This suggests that a proportion of the fibres, most likely to be the fast-twitch glycolytic fibre types, had sustained a temporary depolarisation block due to insufficient N^+-K^+-ATPase activity. Accumulation of K^+ in the extracellular space coupled to the de-activation of the Na^+ channels would cause propagation of the action potential to fail and the M wave to decrease. Assuming that the unexcitable fibres are fast glycolytic then the fibres active in force production are the fast-oxidative and slow oxidative fibres. The physiological recordings reported support this hypothesis, after 1 day the stimulated muscles displayed no twitch potentiation, and increased fatigue resistance and prolonged contraction and relaxation times were recorded **(Hicks *et al.*, 1997)**.

1.8.2 HSP expression may identify specific fibre types experiencing stimulation-induced transformation

Heat shock proteins (HSP) aid polypeptide folding, stabilisation and translocation during protein synthesis. It has been documented that the expression of cytosolic HSP70 in skeletal muscle is proportional to the type 1 fibre composition of that muscle. Neufer *et al.*, 1996 demonstrated that within the first day of continuous low frequency stimulation HSP70 was detected in type 1 and 2A rabbit TA fibres. After 1-3d of stimulation they showed that 2D fibres were completely negative with respect to expression of HSP 70. However, after 21 days of stimulation the expression of HSP 70 remained elevated but the highest level of expression was found in type 2 and the

lowest in type 1 fibres, i.e. there was a shift in expression from type 1 to type 2 fibres **(Neufer *et al.*, 1996)**. Ornatsky *et al.*, 1995 reported that continuous stimulation of rat TA for 10 days showed an increase in HSP70 levels while the muscle showed no transformation from a fast to slow fibre type composition **(Ornatsky *et al.*, 1995)**. This data supports the theory that the adaptive response may proceed in a fibre specific manner. The fibre specific response of HSP 70 may mark those fibres that are actively undergoing the adaptive response. It is feasible that the transformation process may not be initiated simultaneously but occurs sequentially within specific fibre-types in the following sequence 1 2A 2D **(Neufer *et al.*, 1996; Ornatsky *et al.*, 1995)**.

With the onset of stimulation the type 1 fibre population of a fast twitch muscle do not have to transform but their activity will have to be maximal to meet the altered functional demands imposed by stimulation. Thus the reported elevation in HSP70 expression in type 1 fibres is not surprising. The delayed increases in expression of HSP70 in type 2 fibres together with the rapid decreases in force with the onset of stimulation is in agreement with the proposal that type 2 fibres, specifically type 2D, may not be contributing to contractile activity. In addition it suggests that these fast twitch fibres may not be transforming during this quiescent period.

1.9 Reversibility of stimulation-induced transformation

Continuous stimulation of rabbit fast-twitch muscle for 6 weeks induces the expression of a predominantly slow phenotype. However, cessation of stimulation after 6 weeks results in the muscle recovering its fast properties over a more prolonged

time course and on a 'first in last out' basis. The fatigue index regains a fast value after 8 weeks. The capillary density returns to control levels after 9 weeks. The expression of predominately fast myosin isoforms returns after 12 weeks. The proportion of type 1 fibres decreases to control fast-twitch values after 4 weeks of recovery while the proportions of type 2B and 2A fibres return to a typical fast-twitch profile after 12 weeks. The mitochondrial enzymes, CS, SDH, and HAD take between 8 and 20 weeks to return to fast-twitch activity levels. GADPH and LDH, glycolytic and glycogenolytic enzymes, respectively, take 9 weeks to recover to fast enzymatic values. The recovery of a predominately anaerobic metabolism does not exhibit the diphasic response observed upon transformation to an aerobic metabolism. This can be attributed to the presence of the low activity myosin ATPase for a substantial portion of the recovery time period **(Eisenberg *et al.*, 1984; Brownson *et al.*, 1992; Brown** et al., **1989; Salmons, 1990)**

1.10 Force transmission

Sarcomere force depends on the amount of filament overlap. The number of sarcomeres in series determines the active length range of a myofibre. The amount of fibres arranged in parallel, the cross sectional area of the fibres, is an estimate for the amount of force that can be exerted maximally **(Brand *et al.*, 1986)**.

The optimum muscle length is defined as the muscle length at which force is maximal. Sarcomeres are arranged in series in the myofibre however, not all the sarcomeres are identical leading to unstable behaviour at lengths over and above optimum lengths **(Sugi & Tsuchiya, 1988)**.

Dynamic force contractions also depend on the velocity of movement. Force length and force velocity characteristics are independent of each other. In addition the force producing capabilities of the muscle depend on properties that change in time during sustained contractions for example, fatigue (**Meijer *et al.*, 1997**). Fatigue is the failure to maintain force output leading to reduced performance and stiffness (**Edman & Lou, 1990**)

1.10.1 Myotendinous force transmission

Fibres are thought to transmit force generated in the sarcomeres to tendon sheets (aponeuroses) and through the tendon onto the bony structures. The myotendinous junction (MTJ) where myofibrils terminate in the cell membrane at the ends of the muscle fibres is the primary site for longitudinal force transmission to the tendinous tissue (**Trotter, 1993, Monti *et al.*, 1999**).

1.10.2 Myofascial force transmission

Myotendinous (longitudinal) force transmission within the myofibre is not the only mode of force transmission. Myofascial (lateral) force transmission where forces are transmitted laterally to the sarcolemma along the length of muscle fibres and onto the intra-muscular connective tissue has been reported (**Monti *et al.*, 1999; Huijing, 1999a & b**). Street and Ramsey 1965 demonstrated that damage to the plasma membrane of a fibre could induce localised supercontraction of the muscle fibre, where a number of myofibrils in the damaged area may retract from the fibres (**Street & Ramsey, 1965**). They showed that when supercontraction occurred force was

transmitted across the part of the fibre with retracted myofibrils. In this state of supercontraction longitudinal force transmission (from sarcomere to sarcomere) cannot occur. This led them to hypothesis that force may be transmitted in a lateral direction via the sarcolemma, basal lamina and endomysium. Subsequent experiments by Street 1983 presented evidence that force could be transmitted laterally within skeletal muscle. The model employed by Street (Figure 1.3) was comprised of a bundle of twitch fibres dissected from the dorsal arm of frog *semitendinous* muscle. At the proximal end of the bundle the fibres were left intact (splint) while at the distal end the outer fibres were removed so that only one inner fibre was left intact. Essentially the splint acted to cover/immobilise over one half of the fibre but the other half of the fibre was dissected clean and free to actively shorten upon stimulation. The splint was pinned at the end nearest the single dissected fibre and attached to a force transducer at its distal end. The single dissected clean fibre was stimulated with and without its free end pinned. Results showed that when the single fibre was not pinned it could still produce 75% of the force generated when pinned. If longitudinal transmission via the MTJ was the primary mode of force transmission then one would expect the single fibre not to be able to transmit force (just shorten) when pinned at only one end **(Street, 1983)**. Street also described a network of protein filaments attaching the Z- and M-lines to the cell membrane which she proposed may be involved in the transmission of force from the myofilaments through the cell membrane to the extracellular matrix **(Street, 1983)**.

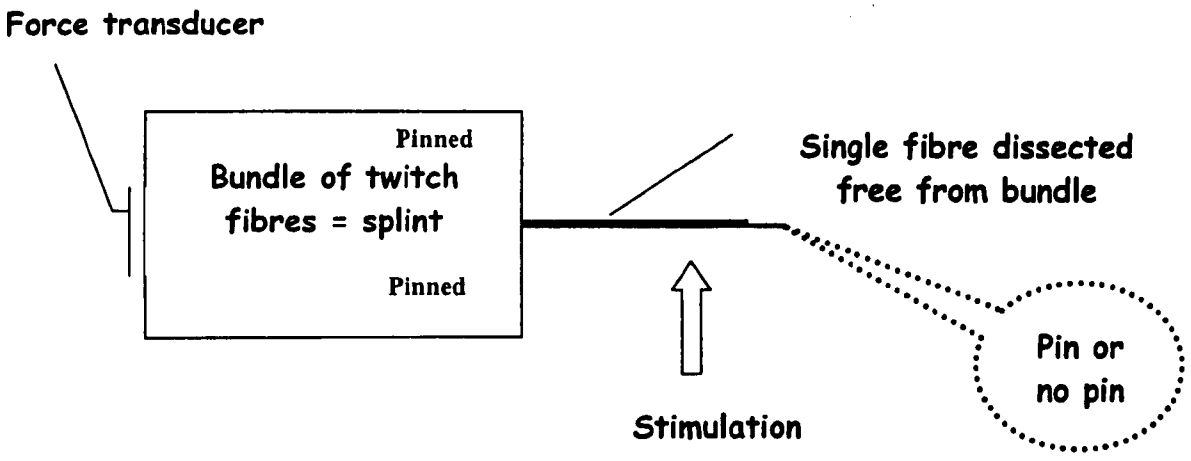

Fig.1.3. Diagrammatic representation of the muscle preparation employed by Street (1983): A bundle of twitch fibres were transected from a frog *semitendinous* muscle. A single fibre was dissected free, for between one-half and one-third of its length, from the bundle of fibres. The bundle (splint) was pinned at the end nearest the isolated fibre and attached to a force transducer at the other end. The isolated fibre was stimulated with and without its free end pinned.

1.10.3 Non-spanning muscle fibres

Myofascial force transmission has also been inferred for non-spanning fibred muscle. Non-spanning fibres do not run or span from one tendon to another tendon or aponeurosis. One end of the fibre is attached to an aponeurosis and the other end terminates intramuscularly. Huijing 1999 described the morphologies of non-spanning fibres, isolated by fixation and treatment with potassium hydroxide, from rat *biceps femoris* muscle. Examination of these isolated fibres under a light microscope identified four non-spanning fibre end morphologies namely tapered ends, myo-myonal, myo-epimysial and myo-endomysial junctions. Tapered ends have no distinguishable specialised microscopic junctional structures and force transmission involves the full periphery of the tapering ends of the muscle fibres. Myo-myonal

junctions are non-tapering ends that exhibit a similarity to the MTJ and may require the full diameter of the muscle fibre. Myo-epimysial junctions also have morphologies typical of MTJ however these junctions are directed at right angles with respect to the direction of the muscle and their invaginations are less deep. Myo-endomysial junctions have the typical invaginated structure of the MTJ but junctional invaginations are filled by endomysial connective tissue **(Huijing, 1999b; Trotter *et al.*, 1993)**.

1.10.4 Protein complexes which may be involved in myofascial force transmission

Transsarcolemmal connections are involved in myofascial force transmission **(Patel & Lieber, 1997)**. Protein complexes including vinculin and dystrophin aid communication between the contractile machinery and the extracellular matrix **(Monti *et al.*, 1999)**. Vinculin is located in regularly spaced subsarcolemma domains called costameres. Costameres connect actin in the myofibril to the extracellular matrix (collagen/laminin). In addition, vinculin has been shown to be located throughout the Z line in skeletal muscle not just at the sarcolemma. Other proteins, including talin and integrin, have been co-localized with vinculin at the costameric structures **(Monti *et al.*, 1999)**.

Dystrophin is present in skeletal muscle costameres although it is more densely distributed at the ends of fibres. Dystroglycan, sarcoglycan and sarcospan are associated with dystrophin and are collectively known as the dystrophin associated protein complex **(Monti *et al.*, 1999)**.

These two protein complexes form links between the sarcomeres and the extracellular matrix and are suspected of operating together to establish connections throughout the cell membrane and may aid myofascial force transmission (**Monti *et al.*, 1999**).

1.10.5 Myofascial force transmission and intra-muscular connective tissue

Myofascial force transmission utilises intramuscular connective tissue. Initial studies using electron microscopy demonstrated that the endomysium is a mesh of randomly oriented collagen fibrils (**Rowe *et al.*, 1981**). More recently Purslow and Trotter, 1994 examined the orientation distribution of collagen fibrils in the endomysial network of bovine *sternomandibularis* muscle at different sarcomere lengths by image analysis of scanning electron micrographs of fixed samples following sodium hydroxide digestion. They reported that at short muscle lengths the collagen fibrils are arranged circumferentially but with increasing muscle lengths the fibrils become oriented with the long axis of the muscle i.e. longitudinally (**Purslow & Trotter, 1994**).

Collagen fibres are re-aligned with muscle contraction and this re-alignment is not immediately reversed upon de-recruitment of a proportion of the motor units. This suggests that a smaller number of motor units, than initially recruited, may utilise this re-arrangement of the intramuscular connective tissue to maintain an increased force output (**Monti *et al.*, 1999**). In other words, force transmission to the skeleton depends not only on neural activation of the motor units, but also on the state of the force transmission mechanisms'. This re-arrangement of collagen fibres following contractions may be one of the causative factors in the beneficial effects of athletes' obligatory stretching regime ('warming-up') prior to a strenuous period of exercise.

Furthermore it has been hypothesised that myofascial force transmission may transmit some of the muscular force onto the compartment connective tissue and not fully onto the tendons. Huijing and Baan 2000 reported that forces exerted at the proximal and distal tendons of EDL (*in vivo*) were not equal **(Huijing & Baan, 2000)**. This disparity between proximal and distal EDL forces suggests that there may be extra-muscular force transmission. As part of my research I investigated the effect of a fatiguing stimulation regime on the relationship between proximal EDL tendon lengths and the forces exerted at the proximal and distal EDL tendons and whether forces exerted at the distal TA and EHL tendon may be influenced by proximal EDL lengths.

1.11 Skeletal muscle damage

A substantial part of my thesis pertains to the protection of skeletal muscle against the potential for muscle damage, which may result from vigorous stimulation regimes. There is a large volume of literature on skeletal muscle damage, which identifies two schools of thought on the primary event causing muscle damage. One contests that mechanical factors i.e. sarcomere popping, see 1.11.1, initiate the process. While others propose that muscle damage is initiated at the cellular level through loss of energy supply, and/or loss of intracellular Ca^{2+} homeostasis, and/or over activity of oxidising free radicals, see 1.11.2. Which mechanical and/or metabolic parameter initiates the damage process has not been conclusively determined **(Bär *et al.*, 1994; Mc Ardle & Jackson, 1994)**. Subsequently a conclusive mechanism by which exercise and/or stimulation-induced muscle damage occurs has not been described. I

will briefly discuss the probable causative and contributory, mechanical and metabolic, factors identified to date.

1.11.1 Mechanical factors in muscle damage

The length-force curve (Figure 1.4) is determined by myofilament overlap and is dependent on sarcomere length.

It has been suggested that during eccentric contractions, where a muscle lengthens during contractions, the passive properties are subjected to excessive strain at muscle lengths on the 'descending limb' of the length–force curve, i.e. at lengths where the overlap of thick and thin filaments is so small that the sarcomeres cannot resist the extending force (**Armstrong *et al.*, 1991; Armstrong *et al.*, 1983; Gordon *et al* 1966**).

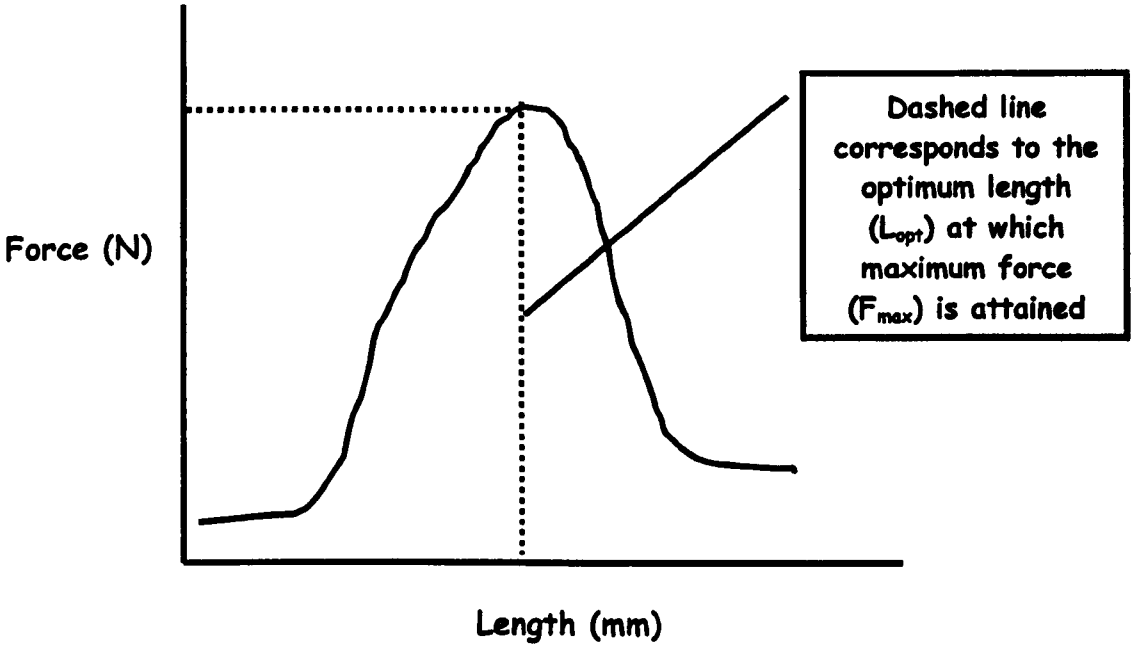

Fig. 1.4. Graph to illustrate the length-force curve.

Wood *et al.*, 1993 reported that immediately after eccentric exercise there was a shift to the right in the length-force curve that is, the passive force associated with a particular length was lower, which showed recovery i.e. shifted left to its original position, 5 hours post-exercise **(Wood *et al.*, 1993)**. Numerous studies have reported that longer muscle lengths showed an increase in the incidence of damage or symptoms of damage **(Lieber & Fridén, 1993; Brooks *et al.*, 1995; Newham *et al.*, 1988)**.

During eccentric contractions a proportion of the sarcomeres may be stretched beyond their filament overlap, this is called sarcomere 'popping'. This 'popping' of the sarcomeres damages the intermediate filaments comprising the passive structures. Electron microscopic analysis has shown damaged muscle to contain Z band streaming and loss of Z band registration in parallel myofibrils i.e. extensive disruption of the intermediate filament ultrastructure. It has been proposed that it is not high force but the magnitude of the strain that precipitates eccentric contraction-induced muscle-damage **(Lieber & Fridén, 1993)**. Whilst others have suggested that it is the culmination of repetitive eccentric contractions that initiates muscle damage **(Warren *et al.*, 1993)**. Which is in some agreement with the hypothesis that muscle damage is a result of the excessive strain placed on the intermediate filaments following sarcomere popping **(Armstrong *et al.*, 1991; Morgan, 1990; Fridén & Lieber, 1992; Wood *et al.*, 1993)**.

Sarcomeric protein filaments include titin, which links myosin filaments in series, and desmin, which links neighbouring Z-disks to each other and the sarcolemma

(Armstrong *et al.*, 1991; Morgan, 1990; Fridén & Lieber, 1992; Wood *et al.*, 1993). In addition, vinculin and its associated proteins, talin and integrin make up costameric structures that interdigitate the sarcolemma. Costameres connect actin to the extracellular matrix. Dystrophin has also been localised in costameres but is more densely distributed at membrane junctions towards the end of the myofibre. Vinculin and dystrophin protein complexes are important for the mechanical and osmotic stability of the sarcolemma **(Monti *et al.*, 1999)**. Eccentric stimulation has been shown to result in the loss of costameric proteins and muscle damage in both fast-twitch and slow-twitch skeletal muscles. The loss of these proteins could be a result of mechanical disruption of the sarcolemma following intensive contractions. Alternatively their loss may be due to reorganisation of the contractile proteins and their connectins to the extracellular matrix following stimulation. This process could destabilise the sarcolemma and make it more susceptible to damage **(Biral *et al.*, 1998)**.

Komulainen *et al.*, 1998 reported 'early' damage to myofibres with coincident disruption of cytoskeletal proteins after eccentric-stimulation of fast-twitch muscles. Immediately after the stimulation regime a proportion of the swollen fibres showed discontinuous dystrophin staining and irregularities in the contour of the cell membrane. After 6 hours they found that the majority of the swollen fibres stained negative for dystrophin and desmin and exhibited disorganised actin and fibronectin, a matrix organising protein showed intramyocellular staining. More prolonged post regime times, 4 and 7 days, showed more advanced muscle damage with dystrophin and desmin negative swollen cells (ghost cells) still present and fibronectin staining

was found throughout the damaged area and in the adjacent endomysium and perimysium. Disruption of the intermediate filaments preceded disturbance of the myofibrillar system and cell plasma membrane. In these experiments swollen fibres, which exhibited disruption of their sarcolemma, showed different staining intensities for disorganised actin and intramyocellular fibronectin. This suggests that disruption of the myofibre may be segmentalised thus eccentric stimulation induced-damage may not occur uniformly within a myofibre. Initial perturbations of sub-membrane cytoskeletal proteins (dystrophin) and intra-sarcomeric cytoskeletal proteins (desmin) may effect other membrane-associated proteins, such as ion channels, which could lead to an increase in intracellular Ca^{2+}. Elevated intracellular Ca^{2+} concentrations may activate calpain, which could further exacerbate the disruption and hydrolysis of cytoskeletal proteins thus precipitating the damage process (**Komulainen *et al.*, 1998**). There is some evidence that eccentric contractions can cause a loss of Ca^{2+} homeostasis. This loss could be promoted by A) Ca^{2+} influx through stretch-activated channels in the sarcolemma, which allow Ca^{2+} to move into the cell down a concentration gradient. B) Ca^{2+} influx through ruptures/lesions in the sarcolemma produced by high tension (**Belcastro *et al.*, 1998**).

1.11.2 Metabolic factors in muscle damage

Loss of energy supply decreases ATP levels and can lead to the fibre being unable to maintain the integrity of its membrane, defective reacylation of phopholipids, thus initiating damaging events including an influx of Ca^{2+} and loss of cellular enzymes. The loss of energy supply and efflux of cellular enzymes from the myofibre are not

coincident which would suggest that decreased ATP levels may act as a catalyst for damaging events which may ultimately lead to the loss of cytosolic components **(Mc Ardle & Jackson, 1994)**. Low frequency stimulation of fast twitch muscles may cause a disparity between the level of work demanded from the muscle and its capacity for generating ATP on a continuous basis. The potential for stimulation-induced damage may be higher during the early stages of stimulation when transformation to an oxidative metabolism is being induced.

It has been shown that the accumulation of intracellular Ca^{2+} i.e. loss of Ca^{2+} homeostasis, can induce ultrastructural damage through the activation of Ca^{2+}-activated proteases and lipolytic enzymes, and mitochondrial overload **(Mc Ardle & Jackson, 1994)**. It has been proposed that a major factor in stimulation-induced damage is the loss of Ca^{2+} homeostasis, which may initiate irreversible ultrastructural damage and ultimately fibre necrosis.

Ca^{2+}-activated proteins are non-lyosomal enzymes of which there are two sub-types namely, calpain type 1 and calpain type 11, they require micromolar and millimolar Ca^{2+} levels, respectively, for activation. In addition, control of these proteases depends on the relative amounts of their associated activator and inhibitor proteins, and whether the enzyme is in the autolyzed or unautolyzed form. This family of Ca^{2+}-activated proteins selectively degrades a variety of proteins including desmin, vimentin, tropomyosin and α-actinin and have been associated with the disruption of the intermediate filaments and Z line streaming. The contractile filaments, actin and myosin, are not substrates for calpain. These enzymes can convert xanthine

dehydrogenase to xanthine oxidase which, acts to generate superoxide radicals **(Belcastro, 1993; Mc Ardle & Jackson, 1994)**.

Ca^{2+}-activated phospholipases can metabolise membrane phospholipids, which may cause disruption of the lipid bilayer and damage the myofibre. However, non-specific phospholipase inhibitors did not inhibit the damage process suggesting that activation of these enzymes is not the primary factor in initiation of muscle damage **(Mc Ardle & Jackson, 1994)**.

Mitochondrial overload is where mitochondria, in the presence of high intracellular Ca^{2+} concentrations, take in large amounts of Ca^{2+} and phosphates concomitantly. Large Ca^{2+} concentrations in the mitochondria inhibit mitochondrial respiration. When Ca^{2+} concentrations become critically high the mitochondria become overloaded and release their Ca^{2+} into the cytoplasm. Research has suggested that mitochondrial overload occurs during damage but is not the initial stimulus for that damage **(Mc Ardle & Jackson, 1994)**.

In addition, to loss of energy supply and Ca^{2+} homeostasis, low frequency stimulation may increase the activity of oxidising free radicals. Over-activity of free radicals can cause damage to myofibres through peroxidation of unsaturated fatty acids in the lipid bilayer, inactivation of plasma membrane Ca^{2+} channels, disruption of intracellular organelles and oxidative damage to DNA and proteins **(Mc Ardle & Jackson, 1994)**. In stimulated muscle, free radicals can be produced by the mitochondrial electron

transport system, cytochrome P-450, membrane bound oxidases, infiltrating phagocytes, xanthine oxidase located in the endothelial tissue and various cytosolic catalytic enzymes. Under normal conditions the potential for oxygen-derived free-radical damage is lowered by anti-oxidant vitamins (vitamin E), thiol containing low molecular weight compounds (reduced glutathione [GSH]), and anti-oxidant enzymes (superoxide dismutase [SOD], GSH peroxidase [GPX], catalase [CAT]) **(Best *et al.*, 1999)**. In stimulated muscles the potential for damage may be compounded by the disparity between the production of oxidising free radicals and anti-oxidising species. It has been hypothesised that free radical formation may mediate the loss of Ca^{2+} homeostasis. The resultant increase in intracellular Ca^{2+} concentrations may cause increased activation of the contractile elements, which will increase ATP consumption thus perturbing the metabolic status of the muscle. In addition the breakdown of ATP provides hypoxanthine as a substrate for xanthine oxidase located in endothelial tissue which, can generate oxygen free radicals **(Mc Ardle & Jackson, 1994)**.

Radák *et al.*, 1995 subjected rats to an exhaustive running regime where the animals had been intraperitoneally injected with a superoxide dismutase (SOD) derivative, SM-SOD. SM-SOD has an advantage over SOD as it has a longer half-life, 6 h to 5 min, respectively. Immediately after the exercise regime untreated soleus and TA muscles showed elevated xanthine oxidase levels while SM-SOD treated muscles exhibited depressed xanthine oxidase levels. They also reported that SM-SOD treatment attenuated the activity of thiobarbituric acid-reactive substances, which gives an estimation of malondialdehyde a peroxidation marker, in soleus and TA

muscles. This suggests that pre-treatment with an anti-oxidant enzyme (exogenous SM-SOD) can diminish the production of free radicals by the xanthine system and attenuate lipid peroxidation (**Radák *et al.*, 1995**). While this study showed that the administration of an anti-oxidant decreased free radical, xanthine oxidase, levels and lipid peroxidation they did not investigate the gross damage status of the exercised muscles and thus did not establish whether their protocol could attenuate the exercise-induced damage process as a whole.

Neuronal type nitric oxide synthase (nNOS) is associated with the sarcolemma of fast muscles (type 2 fibres) and may contribute to the over production of free radicals during exercise and/or stimulation. In addition to nNOS, skeletal muscle contains endothelial nitric oxide synthase (eNOS), albeit at lower levels than nNOS. There is a high expression of nNOS in type 2, and low expressions of this enzyme in type I fibres. Reiser *et al.*, 1997 showed that chronic low frequency stimulation of rabbit TA and EDL muscles increased the expression of nNOS with a concomitant increase in the expression of type 2A and type 1 MHC isoforms at the expense of type 2D isoforms. Stimulation-induced expression of nNOS does not abide by the normal fibre specific pattern of expression (**Reiser *et al.*, 1997**). Furthermore the nNOS is associated with the dystrophin complex (bound to α1-syntrophin) in fast-twitch muscle fibres. If the dystrophin complex is altered during stimulation the nNOS may dissociate from the sarcolemma and this may result in disruption of nNOS regulation and muscle damage (**Brennan *et al.*, 1995**). The disturbance of nNOS may result in higher levels of nitric oxide (NO) in the endothelium which may induce the production

of peroxynitrite, which can decay to the hydroxyl radical. The hydroxyl radical may cause increased adhesiveness of the endothelium for neutrophils and increase the inflammatory response, which may induce further damage **(Reiser *et al.*, 1997; Phan *et al.*, 1994)**.

Exercise causes significant changes in the distribution and function of neutrophils (non-specific defence) which can contribute to the over activity of oxidants. There is an increase in the number of circulating neutrophils with exercise as a result of demargination of these cells from endothelial tissues and bone marrow, or as part of the phagocytic and inflammatory response to exercise-induced damage **(Pyne, 1994)**. Exercise elicits an initial activation of neutrophils primary response, degranulation, with a secondary but variable response in key effector functions such as adherence, phagocytosis and the capacity for the respiratory burst. **(Dufaux *et al.*, 1989; Gray *et al.*, 1993)**. Smith & Weidemann 1990 proposed that moderate exercise might potentiate while intense exercise may suppress the status of the neutrophil function **(Smith & Weidemann 1990)**. Exercise may have an intensity-dependent effect on neutrophil function.

Stimulation-induced muscle damage can result in an inflammatory response, which may increase the number of circulating neutrophils and activate them to release myeloperoxidase (MPO) into the damaged tissue thus exacerbating the damage process **(Pyne, 1994)**. MPO, the heme-containing enzyme found in the primary granules of neutrophils and monocytes, catalyzes the production of hypochlorous acid

(HOCl), a powerful oxidant which is derived from Cl^- ion and H_2O_2 (respiratory burst) **(Bradley *et al.*, 1982 Bozeman *et al.*, 1990)**. Exercise-induced release of granular enzymes (MPO) has been used to indicate neutrophil activation **(Lehrer & Ganz, 1990)**. However, Bury and Pirany 1995 showed that an increase in MPO concentration after prolonged exercise in human subjects did not correlate with modification of neutrophil count, suggesting that neutrophil degranulation maybe independent of their mobilisation **(Bury & Pirany, 1995)**.

Belcastro *et al.*, 1996 subjected rats to eccentric exercise (downhill running to voluntary exhaustion) and showed that, with prolonged exercise, MPO activity is elevated in most rat tissue not exclusively in rat skeletal muscle. In addition they suggested that the metabolic status of muscle might be an important factor for neutrophil infiltration **(Belcastro *et al.*, 1996)**. Raj *et al.*, 1998, demonstrated that following exercise, rat skeletal muscle showed increases in calpain-like and MPO activities. Pre-treatment with a cysteine protease inhibitor (E64c) lowered the calpain-like and MPO activities. It was suggested that Ca^{2+}-stimulated proteolysis (calpain-like activity) and neutrophil accumulation (MPO activity) in skeletal muscle occur along the same time course during exercise **(Raj *et al.*, 1998)**.

Calpain has been implicated in the localisation of neutrophils to damaged tissue. Peptide fragments of calpain have been shown to possess neutrophil chemotactic potential. Dose dependent neutrophil migration has been shown using synthetic peptides of various lengths from the large and small subunits of both calpain isoforms **(Belcastro *et al.*, 1998)**.

This review of muscle damage, albeit brief, shows that it is difficult to differentiate between the influence of mechanical and cellular parameters on the initiation of exercise or stimulation-induced damage. Indeed, it may be that all the aforementioned parameters act in concert with no one factor being totally responsible or indispensable for induction of the damage process as a whole.

1.12 Ischemic-reperfusion induced damage

Historically most of the interest in ischemic-reperfusion damage has focused on cardiac muscle, with the advent of by-pass operations, but similar damage processes occur in skeletal muscle. Ischemic-reperfusion induced damage includes two phases namely, ischemia and then oxygenated reperfusion, the major damage occurs during reperfusion as the examples below illustrate. During ischemia-reperfusion episodes there may be injury to endothelium, which causes inappropriate vasoconstriction, activation of leukocytes and platelets, ultimately resulting in microvascular thrombosis and muscle damage. The primary causative mechanism(s) of ischemic-reperfusion damage is unclear, however free radical mediated processes have been implicated.

During ischemia, endothelial enzymes, NOS and xanthine oxidase, are capable of generating superoxide anions. Damage to endothelial cells triggers the expression of 'leukocyte adhesion molecules' activating circulating neutrophils that infiltrate the reperfused muscle, generating more superoxide anions, causing myonecrosis. **(Smith *et al.*, 1989).**

Ischemic-reperfusion damage in skeletal muscle has been the subject of extensive research and may be instructive in elucidating the mechanism(s) through which stimulation-induced damage occurs.

Harris *et al.*, 1986 subjected canine *gracilis* muscle to 2 or 7 hours of ischemia followed by 4 hours of reperfusion. The shorter ischemia regime (2 hr) caused a transient increase in free radical production during the first 0-60 min of reperfusion. However, free radical production had returned to control levels after 90 min of reperfusion and the muscles exhibited a normal ultrastructure with some swelling of the SR and T-tubules. Muscles that had received more prolonged periods of ischemia (7 hr) showed a persistent increase in free radical production. There was extensive disruption of the ultra-structure with all mitochondria exhibiting swelling and disruption, the nuclei had adopted irregular shapes and a large proportion were swollen. A substantial proportion of the myofibrils exhibited disruption of contraction bands and structural disorganisation. This experimental group incurred extensive muscle damage. This data suggests that the duration of the ischemic episode determines the amount and reversibility of the muscle damage incurred upon reperfusion **(Harris *et al.*, 1986)**.

Following prolonged ischemia a number of capillaries cannot be reperfused upon resumption of blood flow, this is called the 'no flow' phenomenon and has been attributed to an increase in total vascular resistance **(Bagge *et al.*, 1980)**. In addition ischemia may increase interstitial fluid (edema) which is thought to be a result of increased vascular permeability **(Korthuis *et al.*, 1985)**. These symptoms of vascular

post-ischemic damage have been attributed to leukocytes lodging themselves in the capillaries. Korthuis *et al.*, 1988 have demonstrated that in canine *gracilis* muscles reperfusion with granulocyte–depleted whole blood resulted in a dramatic decrease in vascular permeability and resistance compared with whole blood **(Korthuis *et al.*, 1988)**.

Smith *et al.*, 1985 used a canine *gracilis* muscle model, the same model employed by Korthius *et al*, 1985, to evaluate neutrophil influx (MPO activity) and monitor any changes in the antioxidant systems during 4 hours of ischemia and 1 hour of subsequent reperfusion. The tissue MPO levels did not change during ischemia but increased dramatically after reperfusion indicating an influx of neutrophils into the muscle during reperfusion. In addition, the levels of SOD and CAT were not altered after ischemia or reperfusion, but the tissue concentration of GSH decreased after reperfusion. This decrease is indicative of the production of oxidant agents during reperfusion. Skeletal muscle damage induced by ischemia-reperfusion regimes may be attributable, in part, to reactive oxygen species produced by neutrophils **(Smith *et al.*, 1989)**.

Sternbergh and Adelman 1992 subjected rat hind limb muscles to an ischemia (120 min) reperfusion (60 min) regime. The soleus (slow-twitch) and plantaris (fast-twitch) muscles incurred similar levels of damage. No correlation was reported between post-ischemic flow and muscle damage, or microvascular injury. This data suggests that

muscle fibre type composition does not appear to influence the sensitivity of the muscle to ischemia-reperfusion injury **(Sternbergh & Adelman, 1992)**.

In contrast, others have reported that murine EDL (fast-glycolytic) muscles exhibited more damaged mitochondria, SR and myofibrils than soleus (slow oxidative) muscles following an ischemic-reperfusion regime. This suggests that the fibre type composition of a muscle may effect the nature of the ischemia/reperfusion injury **(Woitaske & Mc Carter, 1998)**.

1.13 Protection against muscle damage

Part of my research focused on stimulation-induced protection of rabbit fast twitch muscles against stimulation-induced damage. There is a substantial body of evidence, which shows that the potential for exercise, ischemic-reperfusion and stimulation-induced damage can be ameliorated by subjecting skeletal muscle to moderate episodes of exercise, stimulation and ischemia prior to more intensive regimes. The mechanisms' by which skeletal muscle may impose cytoprotection against damage have not been elucidated.

1.13.1 Repeated bout effect

Muscle damage can be induced by unfamiliar predominantly eccentric exercise **(Faulkner *et al.*, 1993)**. Following eccentric exercise a number of changes are incurred by human skeletal muscle. Initially a loss of strength is experienced followed by pain, muscle tenderness and muscle stiffness. These sensations normally peak around 24 to 48 hours after exercise. Collectively these symptoms are known as

delayed onset muscle soreness (DOMS). Soluble proteins (creatine kinase (CK), myoglobin) are released into the subject's circulation, reaching maximum values 5 to 6 days after the eccentric exercise regime. Muscle damage and infiltration of fibres by mononuclear cells is apparent approximately 10 days after eccentric exercise **(Jones & Round, 1994)**.

Following an initial eccentric exercise regime a repeat of the exercise protocol results in a substantial decrease in muscle damage, this is called the 'repeated bout effect'. Repetition of an exercise regime even in the presence of damaged fibres still causes less damage than an unprepared bout. Thus the protection is not dependent on the full recovery of muscle damage. In addition, the first experience of eccentric exercise does not have to result in significant damage for exertion of the protective effect upon resumption of the exercise regime **(Nosaka & Clarkson, 1995; Brown *et al.*, 1997; Clarkson & Tremblay, 1988)**. Many theories have been proposed to explain the 'repeated bout effect' which pertain to the adaptive capabilities of intra- and extra-cellular parameters of skeletal muscle **(Mc Hugh *et al.*, 1999)**

The 'repeated bout effect' may be attributable to conditioning of the intermediate filament system **(Fridén *et al.*, 1983; Newham *et al.*, 1987; Ebbeling & Clarkson, 1990)** and/or strengthening of the sarcolemma or SR **(Clarkson & Tremblay, 1988; Mc Ardle & Jackson, 1994)** thereby increasing the amount of strain the myofibres can withstand.

It has been proposed that initial periods of eccentric exercise may identify and remove stress susceptible myofibres or sarcomeres. Thus less damage is incurred upon repetition of the exercise regime as a greater population of stress resistant fibres will be participating **(Armstrong *et al.*, 1983)**. However there are problems with this theory as it has been shown that only a minimal amount of muscle injury needs to be experienced and, recovery does not have to be complete for protection upon repeated eccentric exercise. Induction of a minimal amount of damage could not remove all of the stress susceptible myofibres or sarcomeres. Therefore resumption of eccentric exercise would be expected to remove the remaining stress susceptible elements and thus an increase in damage would be expected **(Brown *et al.*, 1997; Clarkson & Tremblay, 1988)**.

It has also been proposed that following an initial period of exercise the longitudinal addition of sarcomeres may occur, thus decreasing the incidence of sarcomere 'popping' upon repeated exercise. Lynn & Morgan 1994 demonstrated that in rat *vastus intermedius* a period of training (uphill running) resulted in an increase in serial sarcomeres compared with non-exercised controls. **(Morgan, 1990; Fridén *et al.*, 1983; Lynn & Morgan, 1994)**. However, there does not have to be full recovery of the trained muscles for the repeated protective effect which suggests that there may not be adequate time for the longitudinal addition of sarcomeres **(Nosaka & Clarkson, 1995; Brown *et al.*, 1997; Clarkson & Tremblay, 1988)**. In addition, Wood *et al.*, 1993 have shown than after an eccentric exercise regime the length-force curve shifts to the right but returns to normal i.e. shifts to the left, after 5 hr. Therefore

additional sarcomeres may be removed upon cessation of stimulation, which would be expected to cause perturbation of the muscle fibre during recovery. Damage has not been recorded during recovery periods (**Wood *et al.*, 1993**).

After eccentric exercise there is an increase in intra-muscular connective tissue. This results in an increase in passive stiffness. Whether this increase is permanent, with respect to control non-exercised muscle, has not been fully elucidated. It has been hypothesised that an increase in intra-muscular connective tissue could increase the amount of strain the passive structures can withstand thus affording the muscle with repeated bout protection. (**Lapier *et al.*, 1995; Howell *et al.*,1993**)

The repeated bout effect has also been attributed to a depressed inflammatory response. Repetition of eccentric contractions following an initial training regime showed a decreased activation of neutrophils and monocytes. Whether depressed activation is due to a decline in the inflammatory response or due to decreased muscle damage is unclear (**Pizza *et al.*, 1996; Nosaka & Clarkson, 1995**).

There is no consensus on a specific mechanism to explain the repeated bout effect. It seems most plausible that a co-ordinated intracellular and extracellular response is needed for the initiation and persistence of the repeated bout effect.

1.13.2 Ischemic pre-conditioning

Ischemic pre-conditioning, repeated brief periods of ischemia followed by reperfusion before a prolonged ischemic-reperfusion regime can ameliorate injury in rat skeletal muscle **(Papanastasiou *et al.*, 1999)**.

Rat *gastrocnemius* muscles were pre-treated with an anti-neutrophil monoclonal antibody (RP3) followed by 3 or 5 hr of ischemia and 24 hr of reperfusion. After 3 hr of ischemia RP3 treated muscles had reduced MPO activities, free radical production, water content and muscle damage. However after 5 hr of ischemia followed by reperfusion the damage was so severe that RP3 treatment, i.e. neutrophil depletion, had no effect on ischemic injury. Reduced neutrophil accumulation and/or activation appears to be involved in protection against ischemia-reperfusion induced damage. However the duration of ischemia determines whether protection can occur or not **(Iwahori *et al.*, 1998)**.

Following ischemia-reperfusion in myocardial tissue both protective and deleterious effects have been attributed to NO. It has been proposed that different redox states of NO can result in cytotoxic or cytoprotective effects. Phan *et al.*, 1994 found that pre-treatment with a NOS inhibitor (nitro-iminoethyl-L-ornithine) resulted in greater muscle viability in pre-treated compared with control groups. Pre-treated muscles showed decreased blood flow, interstitial fluid accumulation and MPO activity compared with control non-treated muscles. NOS inhibitors may protect the muscle by

reducing the accumulation of neutrophils in the muscle and thus attenuating ischemia-reperfusion-induced muscle damage **(Phan *et al.*, 1994)**.

Bushell *et al.*, 1996 examined whether pre-treatments with allopurinol (an inhibitor of xanthine oxidase), ascorbic acid (free radical scavenger), and depomedrone (inhibits neutrophil sequestration and activation) could protect against muscle damage (electron microscopy) in a standardised rabbit model of limb (TA) ischemia (4 hr of ischemia and 1hr of reperfusion). Allopurinol did not have a protective effect against the ischemia-reperfusion-induced damage. This demonstrates that inhibition of xanthine oxidase does not protect skeletal muscle against ischemia-reperfusion damage. High doses of ascorbic acid exerted a protective effect following reperfusion. The ascorbic acid pre-treated animals showed no increase in MPO activity and no change in free radical activity compared with controls. This suggests that inhibition of free radical accumulation may protect against ischemic-reperfusion damage. In addition, corticosteroid pre-treatment demonstrated no increases in MPO and free radical activities when compared to control TA muscles. Steroids may exert their protective effect by inhibiting neutrophil activators and chemoattractants **(Bushell *et al.*, 1996)**.

While no conclusive mechanism for ischemic pre-conditioning has been documented there is considerable evidence that regulation of neutrophil influx to, and accumulation of neutrophils in the reperfused tissue may be involved in protection against ischemic-reperfusion damage.

1.13.3 Neuromuscular stimulation-induced protection

The neuromuscular stimulation protocols employed to condition the skeletal muscle may also damage it. However, damage is not an inevitable consequence of electrical stimulation but is related to the pattern of activation. The incidence of degenerating fibres varies with different patterns and frequencies of stimulation. Damage is not a simple function of the mean stimulation frequency or aggregate number of impulses received by the muscle (**Lexell *et al.*, 1993**).

Stimulation-induced damage is focal and exhibits variability within a cross section and along the length of a muscle. Different anatomical muscles are differentially susceptible to damage. In addition, there are inter-animal variations in response to stimulation-induced damage (**Lexell *et al.*, 1992; Lexell *et al.*, 1993; Lexell *et al.*, 1994**).

It has been documented that the potential for stimulation-induced damage can be abolished or minimised by subjecting the muscle to a period of stimulation with a non-damaging pattern (pre-stimulation) prior to stimulation with a potentially-damaging pattern (**Jones *et al.*, 1997**). Jones *et al.*, 1997 devised a two-stage stimulation protocol, which employed rabbit fast-twitch muscles and programmable stimulators. The fast-twitch muscles were pre-stimulated with a non-damaging pattern of 2.5 Hz continuously for 2, 7 and 14 days. The muscles were then immediately subjected to a potentially damaging pattern of stimulation, 10 Hz continuously for 9 days which, was previously shown to result in a considerable incidence of damage (**Lexell *et al.*, 1992; Lexell *et al.*, 1993**). Protection was not found after 2 days but developed maximally between 7 and 14 days of pre-stimulation. More prolonged periods of pre-stimulation

exerted a greater protective effect. The endomysial tissue content increased in all of the stimulated muscles and showed no significant differences for any of the pre-stimulation times (**Jones *et al.*, 1997**). This would suggest that something other than increased intra-muscular connective tissue has a significant role in the pre-stimulation induced protective effect.

All cells respond to stress by the induction of HSP. These proteins are involved in the folding, stabilisation and translocation of nascent polypeptides into cellular organelles (**Ornatsky *et al.*, 1995**). It has been suggested that HSP may play a role in the protection of muscle against stimulation-induced damage. The expression of HSP70 in a muscle is proportional to the type 1 fibre composition. Neuromuscular stimulation induces the expression of HSP. Ornatsky *et al.*, 1995 showed that chronic stimulation (10 Hz) of rat TA muscles for 10 days increased the expression of HSP70 (10 fold) compared with control muscles. There was no transformation of the stimulated TA fibre type composition which suggests that the 'normal' specificity for higher HSP 70 expression in type 1 fibres may be shifted to type 2 fibres with stimulation (**Ornatsky *et al.*, 1995**).

The potential role of HSP in the stimulation-induced protective effect reported by Jones *et al.*, 1997 is tentative. Chronic stimulation of rabbit TA muscles at 10 Hz for 9 days would be expected to elevate the expression of HSP70 yet considerable histological damage and minimal transformation to slow phenotype have been identified after this period of stimulation at 10 Hz (**Lexell *et al.*, 1992; Lexell *et al.*, 1993; Jones *et al.*, 1997; Ornatsky *et al.*, 1995**). Therefore it is difficult to reconcile

how the inducible HSP may adopt a protective role upon pre-stimulation at a lower 'non-damaging' frequency for between 7 and 14 days when their substantial induction at a higher 'damaging' frequency showed no advantage to muscle viability.

It has been demonstrated that after 14 days of stimulation at 2.5 Hz (the period of pre-stimulation that afforded maximum protection) the fast fibre population of rabbit TA was predominately fast-oxidative 2A fibre types **(Mayne et al., 1996)**. The transformation of the fast-fibre population to a fast-oxidative phenotype after 14 days at 2.5 Hz suggests that specific fibre types, namely fast-oxidative fibre types, may have significant protective consequences for a muscle.

Increased capillarization may be involved in pre-stimulation-induced cyto-protection. Elevations in capillary density occur early in the transformation process **(Skorjanc *et al.*, 1998)** and may increase muscle viability by providing an increased influx of oxygen and metabolites to, and efflux of waste products from the muscle.

The metabolic changes after 14 days at 2.5 Hz are less extreme and more gradual than those associated with neuromuscular stimulation at 10 Hz for the same time period. Only HK showed significant increases after stimulation at 2.5 Hz which may aid synthesis of glycogen and energy production via glycolysis **(Jarvis *et al.*, 1996; Mayne *et al.*, 1996)**.

It has been suggested that cyto-protection afforded to skeletal muscle following pre-stimulation maybe related to metabolic adaptations **(Jones *et al.*, 1997)**. Harris *et al.*,

1986 demonstrated that 7 hr of ischemia followed by 4 hr of reperfusion caused significant ultrastructural damage in canine *gracilis* muscle with persistently high free radical production. However, after 7 hr of ischemia the levels of glycogen were increased. This suggests that fast-twitch muscle can maintain an appreciable rate of glycolysis in the presence of ischemia but muscle damage is still incurred upon resumption of blood flow. Protection against ischemic-reperfusion induced muscle injury may not be wholly based on the metabolic capabilities of fast-twitch muscle **(Harris *et al.*, 1986)**.

Patel *et al.*, 1998 showed that training, discontinuous stimulation for 3 weeks, of rabbit EDL and TA muscles increased CS activity. However, subjecting these trained muscles to 30 min of eccentric exercise showed no differences in maximum tetanic tension, an indirect marker of muscle damage, with untrained muscles. These results suggest that increased oxidative capacity does not protect against exercise-induced muscle damage **(Patel *et al.*, 1998)**.

It is becoming clear that skeletal muscle has protective mechanisms that it can put in place to reduce the potentially damaging effects of future activity, as long as the stimulus is moderate and not overwhelming. The factor(s) that are essential to these protective mechanisms have not been elucidated.

1.14 Clinical applications

Skeletal muscle can be employed in a number of clinical rehabilitation procedures including functional electrical stimulation (FES) and cardiac assistance.

FES exploits neuromuscular stimulation to restore muscle function in stroke patients and patients suffering spinal cord injuries. Functions which can be restored include correction of drop foot, restoration of standing and walking in immobilised patients, **(Veltink *et al.*, 1991; Bajd *et al.*, 1991)**, alleviation of anal incontinence **(Williams *et al.*, 1989)**, and ventilatory assistance **(Glenn *et al.*, 1984)**.

The use of conditioned, fatigue resistant skeletal muscle in a cardiac assist role involves the movement of a pedicled graft of muscle to an appropriate position to assist the heart. There are two categories of cardiac assist procedures namely category 1- and category 2- assists **(Salmons & Jarvis, 1992)**.

Category 1-assist procedures include cardiomyoplasty and aortomyoplasty. Cardiomyoplasty involves wrapping skeletal muscle around the left or right ventricle, or both and, then activating the muscle during systole by electrical stimulation to augment myocardial contraction **(Oakley & Jarvis, 1994)**. Aortomyoplasty involves wrapping the muscle directly around either the ascending or the descending aorta **(Pattison *et al.*, 1991)**.

Category 2-assist procedures involve the construction of independent structures from conditioned fatigue resistant skeletal muscle which are connected to the patient's circulation. In this category two main procedures have been adopted. The construction of skeletal muscle ventricles (SMV) and, utilisation of the power from skeletal muscle to drive an artificial heart or ventricular device via a mechanical, hydraulic or

electrical link (**Acker *et al.*, 1986, Anderson *et al.*, 1991, Pochettino *et al* 1991, Frey *et al.*, 1986, Ugolini, 1986**).

The avoidance of muscle damage is critical in these situations because unless the muscle employed in these clinical procedures can produce force and power on a permanent basis free from the potential of stimulation-induced injuries than these interventions will provide no benefit.

1.15 Research objectives

This thesis can be sub-divided into two main parts. The first section examined the effect of a two-stage stimulation regime on the damage status of rabbit fast-twitch skeletal muscle. The second part of my research investigated the effect of stimulation on force-length relationships within rat fast-twitch skeletal muscles. Both sections of this thesis relate to each other as they examined the viability of skeletal muscles, albeit from different animals, following the challenge of neuromuscular stimulation.

In the first section of this study rabbit TA muscles were pre-stimulated at 2.5 Hz (a non-damaging pattern of stimulation) for 7, 10 or 14 days, either alone or followed by stimulation at 10 Hz (a potentially damaging pattern) for 9 days (Figure 3.1B). The two-stage stimulation model I employed was designed to provide pre-stimulated (2.5 Hz) muscles before and after the challenge (10 Hz).

This part of my research had multiple objectives. The primary aim of this work was to determine the amount of damage incurred by the muscles pre-stimulated alone and the muscles pre-stimulated and challenged with the 10 Hz regime, thus establishing

whether or not low frequency pre-stimulation conferred cytoprotection against the subsequent 10 Hz challenge.

The next objective was to ascertain whether this stimulation regime induced significant changes in capillarization and/or fibre type composition and whether these parameters may be involved in stimulation-induced cytoprotection. As this work progressed an additional objective became apparent namely whether specific fibre types were susceptible to stimulation-induced damage and consequently whether stimulation-induced protection may be fibre specific.

The final aim in this part of the research was to establish the mechanical properties of the muscles pre-stimulated alone and the muscles pre-stimulated and challenged with the 10 Hz regime. Contractile characteristics including the maximum tetanic tension (P_o), the contraction time (C_t), the relaxation time (R_t), and the maximum velocity of shortening (V_{max}) were recorded. The identification of any changes in these physiological measurements following the two-stage stimulation regime may be instructive in identifying cellular factors, which may contribute to stimulation-induced cytoprotection.

In the second section of this study rat EDL, TA and EHL muscles were subjected to three hours of continuous maximal stimulation (30 Hz), via the common peroneal nerve, under isometric conditions.

The primary aim of this work was to establish the effect of passive proximal EDL tendon lengthening on forces exerted at the proximal and distal tendons of rat EDL

muscle and at the distal tendons of TA and EHL muscles before and after the stimulation protocol.

A secondary aim was to elucidate whether a rest period of 10 min, upon completion of the stimulation regime, effected the force-length relationships at the aforementioned EDL and TA and EHL tendons.

2.1 *In situ* low-frequency stimulation of the *tibialis anterior* (TA) muscle in a rabbit model

My research into the cytoprotective effect of pre-stimulation employed adult New Zealand White rabbits of either sex with body weights in the range of 2.5-4 Kg, and miniature electrical stimulators totally implanted in the animal. The TA served as the experimental fast muscle. This muscle was chosen, as there is a large volume of literature on TA and its response to neuromuscular stimulation. The common peroneal nerve, which supplies the TA is predominantly a motor nerve and does not present any complicating sensory effects. In addition the anatomical location of the TA is advantageous as it is not in direct contact with other muscles in the anterior compartment and could be dissected out easily with no adverse effect on mechanical recordings.

In the experimental groups both the left and right TA muscles received stimulation. In the control group the left TA was stimulated, whilst the right TA served as a contra-lateral control.

All experimental animals were treated in strict accordance with the Animals (Scientific Procedures) Act of 1986.

2.2 Stimulators used for low frequency stimulation of rabbit TA muscles

Miniature programmable implantable stimulators were used which allowed the rabbits unrestricted freedom of movement (**Salmons & Jarvis, 1991; Taylor *et al.*, 1996**). An

optical link enabled the stimulators to be switched on or off using a stroboscope, to transmit light pulses over the site of the implant through the skin of the animal.

The stimulators delivered pulses of 0.2 ms duration and had a 3.2 V lithium battery as an internal power source. The amplitude of the stimulus caused supra-maximal stimulation of the motor axons of the TA muscles. The stimulators were encapsulated in several layers of silicone rubber (Dow Corning Ltd) which protected them from corrosive agents and provided an inert surface. A Dacron™ mesh was extended from the silicone rubber to aid suturing. Leads, of PVC-insulated, multi-stranded stainless steel (Cooner Sales Company, California, USA), ended in bared loops mounted on Dacron velour pads (USCI, MA, USA) to facilitate suturing and in-growth (Figure 2.1). Prior to implantation the stimulators were sterilized in 1% benzalkonium for 24 hr.

2.3 Anaesthesia in the rabbit model

Atropine sulphate (3.0 mg kg^{-1} body weight; Sigma) and diazepam (5 mg kg^{-1}; Valium™, Roches Products Ltd., Welwyn Garden City, UK) were administered sub-cutaneously prior to the anaesthetic. After 30 min, the animals were anaesthetised with an intra-muscular injection of fentanyl citrate/fluanisone (0.3 mg kg^{-1}; fentanyl citrate, 0.315 mg ml^{-1} and fluanisone, 10 mg ml^{-1}, Hypnorm™, Janssen Pharmaceuticals, Oxon, UK).

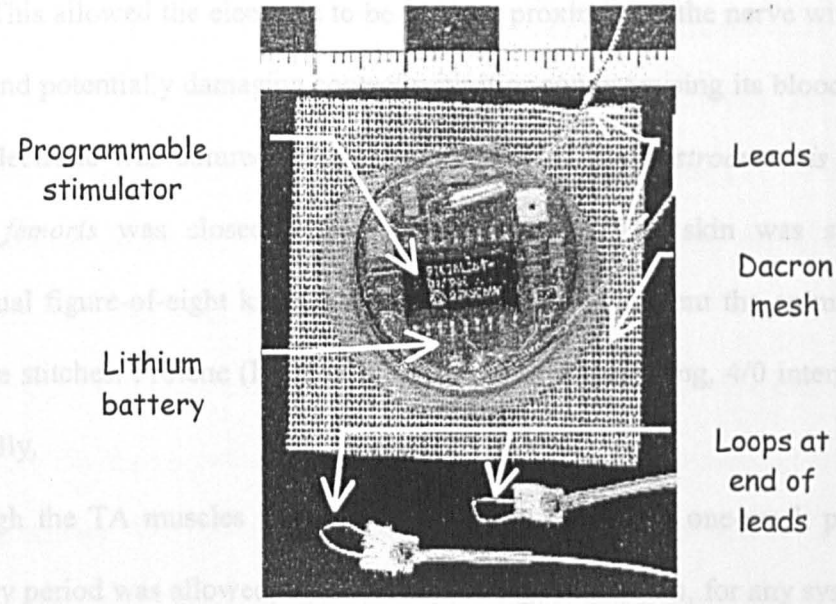

Fig.2.1. Photograph of the programmable stimulator employed for low frequency stimulation of rabbit TA muscles. The programmable stimulator was soldered to a lithium battery (3.2 V) and encapsulated in silicone rubber. A dacron mesh, was attached to the silicone, from which the leads, knotted at the ends to form loops, were extended.

2.4 Implantation of the stimulators into the rabbit model

The flank and limb of the rabbit were shaved and washed with 70% alcohol. All subsequent surgical procedures were carried out under strict aseptic conditions. An incision was made in the flank and the stimulators were implanted intra-peritoneally to the left and right (double implantation) or only to the left (single implantation) side of the experimental or control animals respectively.

Stimulator leads were guided sub-cutaneously through an endotracheal tube, from the flank to a lateral incision in the hind limb. The common peroneal nerve and underlying muscles were exposed with a lateral incision through the *biceps femoris* muscle. The first electrode was passed under the nerve using a 19-gauge needle and sutured in

place. This allowed the electrode to be in close proximity to the nerve without making direct and potentially damaging contact with it or compromising its blood supply. The other electrode was sutured on the lateral head of the *gastrocnemius* muscle. The *biceps femoris* was closed with a running suture. The skin was sutured using individual figure-of-eight knots, which were buried to prevent the animal interfering with the stitches. Prolene (Ethicon Ltd.) was used for suturing, 4/0 internally and 3/0 externally.

Although the TA muscles were not disturbed surgically, a one-week post-operative recovery period was allowed, before commencing stimulation, for any systemic effects of anaesthesia or surgery to subside.

2.5 Low frequency stimulation regime in the rabbit model

Rabbit TA, a muscle composed of predominantly fast fibre types, was stimulated via the common peroneal nerve. Miniature programmable stimulators were implanted into the left and right hand side of experimental rabbits and it was possible to switch each of the stimulators on and off independently. This double implantation design decreased the number of animals' used and thus the potential for inter-animal variation. A different stimulation protocol was applied to each limb. The stimulation start times were staggered with respect to each other so that the experiments would finish at the same time. This allowed mechanical recordings to be taken for both the stimulated right and left TA muscles at the same time.

The stimulation regime was as follows (Figure 3.1): The left and right TA were pre-stimulated for periods within a range previously shown to exert a cytoprotective effect

(**Jones *et al.*, 1997**). The right TA was continuously pre-stimulated at 2.5 Hz for 7 days, 10 days or 14 days (a non-damaging pattern of stimulation). The left TA was continuously pre-stimulated at 2.5 Hz for either 7 days, 10 days or 14 days followed by continuous stimulation at 10 Hz for 9 days (a potentially damaging pattern of stimulation) (**Lexell *et al.*, 1992**).

Following 7-14 days of pre-stimulation the left TA muscles were challenged with a potentially damaging pattern to assess the resistance of the muscles to stimulation-induced damage. The pre-stimulated muscles of the right limb were not challenged (10 Hz) to determine the state of the muscles prior to the challenging pattern.

A control group was incorporated in which the left (positive) control TA was continuously stimulated at 10 Hz for 9 days and the right (negative) control TA received no stimulation. The left TA provided a measure of the normal susceptibility of the muscle to the potentially damaging challenge when there was no pre-stimulation. The right TA demonstrated that any damage recorded could not be attributed to neuromuscular disease or infection.

2.6 Terminal procedures involving stimulation in the rabbit model

2.6.1 Anaesthesia

Rabbits were anaesthetised by an intravenous injection of urethane (Sigma, 250g L^{-1}; 500 mg kg^{-1}) and pentobarbitone sodium (Sagatal™, May and Baker Ltd., Essex, UK; initial dose approximately 30 mg kg^{-1}, given to effect). Supplementary doses of pentobarbitone were given during the procedure to maintain deep anaesthesia. An oximeter was used to monitor the oxygen saturation of the blood throughout the

terminal procedure. The trachea was routinely cannulated and the animals were placed on a respirator. The implanted stimulator was switched off at this point and the stimulated muscles were quiescent for approximately 2-3 hr before the physiological measurements were performed.

2.6.2 Muscle preparations

The following procedures were performed on left and right limbs. A flap electrode (**Barnard *et al.*, 1986**), was sutured around the common peroneal nerve (Figure 2.2). In stimulated limbs this was placed central to the electrodes used for chronic stimulation. The nerve was then cut distally to the flap electrodes and the muscle was sutured and skin incisions closed with Michel clips. The skin covering the anterior compartment of the hind limb was cut to expose the TA. Fascia and connective tissue were dissected away to reveal the TA muscle with no disruption of its vascular supply. The TA tendon above and below the transverse (crural) ligament was dissected free. Muscle length measurements were taken from the tibial crest to the furthest extent of the muscle fibres with the ankle at full extension, full flexion and at 90° to the tibia. After these measurements the tendon was cut below the extensor retinaculum, freed and secured in a miniature titanium clamp (**Jarvis & Salmons, 1991**). The TA was partially freed from the underlying EDL muscle, without disturbing the blood supply to either muscle. The animal was placed supine on an ergometer table; limbs were clamped at the lower end of the femur at the knee and on the malleoli of the tibia at the ankle with no interference to their femoral blood supply. The tendon clamp was connected via a lightweight, non-compliant carbon fibre-epoxy link to a Dual Mode

Servo System (Cambridge Technology, Inc., MA., USA; Model 310B), designed to generate and measure controlled forces up to 50 N and lengthening up to 20 mm on either side of the neutral position. Servomotors were positioned so that the TA was at full extension over the most accurate part of the displacement range of the servomotor (-10 to +10). An IBM compatible PC running programs written in-house in Borland Turbo C++ provided synchronized control of the servomotor, muscle stimulation and data acquisition. Supramaximal impulses (20 volts, 0.05 ms duration) were delivered to the muscles via isolated stimulators (Isolated Stimulator Mk. IV, Devices, Herts, UK), and controlled by pulses from the PC (Figure 2.3). Loss of body heat from the rabbit was prevented by polystrene and cotton wool insulation. Muscle temperature was kept at 37°C using tungsten lamps; applying liquid paraffin prevented drying out of the exposed muscles.

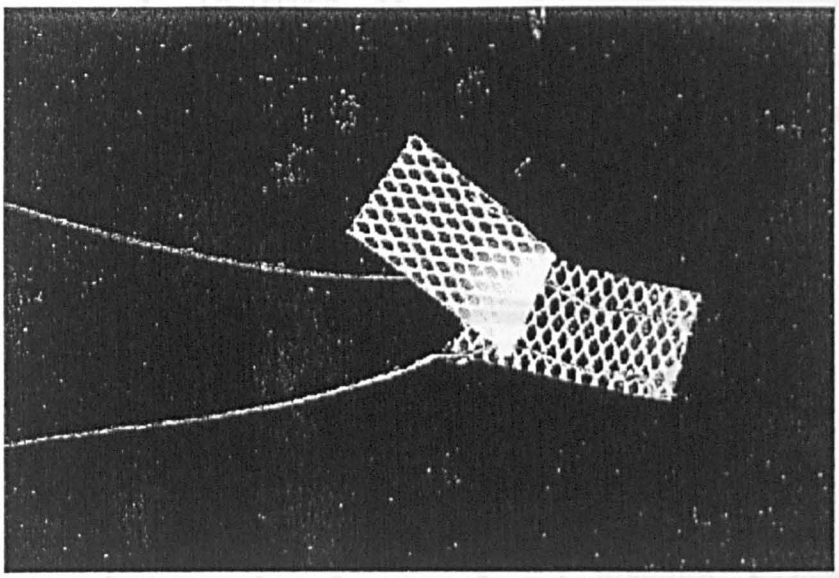

Fig.2.2. Photograph of a flap electrode, which was employed in the acute physiological measurements of rabbit TA. The lower silicone flap with bared wires was fed under the common peroneal nerve, which was dissected away from the *gastrocnemius*. The upper flap was placed over the nerve and the whole electrode was sutured to the *gastrocnemius*.

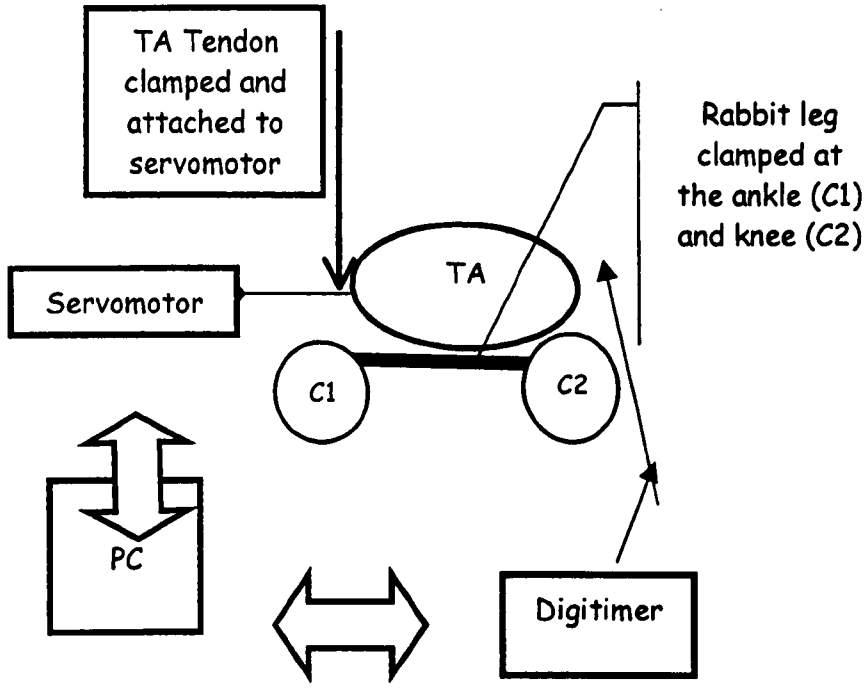

Fig.2.3. Schematic diagram of the experimental set-up for the physiological measurements of the rabbit TA muscle, only one leg has been included in this illustration however all measurements were performed on the right and left TA. The rabbit was placed on its back on the table. The flap electrode was sutured to the common peroneal nerve. The ankle and knee were clamped and the TA tendon was attached to a titanium clamp, which was attached to the servomotor via a carbon fibre epoxy link. The PC controlled the servomotor and the isolated stimulators.

2.7 Physiological measurements in the rabbit model

2.7.1 Force-length

Optimum loading conditions were determined using force-length and force-frequency measurements to ensure that accurate physiological records were made. The TA was stimulated isometrically at successively longer lengths on the servomotor ranging from full flexion to full extension. Optimum length (L_o) was chosen as the length at which the developed force was highest (or 95% of the highest value), with the resting

tension remaining low. This length was generally 2mm lower than L_o and generated 95% of maximum tetanic tension (P_o). The shorter length was chosen to minimise the release of stored elastic energy and prevent misleading recording during shortening contractions at longer lengths. Force-length data was analyzed using Easyplot and the amplitude (twitch force, P_t), contraction time (C_t) and half-relaxation time (R_t) were calculated. The muscle was placed at L_o for all subsequent measurements.

2.7.2 Force-frequency

The muscle was stimulated with a single impulse and then with 400ms bursts at frequencies up to 200 Hz. Resting and developed tensions were again measured and using Easyplot the maximum tetanic tension (P_o) was determined.

2.7.3 Cross-sectional area (CSA)

To measure specific force (force produced per CSA) the CSA area was calculated by dividing the mass by the L_o. This was derived from the following equations: Density = mass / volume. In the literature the density of muscle has been given as 1.072 and 1.0564 **(Gollnick *et al.*, 1981; Roy *et al.*, 1982)**. The density has been approximated to 1 g cm^{-3} where 1 = mass / volume, but volume is equal to CSA x L_o, therefore CSA = mass / L_o. This equation assumes that CSA is constant along the length of muscle and that the fibres run parallel from one end of the TA to the other. This is a reasonable approximation for the TA thus this equation should only be used to compare TA muscles with each other.

2.7.4 Force-velocity

The force-velocity relationship represents the relationship between the load on a muscle and the speed at which it contracts against that load. Software controlled the application of a series of increasing loads, the stimulation of the muscle and the measurement of the corresponding velocity. The muscle was placed at L_o and P_o was the maximum load applied. Stimulation was applied to the muscle at a frequency of 200 Hz for a duration of 400 ms. The force-velocity curve was calculated using Easyplot and the values for the maximum velocity of shortening (V_{max}) was obtained.

2.7.5 Fatigue test

The fatigue resistance of a muscle is assessed by its ability to sustain a certain level of work over a specific time period. The Burke fatigue test was employed **(Burke *et al.*, 1973)**.

The muscle was placed at L_o, and subjected to isometric stimulation at 40 Hz for 330 ms every sec for 5 min. The developed force was recorded using CODAS.

2.7.6 Termination of the rabbit and removal of tissues

Following the completion of physiological measurements the rabbits were killed by delivering an overdose of pentobarbitone intravenously. The left and right TA muscles were immediately excised. For morphometric assessment of damage, fibre types and capillary density transverse blocks were cut from the widest part of the muscles, orientated and mounted on cork discs with Cryo-M-Bed (Bright, Cambs, UK). All blocks were frozen in isopentane, pre-cooled above liquid nitrogen. The remaining muscle was placed in aluminium foil, and frozen rapidly in liquid nitrogen. All muscles were stored at -77° pending further experimentation and analysis.

2.7 Low frequency stimulation of *extensor digitorium longus* (EDL), TA and *extensor hallicus longus* (EHL) muscles in a rat model

My research into the effect of passive proximal EDL tendon lengthening on forces exerted at the proximal and distal tendons of rat EDL muscle, and at the distal tendon of TA and EHL muscles employed male Wistar rats with body weights in the range of 0.3 Kg. Rat biceps muscles of the left hind limb namely EDL, TA and EHL were employed for this series of experiments. These muscles were chosen as the connective tissue that covers the biceps muscles envelops the anterior compartment accommodating a very long insertion along the tibia making it a suitable model for the study of myofascial force transmission.

All surgical and experimental procedures were carried out in agreement with the animal welfare regulations as described by Dutch law and were approved by an Animal Experimentation Committee at the Vrije Universiteit, Amsterdam.

2.9 Anesthesia in the rat model

Animals were anaesthetised with an intra-peritoneal injection of diluted urethane (1.2 ml (12.5% urethane solution) / 100g body mass). Supplementary injections of urethane (0.5 ml (12.5% urethane solution)) were administered (maximally 3 times) to maintain deep anaesthesia. The animals were placed on a heater water pad (37°C) during surgery and experimentation.

2.10 Surgical procedures in the rat model

The skin was removed from the upper and lower area of the left hind limb. Fascia and a section of the *biceps femoris* muscle were removed to expose the anterior compartment. The preparatory removal of the *biceps femoris* was the only disturbance of the proximal segment of the anterior compartment. Thus intra- and extra-muscular connective tissue design and relationships were maintained.

The distal portion of the anterior compartment was also opened to expose the distal tendons of the EDL, EHL and TA muscles. The knee joint was placed at 90° and the angle between the foot and the tibia was set at 90° ('reference position'). The four distal tendons of the EDL were tied together and the distal EHL and TA tendons were tied together. Tying the muscle tendons together acted to mechanically couple the tendons. Matching markers were placed on the distal tendons of EDL and TA-EHL, as well as on a fixed position on the lower leg. These markers would allow the distal muscle tendon complexes to be set at known lengths in the experimental set up. The distal EDL and TA-EHL tendon complexes were then cut as distally as possible and removed from their retinaculae near the ankle joint. Freeing the distal tendon groups allowed the respective muscles to be placed at specified lengths during the experiment. Each distal tendon group was tied (polyester thread) to looped Kevlar threads (4% elongation at a break load of 800N). The looped Kelvar threads were used to link the muscle tendon complexes to their respective force transducers. The foot was attached firmly to a plastic foot-plate using iron thread (Sorbo) to facilitate mounting the muscles in the experimental set-up.

The femoral compartments were also opened to allow access to the proximal tendon of the EDL, the sciatic nerve and the femur.

The proximal EDL tendon was freed and attached to looped Kevlar thread (4% elongation at a break load of 800N). Freeing the proximal EDL tendon complex allowed it to be passively lengthened as required during the experiment. The sciatic nerve was dissected and cut proximally. The sural, tibia and articular branches of the sciatic nerve were severed. This allowed for the exclusive stimulation of the full motor segment of the common peroneal nerve. A clamp was attached to the femur to aid fixation of the animal during physiological readings.

Dehydration of the exposed tendon groups was prevented by applying silicone grease (art.no.7746LAB, Merck) carefully along the tendons prior to mounting the animal in the experimental set-up.

2.11 Mounting the rat in the experimental apparatus

After mounting the rat in the experimental apparatus, the femur was secured by means of a metal clamp. The plate with the foot attached was manipulated such that the ankle was in extreme plantar flexion to allow space for the passage of the distal tendon groups and their attached Kevlar threads. Following this manipulation the plate was firmly attached to the experimental apparatus.

The distal EDL and TA-EHL tendons were brought to lengths corresponding to their reference positions. All Kevlar threads were connected to force transducers (Hottinger Baldwin, maximal output error <0.1%, compliance 0.0048 mm/N). The tendon groups were correctly aligned with respect to each other and, the distal end of the severed

sciatic nerve was placed on a bipolar cuff electrode with stainless steel electrodes (Figure 2.4 & 2.5).

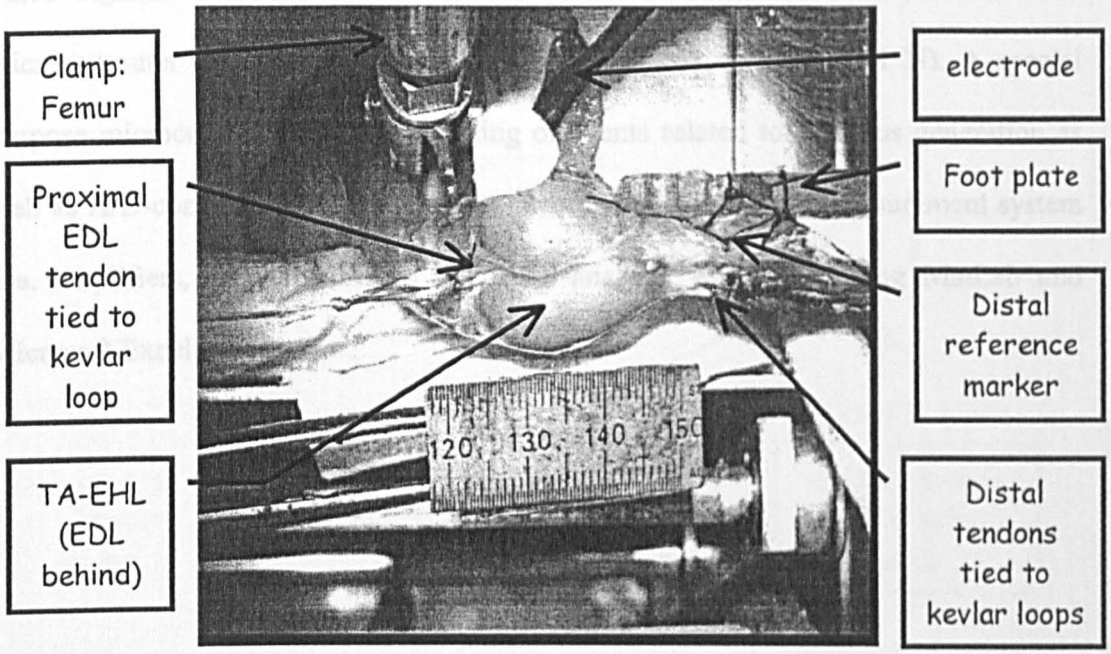

Fig.2.4. Photograph of the rat biceps muscles mounted in the experimental apparatus. Only the TA is visible as the EDL is located behind the TA.

During experimentation, ambient room temperature was kept at 22° ± 0.5°C and air humidity was kept at 80 ± 2% by a computer-controlled air conditioning system (Holland Heating) creating a down flow of air onto the experimental table. The surface of the anterior compartment was protected with a layer of paraffin viscous (art. no. 7160.00, Merck).

2.12 Low frequency stimulation of rat EDL and TA-EHL muscles

TA, EHL and EDL muscles (all innervated via the deep peroneal nerve), were excited simultaneously and maximally. This was done by stimulating the, distal end of the severed, sciatic nerve supra-maximally, using a pair of silver electrodes connected to a

constant current source (3mA, square pulse width 100 microsecond, pulse train 1000ms, 30 Hz).

Force signals were acquired using a 12-bit A/D converter and recorded on a microcomputer (sample frequency 1000 Hz, resolution of force 0.01 N). A special purpose microcomputer controlled timing of events related to stimulus generation as well as A/D-conversion. The output was recorded with the same measurement system (i.e. amplifiers, A/D converters). All data analysis was done using MatLab and Microsoft Excel.

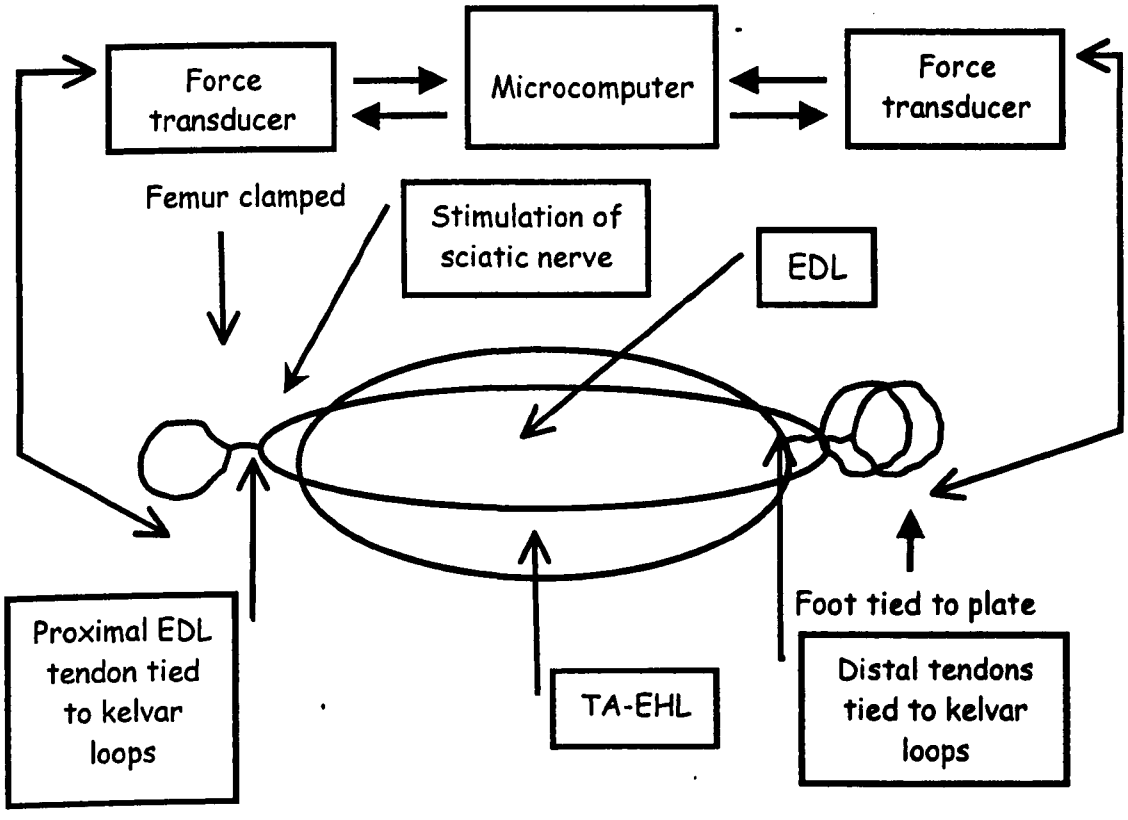

Fig.2.5. Schematic diagram of the experimental set-up for the physiological measurements of the rat biceps muscles. The rat was lying on its back on the table. The femur was clamped and the foot, with the ankle manipulated to extreme plantar flexion, was firmly positioned in the experimental apparatus using the foot plate. The distal tendons of TA-EHL and EDL were placed at there respective 'reference lengths' and attached, via kevlar loops, to force transducers. The proximal EDL tendon was attached, via kevlar loop, to its force transducer. The tendon groups were aligned to each other and a bipolar cuff electrode was placed on the distal end of the severed sciatic nerve.

2.13 Physiological measurements in the rat model

2.13.1 Force-length measurements before stimulation

Prior to the onset of the stimulation regime force-length measurements, where only the proximal EDL tendon was lengthened, were recorded at the proximal and distal tendons of the EDL and at the distal tendon of the TA-EHL muscle complex. Moving the proximal force transducer (1mm increments) lengthened the proximal EDL tendon. The distal EDL tendon was kept at reference position and the distal TA-EHL tendon complex was kept at a relatively low length. The position of the distal tendons of the EDL and the TA-EHL complex were kept constant during the entirety of the experiment. Isometric tetanic EDL and TA-EHL forces were measured for 10 proximal EDL tendon lengths where the starting length corresponded to several mm over slack length (i.e. the lowest muscle length at which active muscle force approaches zero).

2.13.2 Force length measurements after stimulation

The rat biceps muscles (TA, EDL and EHL) were subjected to 3 hr of continuous stimulation at 30 Hz under isometric conditions with the proximal EDL tendon length at L_o, the distal EDL tendon at reference length and the distal TA-EHL tendon at a relatively low length.

Upon completion of this regime a second set of force-length data was collected. Force-length measurements were recorded as previously described (2.13.1 force-length measurements before stimulation).

2.13.3 Force length measurements after a 10 min recovery period

Upon completion of the aforementioned stimulation regime the muscles were allowed to rest (i.e. no stimulation) for 10 min. After this rest period a third set of force-length measurements were recorded as previously described (2.13.1 force length measurements before stimulation).

2.13.3 Termination of the rat and removal of muscles

Upon completion of the experiment a double-sided pneumothorax was performed followed by the immediate administration of an overdose of pentobarbital. For morphometric assessments of damage transverse blocks were cut from the widest part of the muscles, orientated and mounted on cork discs with Cryo-M-Bed (Bright, Cambs, UK). All blocks were frozen in isopentane, pre-cooled above liquid nitrogen. All muscles were stored at -77° pending analysis.

2.14 Histochemistry

Histochemical analysis used rabbit and rat muscle blocks mounted on cork. Serial transverse sections of 10 μm thickness were cut on a cryostat (Bright Instrument Company Ltd) with a chamber temperature of -23°C and a specimen temperature of –19°C. Sections were picked up onto subbed glass slides (Appendix 1), air dried for 5-10 min and stored at -70°C.

2.15 Haematoxylin and eosin stain for damage in rabbit and rat muscles

General morphology was assessed using the regressive haematoxylin and eosin stain (Appendix 2). This technique involved overloading the sections with haematoxylin (10 min incubation) and eosin (5 min incubation) stain. The over stained sections were washed in running tap water to progressively remove excess stain and dehydrated through graded alcohols. Sections were then cleared in xylene and mounted in histomount (Gibco). Haematoxylin stains the cells sarcolemmal nuclei blue-black. Whilst the eosin stains the cells cytoplasm and connective tissue fibres a vibrant and pale pink respectively **(Lexell *et al.*, 1992)**.

2.15.1 Quantification of damage

Point-count morphometry was used to quantify the percentage damage **(Lexell *et al.*, 1992)**. Transverse sections (10 μm) were stained with haematoxylin and eosin as described above. A grid composed of 1 mm squares was photographed onto clear, colourless film and placed over the coverslip of the sections. The top-left most square which covered part of the section was located on a X25 magnification of a Leitz Diaplan microscope. An eyepiece graticule (10 x 10 lines) was fitted within the area of the 1 mm squares. The section and the graticule were brought into focus and 121 intersections were seen. The number of intersections falling on damaged, non-damaged and endomysial tissue were recorded. Intersections at the upper and left-hand borders were included and whilst those at the lower and right hand borders were excluded, giving a total of 100 intersections. This counting procedure was repeated for every fourth 1 mm square, between 8 and 10 squares were quantified. The histological

parameters used to define damage included: invasion of fibres by mononuclear cells; the presence of small rounded fibres with internal nuclei, hypercontracted fibres and vacuolated fibres; general cytoplasmic disruption within the fibres; abnormal swelling of the fibres. The total number of damaged and endomysial fibres within the graticule grid were pooled and the percentage volume of damaged and endomysial tissue was calculated.

2.16 Tunell and Hart stain for fibre types in rabbit muscle

This methodology is a modification of Guth & Samaha (1970) which uses myofibrillar activity to demonstrate the presence of three fibre types, 2A, 2D and 1 in muscle sections **(Tunell & Hart, 1977)**. The major modification is a pre-incubation in an alkali solution for 50 min (Appendix 3).

The Tunell and Hart stain exploits qualitative differences in the myosin ATPase enzyme in type 1 and 2 fibres. In type 2D and 2B fibres the myofibrillar ATPase is acid labile and base stable, in type 2A fibres the ATPase enzyme exhibits intermediate stability in both acid and alkali solutions while in type 1 fibres the myofibrillar ATPase is acid stable and base labile.

The Tunell and Hart stain uses the difference in stability of the myosin ATPase, in fast and slow fibre types, to pre-incubation in an alkali solution (formaldehyde and glycine), to differentiate between fast and slow fibre types **(Tunell & Hart, 1977)**. A limitation of this staining technique is that it can not differentiate between fast type 2B and 2D fibre types as their respective ATPase enzymes are base stable and exhibit high ATPase activities.

Pre-incubation in an alkali solution (glycine, formaldehyde and calcium chloride) inactivates the myofibrillar ATPase in type 1 fibres while glycine and formaldehyde work synergistically to distinguish between fibre types 2A and 2D.

Incubation in a solution of ATP and Ca^{+} at pH 9.4 induces the ATPase in type 2 fibres to split releasing inorganic phosphate, which precipitates as Ca^{2+} phosphate. At an alkaline pH the Ca^{2+} phosphate is insoluble and is deposited at the sites of ATPase activity.

Incubation in cobalt chloride solution results in the Ca^{2+} being replaced by the cobalt forming cobalt phosphate. The phosphate is replaced by sulphide upon immersion in an ammonium sulphide solution. The areas of ATPase activity in the muscle section can be distinguished by the deposition of a brownish-black precipitate of cobalt sulphide at these sites.

Type 2D fibres are stained dark (high ATPase activity), type 2A fibres are stained intermediate (intermediate ATPase activity) and type 1 fibres pale (low ATPase activity).

2.16.1 Quantification of fibre type composition

Point count morphometry was used to qualify the percentage fibre type and the area they occupied for each experimental group (**Lexell *et al.*, 1991**). The number of cross sections falling on each fibre type, identified by the Tunell and Hart stain, and on extra-cellular space, were counted using the same 1-mm-square grids as described previously (2.15.1 quantification of damage). The total number of fibres was also

counted within each square. The number of each fibre type from all the counted squares was pooled and the proportions of each fibre type were calculated.

2.17 Tunell and Hart stain for capillary density in rabbit muscle

This method is a modification of the Tunell and Hart stain (1977). This protocol employs the ATPase reaction with an acid pre-incubation, to visualise capillaries within the skeletal muscle **(Sillau & Banchero, 1977)**. This stain differentiates between the myosin and endothelial ATPase by pre-incubation in an acidic solution (Appendix 4). The transverse muscle sections are processed using the Ca^{2+} method with ATP as substrate. The sections were pre-incubated in an acid medium for between 5-10 min, which demonstrated acid ATPase activity. Immersion in ATPase incubating solution formed Ca^{2+} phosphate, which was made visible by cobalt chloride and ammonium sulfide. This produced an insoluble dark cobalt sulfide deposit on the capillaries, around the perimeter of the fibres only, and made them visible.

2.17.1 Quantification of capillary density

Point count morphometry was used to quantify the total number of capillaries in the experimental tissues.

The number of cross sections falling on each capillary, identified by the Tunell and Hart stain with an acid pre-incubation, and on extra-cellular space was counted using the same 1-mm-square grids as described previously (2.15.1 quantification of damage). The total numbers of fibres were also counted within each square. The total

number of capillaries from all the counted squares were pooled and the capillary density was calculated.

2.18 Enzyme analysis of myeloperoxidase (MPO) in rabbit muscle: MPO assay

Muscle tissue was analyzed to determine the MPO activity. This heme-containing enzyme is found in the secretory granules of neutrophils and monocytes and catalyzes the production of hypochlorous acid (HOCl), a powerful oxidant which is derived from Cl^- ion and H_2O_2. **(Bradley *et al.*, 1982 & Bozeman *et al.*, 1990).**

The MPO assay involved disrupting, extracting and rendering the MPO granules soluble in an aqueous solution (Appendix 5). This colormetric assay is based on the catalysis of H_2O_2, which can be recorded by measuring the optical density at 405 nm over 30 min at 15^0C. Frozen muscle homogenate were diluted in a stabilizing aqueous solution across a 96-well Immulon II microtitre plate. Each muscle sample was assayed in duplicate, together with a set of four standards (purified human MPO (Sigma)), a set of negative controls and a set of background samples (contained the assay solution alone). Plates were read using a microplate reader (Molecular Devices, UK). Enzyme activities were expressed as units of activity per gram of muscle **(Tang *et al.*, 1998).**

2.19 Myosin analysis in rabbit muscle

2.19.1 Extraction and purification of myosin from whole muscle samples

The myosin was extracted and purified from a pulverised muscle sample by suspension in a high ionic strength extraction buffer followed by precipitation in a low

ionic strength extraction buffer (Appendix 10). Actin was dissociated from the myosin by the addition of $MgCl_2$ and ATP. Both muscle proteins were then precipitated in solutions of increasing ammonium sulphate concentration and the pellets re-suspended in high ionic strength buffer. Following dialysis overnight at 4°C, SDS was added to some samples (0.5% (w/v) for myosin light chain (MLC) analysis.

2.19 SDS polyacrylamide gel electrophoresis (SDS-PAGE) of MLC

SDS–PAGE was used to examine the MLC isoforms of the purified myosin samples. Separation of the MLC was achieved using a Biorad Protean II vertical slab unit and the methodology previously described by Laemilli 1970 with modifications as described by Brown *et al.*, 1983 The separating gel contained 15% acrylamide and 0.125% bisacrylamide. The stacking gel contained 5% acrylamide and 0.13% bisacrylamide. The samples buffer contained a final concentration of 1% SDS. Electrophoretic separation occurred at 35 mA per gel until the bromophenol tracking dye reached the bottom of the gel (Appendix 11).

2.20 Staining of gels

Gels were stained with Coomassie Blue R250, and incubated in de-stain (Appendix 13) over-night on a Rotatest R-100 shaker (Luckham Ltd.). Gels were incubated for 2 hr in Coomassie Blue staining solution and immersed in three changes of de-stain to give good intensity of staining of the bands.

2.21 Photomicrography

Photomicrography employed a Leitz Diaplan microscope and a Leitz Orthomat photomicrographic system. The precise magnification of each section was determined using a stage graticule.

2.22 Statistics

Statistical analysis was done using either Instat (work done in England) and SigmaStat (work done in Holland). Multiple comparisons between respective experimental groups were made using one-way analysis of variance (ANOVA). When significant effects were found ($P<0.05$) differences between group means were analyzed using Tukey-Kramer post hoc comparison tests.

Relationships between selected variables were made using the Pearson correlation test. All results are expressed as mean ± SEM.

Cyto-protection of rabbit TA muscles against stimulation-induced damage

3.1 Introduction

Stimulation-induced transformation, from a fast to slow phenotype, involves many changes in the properties of muscle fibres including the ultra-structure, mitochondrial volume, capillary density, Ca^{2+} transport kinetics, metabolism, and myosin isoform content **(Salmons & Vrbová, 1969)**. There is an increasing body of indirect evidence which suggests that different fibre types do not respond uniformly to stimulation but that transformation may occur sequentially within specific fibre-types in the following sequence 1 2A 2D. Fast-twitch muscles exhibit rapid stimulation-induced force depressions which are only partially alleviated after substantial stimulation periods **(Cadefau *et al.*, 1993; Mayne *et al.*, 1991; Green *et al.*, 1992; Green *et al.*, 1997)**. By means of explanation it has been hypothesised that with the onset of stimulation specific fibre types, most likely to be the fast-twitch glycolytic (2B), experience transient depolarisation blocks, due to insufficient N^+-K^+-ATPase activity **(Hicks *et al.*, 1997)**.

Stimulation protocols employed to increase the fatigue resistance of fast-twitch muscles (transformation from a fast to slow phenotype) may induce muscle damage. However, damage is not an inevitable consequence of stimulation or a pre-requisite for transformation to occur **(Lexell *et al.*, 1994b; Jarvis *et al.*, 1996; Mayne *et al.*, 1996; Lexell *et al.*, 1993)**.

The are two schools of thought on the primary initiation factor in the damage process namely mechanical initiation, i.e. sarcomere popping, or metabolic initiation, i.e. loss of energy supply, and/or loss of intracellular Ca^{2+} homeostasis, and/or over activity of oxidising free radicals. Which mechanical and/or metabolic parameter initiates muscle damage has not been elucidated (**Bär *et al.*, 1994; Mc Ardle & Jackson, 1994**).

Intuitive proposals that exercise-, ischemic-reperfusion- and stimulation-induced damage may be minimised or ameliorated by conditioning a muscle with a moderate yet progressive 'training' regime prior to a more intensive protocol have been verified. Pre-training a muscle with a moderate exercise regime protects against exercise-induced damage upon resumption of a more strenuous exercise protocol, this is known as the 'repeated bout effect' (**Nosaka & Clarkson, 1995; Clarkson & Tremblay, 1988; Mc Hugh *et al.*, 1999**). Pre-conditioning a muscle with short ischemic-reperfusion episodes protects against ischemic-reperfusion-induced damage with more prolonged ischemic-reperfusion regimes (**Papanastasiou *et al.*, 1999**). It has been demonstrated that stimulation-induced damage can be minimised by subjecting fast-twitch muscle to pre-stimulation, with a non-damaging pattern, prior to stimulation with a potentially-damaging pattern (**Jones *et al.*, 1997**).

Jones *et al* employed a two-stage stimulation protocol in which rabbit fast-twitch, muscles were pre-stimulated with a non-damaging pattern of 2.5 Hz continuously for 2, 7 and 14 days followed by stimulation with a potentially damaging pattern of stimulation, 10 Hz continuously for 9 days (Figure 3.1A). Protection was afforded to

muscles after 7 days of pre-stimulation, with longer periods of pre-stimulation exerting greater protective effects in terms of a lower volume of damaged fibres at the end of the experiment (**Jones *et al.*, 1997**).

3.2 Methods

In this study rabbit TA muscles were pre-stimulated at 2.5 Hz (a non-damaging pattern of stimulation) for 7, 10 or 14 days, either alone or followed by stimulation at 10 Hz (a potentially damaging pattern) for 9 days, (Figure 3.1B). In contrast to the initial research conducted by Jones *et al.*, 1997 this work provided pre-stimulated muscles (right hind-limb) that were not challenged with stimulation at 10 Hz and pre-stimulated muscles that were challenged with the potentially damaging pattern of 10 Hz (left hind-limb). This allowed for the analysis of pre-stimulated muscles prior to the 10 Hz challenging pattern, and for assessment of the resistance of the pre-stimulated muscles to stimulation-induced damage. The left control TA provided a measure of the 'normal' susceptibility of the muscle to the 10 Hz challenge with no pre-stimulation. While the right control TA, no stimulation, demonstrated the state of the muscle under 'normal' physiological conditions i.e. that there were no inherent pathological problems that could interfere with the reliability of the experiments.

Muscles were excised and transverse (10μm) sections were stained with haematoxylin and eosin (H&E) for morphological assessment of damage (**Jones *et al.*, 1997; Lexell *et al.*, 1992; Lexell *et al.*, 1993**). Stimulation-induced muscle damage was also measured using a myeloperoxidase (MPO) assay, (**Tang *et al.*, 1998**). MPO is a heme-containing enzyme found in the primary granules of neutrophils and monocytes.

Release of this granular enzyme has been used to indicate neutrophil activation and thus was included in this study to provide an additional measure of muscle damage i.e. neutrophil infiltration as part of the inflammatory response to damage **(Lehrer & Ganz, 1990; Pyne, 1994)**.

Increased capillarization occurs early in the transformation process **(Skorjanc *et al.*, 1998)**. To ascertain whether changes in capillary densities occurred during the pre-stimulation regimes transverse (10μm) muscle sections were subjected to a modified Tunell and Hart (acid pre-incubation) staining procedure **(Sillau & Banchero, 1977; Tunell & Hart, 1977)**.

It has been proposed that specific fibre types may respond sequentially to the increased functional demand imposed on them during low frequency stimulation **(Hicks *et al.*, 1997; Skorjanc *et al.*, 1998; Neufer *et al.*, 1996; Ornatsky *et al.*, 1995)**. Therefore, it is conceivable that stimulation-induced damage and/or protection may also proceed in a fibre specific manner. The fibre type composition, demonstrated using the Tunell and Hart technique, of pre-stimulated alone and pre-stimulated plus challenged (10 Hz) muscle sections were used in conjunction with the H&E data to determine whether stimulation-induced damage exhibited fibre-type-specificity **(Tunell & Hart, 1977)**.

One way analysis of variance (ANOVA) and subsequently Tukey-Kramer multiple comparison post tests (when ANOVA found significant differences) were employed to identify significant changes between the pre-stimulation alone, pre-stimulation followed by the 10 Hz challenge and control groups.

There were three main aims in this part of my study. The first objective was to determine the amount of damage incurred by muscles pre-stimulated alone and muscles pre-stimulated and challenged with the 10 Hz regime. Thus establishing the state of the pre-stimulated muscles before and after the challenge (10 Hz) and gaining further insights into the stimulation-induced protective effect. The second objective was to ascertain whether stimulation-induced protection may, or may not, be attributed, to changes in capillarization. The final objective was to identify whether susceptibility to stimulation-induced damage exhibited fibre type specificity.

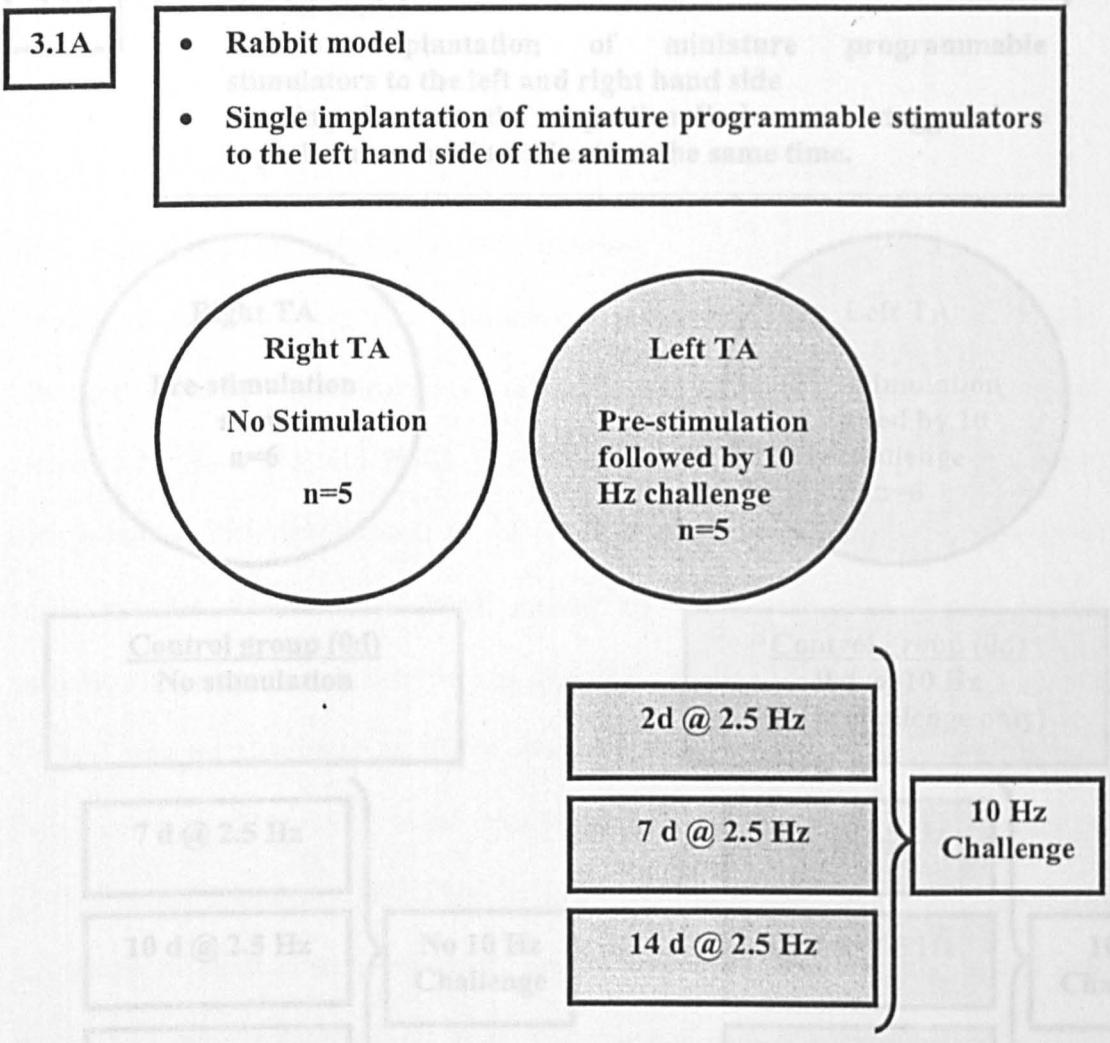

Fig.3.1A Schematic representation of the stimulation protocol used in the Jones *et al.*, 1997 study. The left TA received pre-stimulation at 2.5 Hz for 2, 7 and 14 days followed by the 10 Hz challenge. The right TA received no stimulation i.e. fast control.

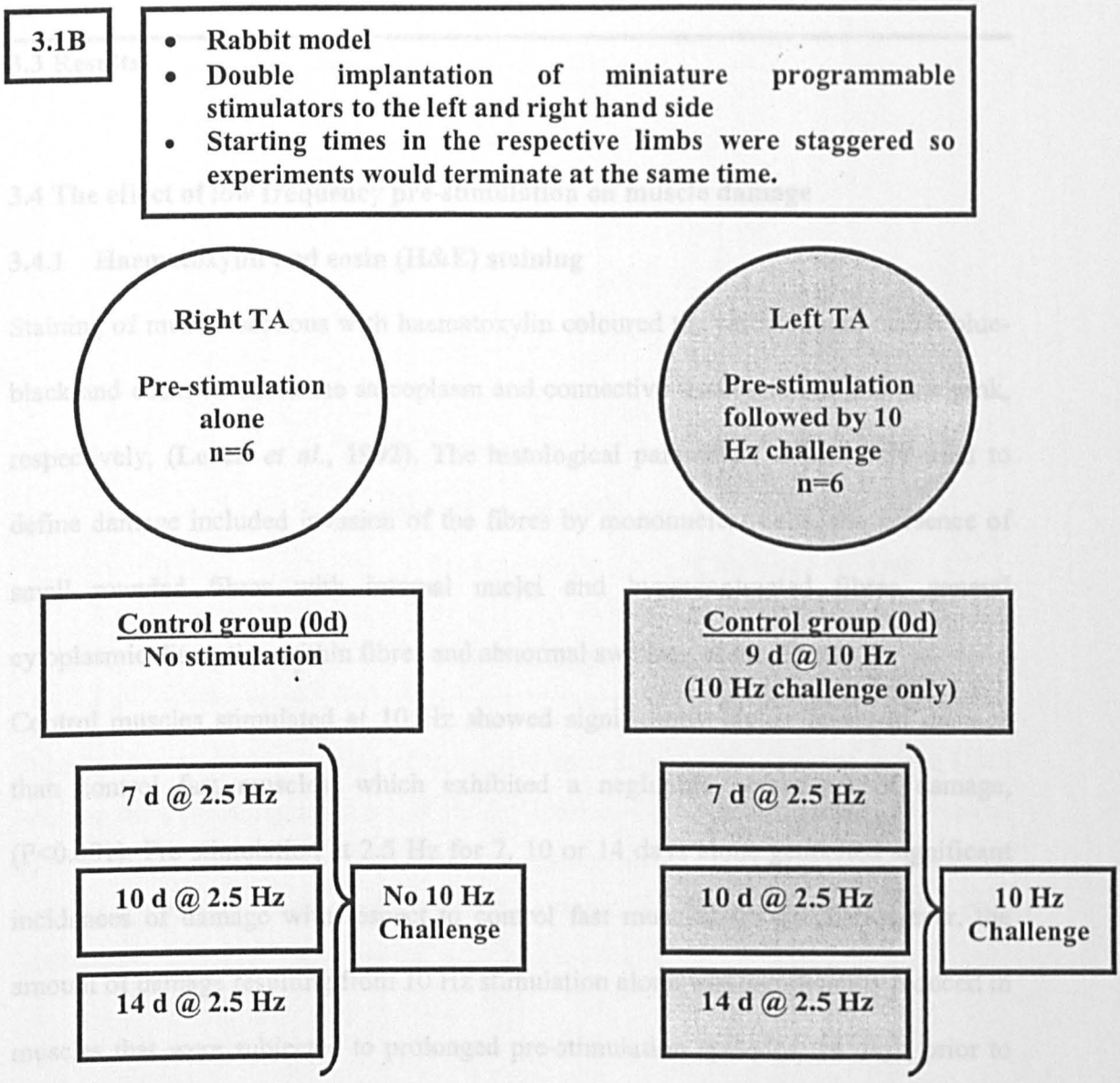

Fig. 3.1B Schematic illustration of the stimulation regimes used in this study. The right TA received pre-stimulation at 2.5 Hz for 7, 10 and 14 days alone while the left TA received pre-stimulation for the aforementioned times followed by the 10 Hz challenge. Control groups included right control TA muscles that received no stimulation and left control TA muscles that were subjected to the 10 Hz challenge (9 days at 10 Hz) alone.

3.4 The effect of low frequency pre-stimulation on muscle damage

3.4.1 Haematoxylin and eosin (H&E) staining

Staining of muscle sections with haematoxylin coloured the sarcolemmal nuclei blue-black and eosin coloured the sarcoplasm and connective tissue vibrant and pale pink, respectively, (**Lexell *et al.*, 1992**). The histological parameters which were used to define damage included invasion of the fibres by mononuclear cells, the presence of small rounded fibres with internal nuclei and hypercontracted fibres, general cytoplasmic disruption within fibres and abnormal swelling of the fibres.

Control muscles stimulated at 10 Hz showed significantly higher levels of damage than control fast muscles, which exhibited a negligible percentage of damage, ($P<0.001$). Pre-stimulation at 2.5 Hz for 7, 10 or 14 days alone generated significant incidences of damage with respect to control fast muscles ($P<0.05$). However, the amount of damage resulting from 10 Hz stimulation alone was significantly reduced in muscles that were subjected to prolonged pre-stimulation episodes, 14 days, prior to the 10 Hz challenge ($P<0.05$). The extent of damage recorded within or between the pre-stimulated alone or pre-stimulated followed by 10 Hz stimulation muscle groups did not significantly differ from one another, (Figure 3.2 & 3.3).

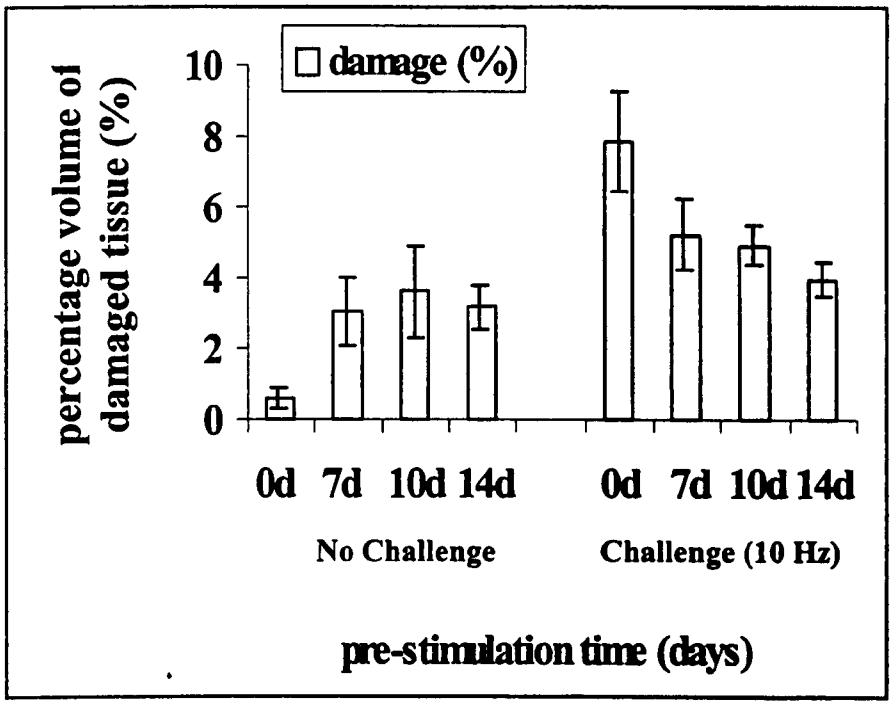

Fig.3.2. The volume percentage of damaged tissue in rabbit TA, assessed using H&E staining, after pre-stimulation at 2.5 Hz for 7, 10 or 14 days either alone or followed by stimulation at 10 Hz for 9 days. Control groups include non-stimulated TA (fast) muscles (0d-no challenge) and muscles stimulated at 10 Hz for 9 days only (0d-challenge 10 Hz), (mean data points, error bars ± SEM, n=6).

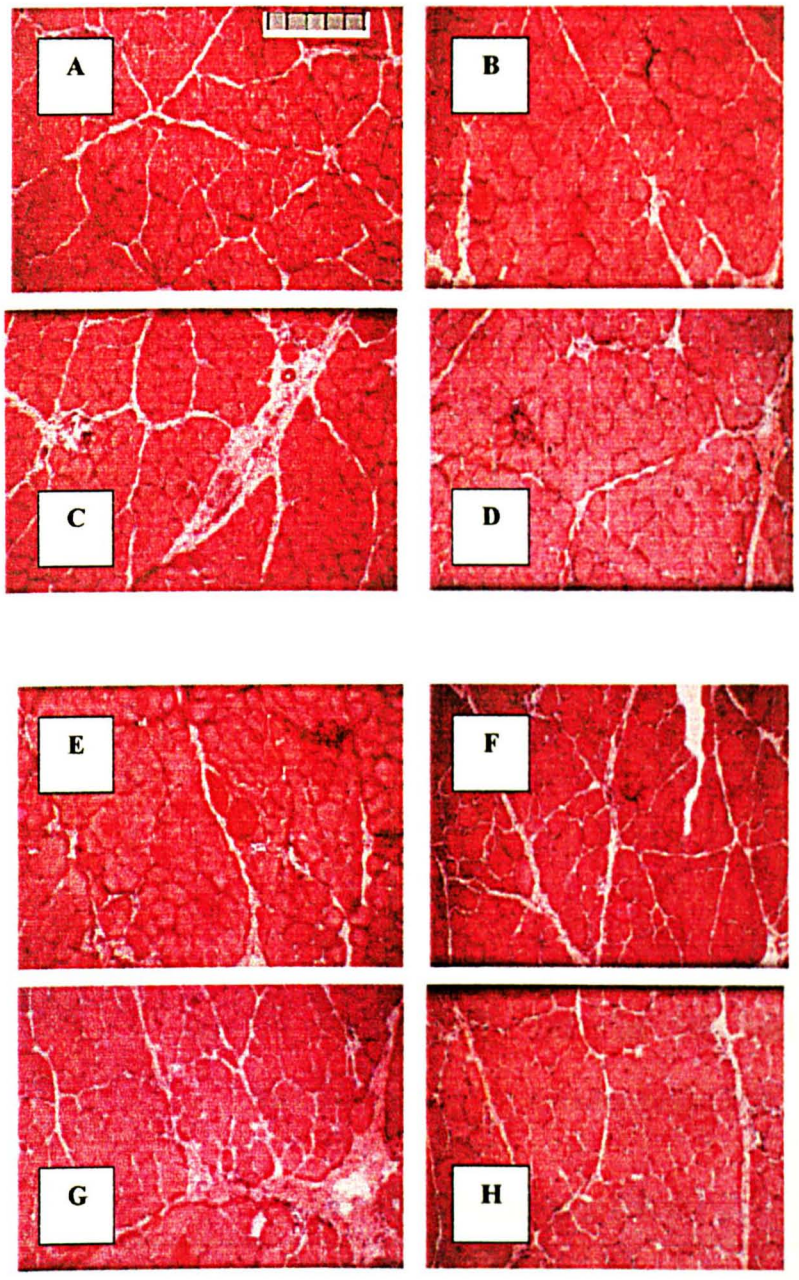

Fig.3.3 Photomicrographs of transverse rabbit TA sections (10μm) stained with H&E for damage after either pre-stimulation at 2.5 Hz for 7-14 days alone or followed by the 10 Hz pattern. A, represents control fast TA muscle; B, C and D, represents TA that has been pre-stimulated (2.5 Hz) for 7, 10 and 14 days respectively, with no 10 Hz challenge; E, represents TA that has been stimulated at 10 Hz for 9 days; F, G and H, represent TA that has been pre-stimulated at 2.5 Hz for 7, 10 and 14 days respectively followed by the 10 Hz challenge (bar = 50 μm).

Muscles that were subjected to the 10 Hz challenge alone showed significant increases in endomysial tissue with respect to control fast muscles ($P<0.05$). Comparisons with control fast muscles showed that only pre-stimulation for 10 days followed by the 10 Hz challenge showed significant increases in endomysium ($P<0.05$). The percentage volume of endomysial tissue in muscles that received pre-stimulation followed by 10 Hz stimulation appeared to increase but did not attain significance with respect to muscles that were subjected to pre-stimulation alone (Figure 3.4 & 3.3).

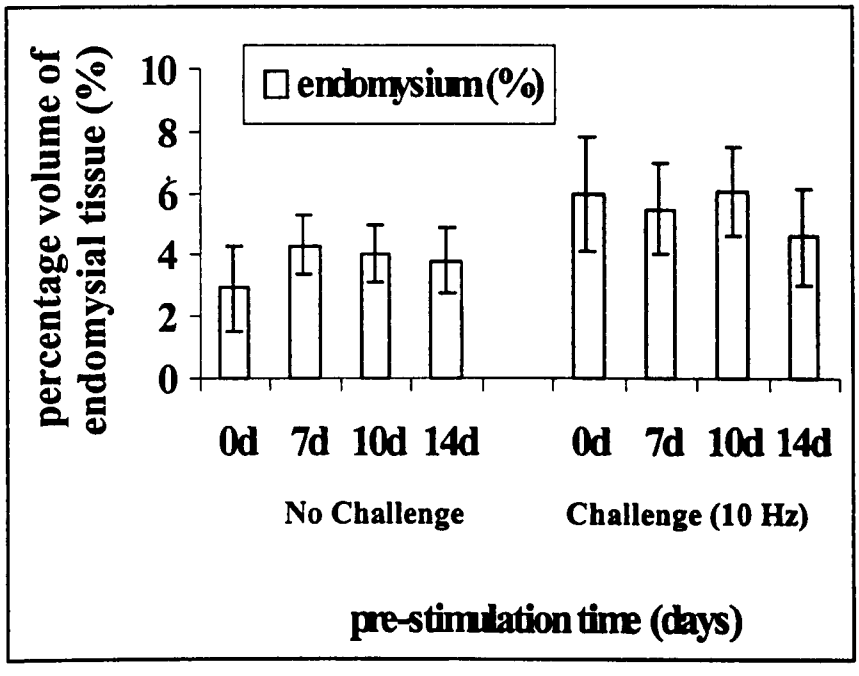

Fig.3.4. The volume percentage of endomysial tissue in rabbit TA, determined using H&E staining, after pre-stimulation at 2.5 Hz for 7, 10 or 14 days either alone or followed by stimulation at 10 Hz for 9 days. Control groups include non-stimulated TA (fast) muscles (0d-no challenge) and muscles stimulated at 10 Hz for 9 days only (0d-challenge 10 Hz), (mean data points, error bars ± SEM, n=6).

3.4.2 Myeloperoxidase (MPO) activity

The damaging pattern of 10 Hz stimulation showed an increase in MPO activity, which did not appear to reach significance with respect to control fast muscles. Low frequency pre-stimulation at 2.5 Hz for 14 days showed significantly elevated MPO values compared with control fast ($P<0.01$) and control 10 Hz stimulation ($P<0.05$) MPO activities. Prolonged periods of pre-stimulation for between 10 and 14 days followed by the 10 Hz stimulation showed significantly higher MPO values with respect to stimulation at 10 Hz for 9 days alone ($P<0.01$) and control fast muscles ($P< 0.001$), (Figure 3.5).

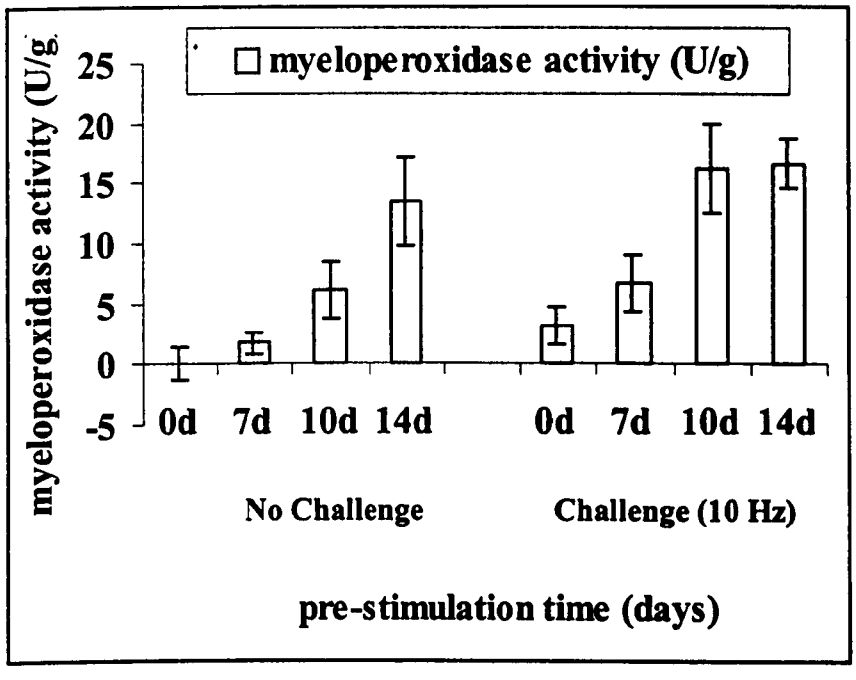

Fig.3.5. Changes in myeloperoxidase (MPO) activity in rabbit TA after pre-stimulation at 2.5 Hz for 7, 10 or 14 days alone or followed by stimulation at 10 Hz for 9 days. Control groups include non-stimulated TA (fast) muscles (0d-no challenge) and muscles stimulated at 10 Hz for 9 days only (0d-challenge 10 Hz), (mean data points, error bars ± SEM, n=4).

The MPO activities recorded for the pre-stimulated alone and pre-stimulated followed by the 10 Hz challenge muscles was an unexpected finding and demonstrates that MPO activity does not correlate with the appearance of morphological abnormality.

3.5 The effect of low frequency pre-stimulation on capillarization

Histochemical staining of muscle sections with a modified version of the Tunell and Hart stain (acid pre-incubation) coloured the capillaries black-brown with no staining of fibres, **(Tunell & Hart, 1977).**

Muscles that received pre-stimulation, 7 to 14 days, alone or followed by the 10 Hz stimulation pattern did not show substantial changes in their respective capillary densities when compared to control fast or control 10 Hz challenged muscles. No discernible differences in capillarization were found between pre-stimulation alone or followed by the 10 Hz challenge groups, (Figure 3.6 & 3.7).

3.6 Fibre specificity of stimulation-induced damage

Staining of muscle sections for the demonstration of myofibrillar ATPase, using the Tunell & Hart methodology, stained type 2D fibres dark black-brown, type 2A fibres intermediate black-grey and type 1 fibres pale grey-white, **(Tunell & Hart, 1977).**

Control muscles stimulated at 10 Hz showed negligible differences in their type 1 fibre composition to the non-stimulated fast controls. Pre-stimulation for 7-14 days demonstrated marginal increases in type 1 fibres, which did not reach significance with respect to fast control type 1 populations. Pre-stimulation for 7-14 days followed by 10 Hz stimulation showed significant increases in the proportion of type 1 fibres

with respect to control fast ($P<0.05$) and control 10 Hz stimulation ($P<0.01$) muscle groups. (Table 3.2 & Figure 3.8). No linear correlation was found between the increasing type 1 fibre populations with stimulation duration and the incidence of histological damage.

Pre-stimulation for between 7 and 14 days alone and followed by the 10 Hz challenge and 10 Hz stimulation alone did not show any substantive change from the fast type 2A and 2D, fibre type composition identified for the control fast TA muscle, (Table 3.2 & Figure 3.8).

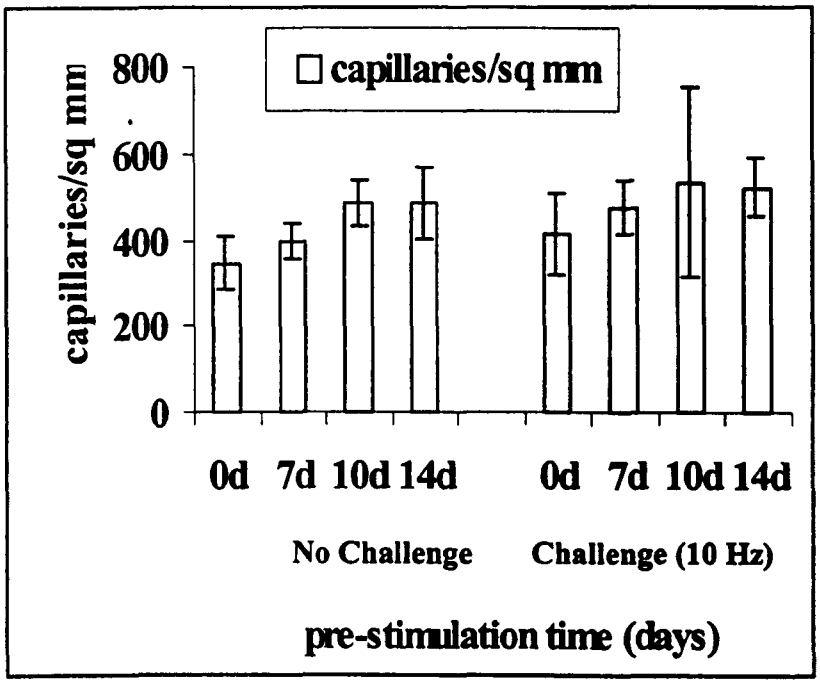

Fig.3.6. Changes in the capillary density of rabbit TA, determined using the Tunell and Hart stain with an acid pre-incubation, after either pre-stimulation at 2.5 Hz alone for 7, 10 or 14 days or followed by the 10 Hz challenging regime. Control groups include non-stimulated TA (fast) muscles (0d-no challenge) and muscles stimulated at 10 Hz for 9 days only (0d-challenge 10 Hz), (mean data points, error bars ± SEM, n=6).

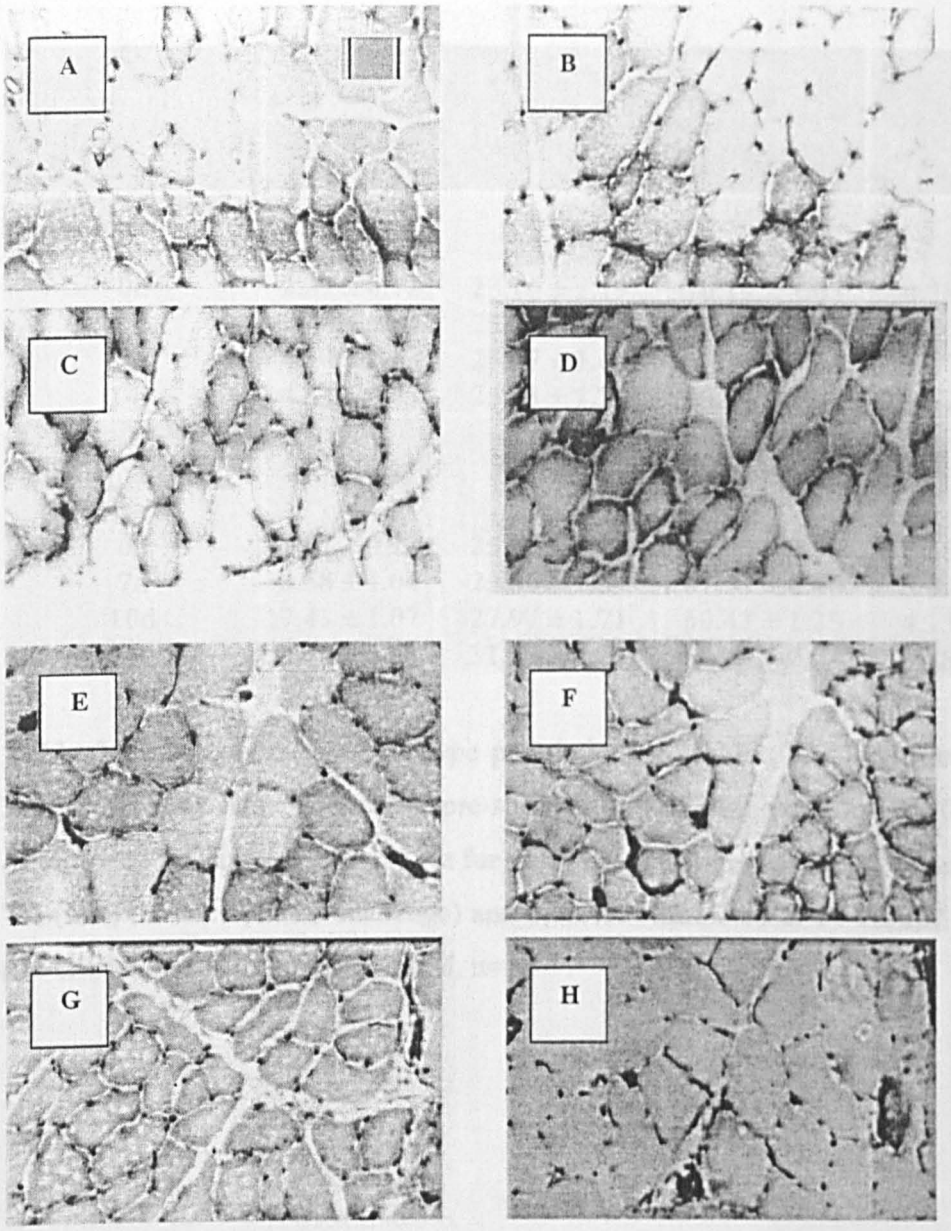

Fig.3.7 Photomicrographs of transverse rabbit TA sections (10μm) treated with the Tunell and Hart stain for capillary density after either pre-stimulation at 2.5 Hz for 7-14 days alone or followed by the 10 Hz pattern. A, represents control fast TA muscle; B, C and D, represents TA that has been pre-stimulated (2.5 Hz) for 7, 10 and 14 days respectively, with no 10 Hz challenge; E, represents TA that has been stimulated at 10 Hz for 9 days; F, G and H, represent TA that has been pre-stimulated at 2.5 Hz for 7, 10 and 14 days respectively followed by the 10 Hz challenge (bar = 8.4 μm).

Pre-stimulation time (days)	Type 1 fibres (%)	Type 2A fibres (%)	Type 2D fibres (%)	Extra-cellular space (%)
No Challenge				
0d	2.27 ± 0.72	23.16 ± 2.19	70.19 ± 1.63	4.28 ± 0.95
7d	3.84 ± 0.84	25.62 ± 1.85	67.49 ± 2.27	3.06 ± 0.71
10d	4.80 ± 1.13	25.67 ± 1.68	65.87 ± 2.24	3.67 ± 0.36
14d	4.33 ± 0.48	25.53 ± 1.25	65.57 ± 1.61	4.57 ± 0.55
Challenge 10 Hz				
0d	2.01 ± 0.23	25.27 ± 1.23	65.04 ± 0.58	7.68 ± 1.11
7d	6.58 ± 1.04	25.80 ± 1.34	61.53 ± 0.46	6.09 ± 1.00
10d	7.47 ± 1.07	27.97 ± 1.71	60.43 ± 1.25	4.13 ± 0.51
14d	6.77 ± 0.61	31.58 ± 1.27	58.27 ± 2.04	3.38 ± 0.93

Table 3.1 Changes in the fibre type population of rabbit TA, identified using the Tunell and Hart stain, after either pre-stimulation (2.5 Hz) alone for 7, 10 or 14 days or followed by stimulation at 10 Hz for 9 days. Control groups include non-stimulated TA (fast) muscles (0d-no challenge) and muscles stimulated at 10 Hz for 9 days only (0d-challenge 10 Hz), (mean ± SEM, n=6).

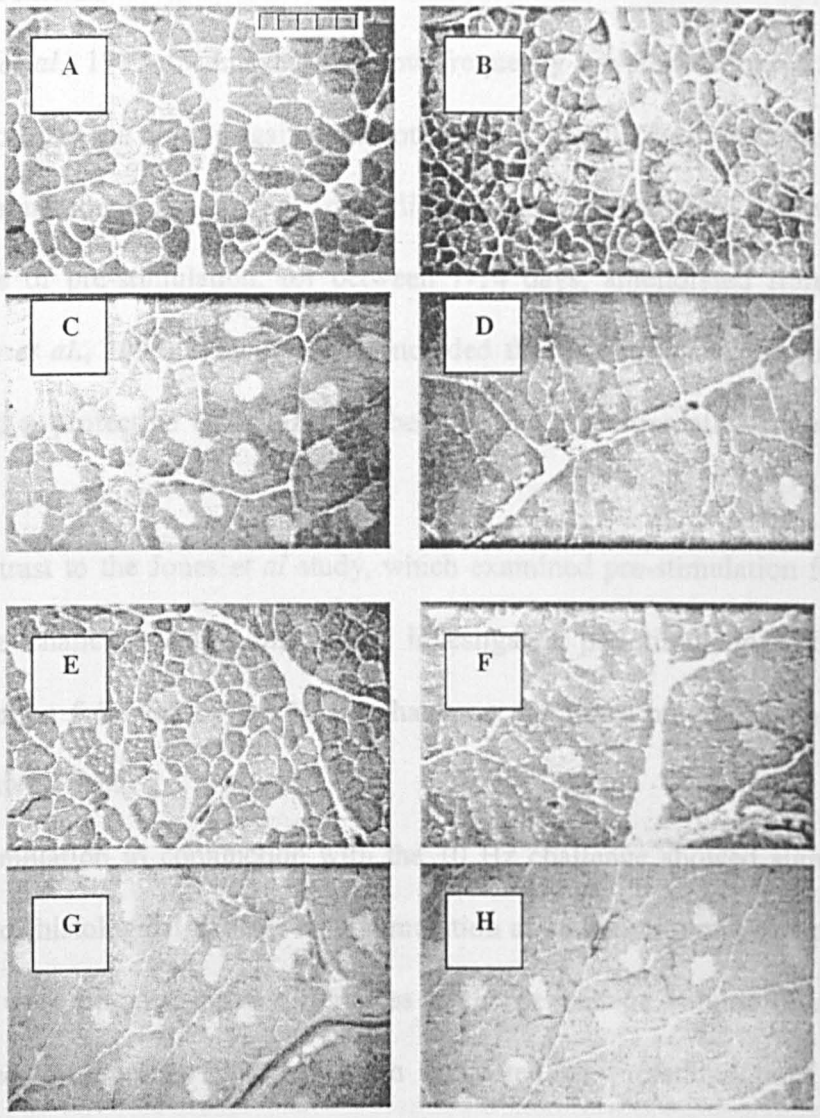

Fig.3.8 Photomicrographs of transverse rabbit TA sections (10μm) treated with the Tunell and Hart stain for fibre types after either pre-stimulation at 2.5 Hz for 7-14 days alone or followed by the 10 Hz pattern. A, represents control fast TA muscle; B, C and D, represents TA that has been pre-stimulated (2.5 Hz) for 7, 10 and 14 days respectively, with no 10 Hz challenge; E, represents TA that has been stimulated at 10 Hz for 9 days; F, G and H, represent TA that has been pre-stimulated at 2.5 Hz for 7, 10 and 14 days respectively followed by the 10 Hz challenge (bar = 50 μm).

3.7 Discussion

Jones *et al.*, 1997 documented that low frequency pre-stimulation (2.5 Hz) of rabbit TA protected the muscle against the potential for stimulation (10 Hz)-induced damage. Pre-stimulation at 2.5 Hz for 2 days did not exert a protective effect while increased periods of pre-stimulation, for between 7-14 days, ameliorated fibre degeneration, **(Jones *et al.*, 1997)**. Thus it was concluded that pre-stimulation at low frequencies exerted a protective effect against the potential for stimulation-induced damage at higher frequencies.

In contrast to the Jones *et al* study, which examined pre-stimulation followed by the 10 Hz challenge only, this study investigated pre-stimulation alone, and pre-stimulation followed by the 10 Hz challenge, for times previously shown to exert a protective effect.

Pre-stimulation in conjunction with the 10 Hz challenge showed significantly lower levels of histological damage than stimulation at 10 Hz with no prior pre-stimulation. There were no substantive differences in the percentage volume of damaged tissue incurred by muscles that had been subjected to pre-stimulation alone or pre-stimulation followed by the 10 Hz challenge. This suggests that decreased damage, with pre-stimulation prior to 10 Hz stimulation, may be due to protective effects exerted by the low frequency conditioning pattern.

Pre-stimulation (2.5 Hz) for 7, 10 or 14 days resulted in 3, 3.6 and 3.2%, respectively, of the TA tissue volume experiencing damage. The fact that low frequency stimulation at 2.5 Hz resulted in significant fibre degeneration was unexpected however Jarvis *et al.*, 1996 reported that continuous stimulation at 2.5 Hz for 14 days resulted in a

significant percentage of rabbit TA fibres exhibiting histological abnormalities **(Jarvis *et al.*, 1996)**.

Pre-stimulation for the maximum time period, 14 days, followed by the 10 Hz challenge did not show the complete amelioration of histological damage previously recorded by Jones *et al.*, 1997. This may reflect inter-animal differences and the subjective nature of the morphometric analysis of H&E staining. It has been documented that the incidences of stimulation-induced damage may vary considerably from one study to the next even when identical stimulation regimes and animal models have been employed **(Jones *et al.*, 1997; Jarvis *et al.*, 1996; Lexell *et al.*, 1992, Lexell *et al.*, 1993)**.

Stimulation-induced damage may result in an inflammatory response which may increase the number of circulating neutrophils, which upon activation may release MPO from their primary granules into the damaged muscle **(Lehrer & Ganz, 1990; Pyne, 1994; Smith & Weidemann 1990; Dufaux *et al.*, 1989; Gray *et al.*, 1993)**. In this study MPO activities increased with stimulation time and did not, as would be expected, decrease with decreasing volumes of histological damage, as determined with H&E staining. In an attempt to verify the MPO data, MPO assays were performed using the experimental TA muscles from the initial Jones *et al* study. Preliminary results mirrored the MPO data recorded for the pre-stimulated muscles in this study, where MPO activities for pre-stimulated muscles increased with increasing stimulation times. After 2 days of pre-stimulation followed by 10 Hz stimulation Jones *et al* reported large volumes of fibre degeneration, comparable to damage levels

reported after simulation at 10 Hz for 9 days (**Lexell *et al.*, 1992; Jones *et al.*, 1997**)). However, preliminary assays showed that the MPO activities at 2 days were low and comparable to enzyme activities recorded for non-stimulated control TA muscles. MPO activities were greatest at 14 days when Jones *et al* reported that maximal protection was afforded to the muscle.

MPO has been routinely used as a marker for neutrophil content. However, it must be borne in mind that the extraction of neutrophils from skeletal muscle and the subsequent solubilisation of MPO from their primary granules may underestimate both the number of neutrophils reaching the tissue to contribute their MPO and the MPO concentration (**Bradley *et al.*, 1982**). Furthermore it has been reported that increases in MPO concentration do not correlate with changes in neutrophil count thus suggesting that neutrophil degranulation may be independent of neutrophil mobilisation (**Bury & Pirany, 1995**). Smith & Weidemann proposed that exercise may have an intensity dependent effect on neutrophil function. They hypothesised that moderate exercise regimes may potentiate while intensive exercise protocols may attenuate neutrophil function i.e. degranulation (**Smith & Weidemann, 1990**).

While MPO assays may accurately quantitate MPO activity (**Tang *et al.*, 1998**), they do not provide any information on the state of the neutrophils i.e. whether these cells, upon migration to the muscle have been activated or not. This suggests that immunological assays should be co-operatively employed with the MPO assay to accurately quantitate the neutrophil and/or MPO content of muscle samples (**Edwards *et al.*, 1987**).

The activity of MPO was shown to increase with increasing stimulation times irrespective of the intensity of the stimulation patter employed or the damage status of the pre-stimulated muscles. It is conceivable that neutrophil infiltration in response to stimulation-induced damage may culminate in time dependent, as opposed to intensity or damage-dependent, degranulation of a proportion of the invading neutrophils.

While the objective nature of the MPO assay made it an attractive candidate for quantifying muscle damage in this study, these results demonstrate that employing an MPO assay alone to assess muscle damage was not a good choice.

Mayne *et al.*, reported that low frequency stimulation at 2.5 Hz for 14 days showed hexokinase (HK) to be the only metabolic enzyme exhibiting an increase in activity thus increasing the potential for aerobic glycolysis. Succinate dehydrogenase (SDH) and citrate synthase (CS) showed no significant changes indicating that there had been no increase in the influx of substrates through the TCA cycle **(Mayne *et al.*, 1996)**. Analysis of the changes in capillarization after either 7, 10 or 14 days of pre-stimulation at 2.5 Hz showed no significant increases in their capillary density with respect to non-stimulated TA muscles. In contrast, 4 days of 10 Hz stimulation has been shown to result in a 20 % increase of capillary density reaching up to 50% after 14 days **(Cotter *et al.*, 1973; Brown *et al.*, 1976)**. In addition, SDH and CS showed increases in their activities after 14 days of stimulation at this higher frequency (10 Hz) **(Mayne *et al.*, 1996)**. Taken together this data would appear to be in agreement with the proposal by Skorjanc *et al* that increases in capillarization may precede mitochondrial, CS and SDH, induction **(korjanc *et al.*, 1998)**. However, this

hypothesis may only pertain to stimulation at higher frequencies, as lower frequencies do not appear to induce significant changes in either capillarization or SDH and CS activities after 14 days.

Capillary density results from this study suggest that the pre-stimulation protective effect may not be attributable to capillary development alone. Transformation from a fast-twitch glycolytic to an oxidative-glycolytic metabolism has been initiated at a time point when pre-stimulation (2.5 Hz) exerts a protective effect (**Mayne *et al.*, 1996; Jones *et al.*, 1997**). Whether stimulation-induced protection can be solely attributed to this adaptation is contentious. Further research into the metabolic state of muscles after a range of pre-stimulation times needs to be conducted.

It has been reported that after 14 days of stimulation at 2.5 Hz the type 2D fibre population decreased with a concomitant increase in the type 2A fibre population. In addition significant, albeit small increases in the type 1 fibre population were recorded (**Mayne *et al.*, 1996**). In direct contrast, this study showed that the proportions of type 2A and 2D fibres did not differ from control TA fast fibre populations after either pre-stimulation alone or pre-stimulation followed by the 10 Hz challenge. However, in agreement with the Mayne *et al* study small increases in type 1 fibre populations were recorded for pre-stimulated muscles alone, with respect to control TA muscles. Differences in the fibre populations between these two studies may be attributable to the fact that in the Mayne *et al* study the number of rabbit TA muscles employed were lower than those included in this work, n=2 verses n=6, respectively.

The control 10 Hz stimulated muscles demonstrated significant increases in the incidences of fibre degeneration with respect to control TA muscles and their type 1, 2A and 2D fibre populations showed no significant differences to one another. Pre-stimulation prior to the 10 Hz challenge incurred less incidences of histological damage and showed significant, albeit small, increases in the proportion of type 1 fibres with respect to the control 10 Hz challenge group. There was no correlation between specific fibre types and histological manifestations of damage for any of the experimental or control muscle groups. While this data is by far from conclusive the influence of fibre type on stimulation-induced damage and/or protection remains tentative.

Chapter 4

The mechanical profile of rabbit TA muscles subjected to low frequency pre-stimulation alone and followed by a 10 Hz challenge.

4.1 Introduction

Numerous studies have established that low frequency stimulation (10 Hz) of rabbit TA, fast twitch, muscles induces a rapid, within minutes, and persistent decrease in force (**Mayne *et al.*, 1991; Hicks *et al.*, 1997; Jarvis *et al.*, 1996**). Jarvis *et al.*, 1996 reported that stimulation at 2.5 Hz and 10 Hz initially induced similar force deficits but stable recovery of force was attained after 4 weeks of 2.5 Hz stimulation compared with progressive decreases in force at this time point for 10 Hz stimulation (**Jarvis *et al.*, 1996**). This suggests that a fast twitch muscle can accommodate the functional changes imposed on it by a moderate yet progressive stimulation regime (2.5 Hz for up to 12 weeks) more effectively than those incurred by a more intensive stimulation protocol (10 Hz for up to 12 weeks).

The metabolic changes accompanying stimulation-induced force deficits were found to occur in two phases. Phase one comprised of an early decrease, within minutes, in high energy phosphate metabolites and compounds involved in the purine nucleotide cycle. Phase two occurred within hours and involved full metabolic recovery albeit with continued force depressions. This has lead to the suggestion that metabolic exhaustion was not responsible for the persistence of the force deficit (**Hicks *et al.*, 1997; Mayne *et al.*, 1991**). Whether the phasic nature of the metabolic response to

low frequency stimulation may be instructive in the induction of force fatigue in fast twitch muscles has not been elucidated.

Low frequency stimulation may induce the loss of muscle mass. Stimulation-induced decreases in the mass of fast twitch muscles have been attributed to decreases in the cross-sectional area and not to decreases in the number of fibres **(Salmons & Vrbová 1969, Pette *et al.*, 1976, Eisenberg & Salmons 1981; Salmons & Henrikkson 1981)**. Hicks *et al.*, 1997 reported that the decreases in cross-sectional area (CSA) and mass, in fast twitch muscles, were progressive and increased with the duration of stimulation **(Hicks *et al.*, 1997)**. Thus stimulation-induced force depressions may be partially attributed to decreases in CSA and muscle mass however they cannot account for either the rapid decreases in force with the onset of stimulation or account for the totality of the force deficit after prolonged periods of stimulation.

Coincident with stimulation-induced force decreases are reductions in the mass action potentials of fast twitch muscle **(Mayne *et al.*, 1991; Hicks *et al.*, 1997)**. Hicks *et al.*, 1997 hypothesised that the stimulation-induced decrease in M wave amplitude for fast twitch skeletal muscle may be caused by a significant portion of the fibre population, most likely fast glycolytic fibres, being temporarily refractory to stimulation. They reported progressive increases in the Na^+-K^+-ATPase with stimulation (10 Hz) which showed a positive correlation with the increasing M wave amplitude. This supported their proposal that the refractoriness of muscle fibres may be related to insufficient Na^+-K^+-ATPase activity, particularly in the fast glycolytic fibres, relative to the increased functional demands imposed by stimulation. Insufficient Na^+-K^+ pumping

may cause the accumulation of K^+ in the extracellular space leading to depolarisation of the surface membrane and ultimately deactivation of the Na^+ channels and action potential failure **(Hicks *et al.*, 1997)**. Low frequency stimulation (2 Hz) of canine *latissimus dorsi*, fast twitch, muscle for between 6-8 weeks was found to decrease the amount of the dihydropyridine (DHPR) and ryanodine (RyR) receptor proteins, two components of E-C coupling. Upon activation the DHPR acts as a voltage sensor which regulates the release of Ca^{2+} ions via the SR RyR **(Hicks *et al.*, 1997; Ohlendieck *et al.*, 1991)**. Reduced expression of junctional SR 90 kDa and 94 kDa proteins which are located near the RyR junctional face membrane of SR suggests that these proteins may be involved in regulating E-C coupling or Ca^{2+} release. It has been established that skeletal and not cardiac isoforms of RyR and DHPR are detectable in fast and slow twitch fibres with the skeletal isoforms of RyR and DHPR present in lower amounts in the slow twitch fibres. Furthermore the junctional transverse tubules and feet occupy approximately 50% less volume in slow twitch fibres than in fast twitch fibres. The RyR and DHPR are associated with these structures and therefore a stimulation-induced decrease in the amount of RyR and DHPR may be expected **(Ohlendieck *et al.*, 1991)**. Whether changes in E-C coupling are instructive in the initiation of force fatigue has not been fully determined.

Stimulation-induced changes in the total amount and/or specific activity of the SR Ca^{2+} ATPase may be involved in force fatigue. It has been demonstrated that stimulation (10 Hz) of fast twitch muscles evoked significant increases in the contraction (C_t) and relaxation (R_t) times (56 and 158% of control fast twitch muscle

respectively) after 1 day. Longer periods of stimulation, 20 weeks, have been shown to increase the contractile speed to values that exceeded the contractile speed recorded for control soleus muscles **(Hicks *et al.*, 1997; Jarvis *et al.*, 1996; Salmons & Sréter, 1976).**

Increases in the C_t and R_t have been attributed to decreases in the total amount or specific activity of the SR Ca^{2+} ATPase activity. The SR Ca^{2+} ATPase acts to transport Ca^{2+} into the lumen of the SR and plays an essential role in the contraction-relaxation cycle, largely determining the relaxation rate, of a muscle. The time disparity between stimulation-induced increases in contractile speed (days) and induction of the slow SERCA2 Ca^{2+} ATPase isoform (weeks) suggests that the changes in contractile speed are not due to the changes in the expression of specific Ca^{2+} ATPase isoforms **(Simonides & van Hardeveld, 1990)**. It has been suggested that stimulation (10 Hz) of fast twitch muscle may induce alterations at the nucleotide binding site of the Ca^{2+} ATPase enzyme which may decrease the catalytic activity of this enzyme **(Leberer *et al.*, 1987; Dux *et al.*, 1990)**. Changes in Ca^{2+} ATPase activity may also be partly attributed to the fact that fast twitch fibres contain a larger volume of SR, 9% of cell volume, compared with slow twitch fibres, 4.5% of cell volume **(Warmington *et al.*, 1996)**. It has been reported that after 2 weeks of stimulation (10 Hz) the volumes of the terminal cisternae, the T tubules, the SR and the Z disc decrease to levels similar to those observed in control slow muscle **(Salmons *et al.*, 1978; Eisenberg & Salmons, 1981; Sréter *et al*, 1974; Heilmann & Pette, 1979).**

A reduction in the maximal activity and total amount of the Ca^{2+} ATPase may lead to a reduction in the amount of Ca^{2+} available for release by the SR, via the SR Ca^{2+} release

channels, upon activation, thus facilitating a rapid and persistent depression of maximal force. In addition efficient functioning of the Ca^{2+} release channels depends on optimal ionic and metabolic conditions. Disruption of the Ca^{2+} ATPase may disrupt the functioning of the Ca^{2+} release channels and exacerbate the force deficit **(Warmington *et al.*, 1996; Simonides & van Hardeveld, 1990)**. Whether changes in Ca^{2+} trafficking to and from the SR, are important initiators of or contributory factors to force fatigue and/or muscle damage has not been fully elucidated.

4.2 Methods

Rabbit TA muscles was pre-stimulated (2.5 Hz) for times within the range previously shown to exert a protective influence. The left TA was pre-stimulated at 2.5 Hz for 7, 10 or 14 days followed by stimulation at 10 Hz for 9 days and the right TA was pre-stimulated at 2.5 Hz for 7, 10 or 14 days alone (Figure 3.1). Prior to the removal of the stimulated muscles a number of physiological measurements were performed to establish the mechanical properties of the muscles. The force-length relationship was determined from successive twitch contractions at increasing muscle lengths. The muscle length (optimum length, L_o) at which maximal twitch tension developed was identified. This length was then reduced to 95% L_o as a 5% reduction in L_o was found to decrease resting tension without affecting the development of tetanic force **(Jarvis, 1993)**. All subsequent measurements were performed at this length. The C_t and R_t and the amplitude of the isometric twitch (P_t) were measured. The force-frequency curve was then determined by stimulating muscles with a series of pulses (400 msec) at frequencies up to 200 Hz. The maximum tetanic tension (P_o) was used as the highest

load in a series of isotonic contractions to establish the force-velocity relationship. The maximum velocity of shortening (V_{max}) was derived from the force-velocity curve. To ascertain the specific tetanic tension, the cross sectional area (CSA) was estimated from mass/L_o taking the density at 1000 Kg M^{-3}. Finally fatigue tests were performed, these involved measuring the tension developed after 5 min of acute tetanic stimulation, 40 Hz for 330ms every sec **(Burke *et al.*, 1973)**. At the end of the fatigue test, the rabbit was killed, overdose of pentobarbital, and the left and right TA muscles were removed and stored at -77°C.

Analysis of variance (ANOVA), followed by Tukey-Kramer multiple comparisons post tests when significant differences were found, were employed to identify significant changes between the pre-stimulation alone, pre-stimulation followed by the 10 Hz challenge and the control groups.

Previous research into the cytoprotective effect of low frequency pre-stimulation did not investigate whether or not pre-stimulation followed by the 10 Hz challenge evoked changes in the mechanical profile of fast twitch muscles **(Jones *et al.*, 1997)**. This section of my thesis had two main objectives. The primary aim was to identify which mechanical parameters, if any, showed significant alterations in muscles pre-stimulated at 2.5 Hz for 7, 10 or 14 days alone. The secondary aim was to determine whether pre-stimulation at 2.5 Hz for the aforementioned times followed by the 10 Hz challenge exhibited the same mechanical profile as the pre-stimulated alone muscles. In conjunction with the control groups these physiological measurements were used to

aid preliminary identification of any cellular changes, which may be involved, in pre-stimulation induced cytoprotection.

4.3 Results

4.4 The effect of low frequency pre-stimulation on force production

4.4.1 Maximum tetanic tension (P_o)

Muscles that were subjected to stimulation at the potentially damaging pattern of 10 Hz for 9 days exhibited significant decreases in P_o ($P<0.001$) when compared to control fast TA muscles. Pre-stimulation at 2.5 Hz evoked significant depression of the P_o after 7 days ($P<0.05$) with stabilisation of the force deficit after 10 and 14 days ($P<0.01$) with respect to control fast muscles. Muscles that received pre-stimulation for 7 and 10 days followed by the 10 Hz challenge exhibited significant decreases ($P<0.001$) in P_o while longer duration's of pre-stimulation, 14 days, showed less profound ($P<0.01$) P_o deficits, relative to control fast values. Pre-stimulation for the aforementioned times followed by stimulation at 10 Hz for 9 days did not induce substantive changes in the P_o when compared with P_o values for the control 10 Hz for 9 days muscles (Figure 4.1).

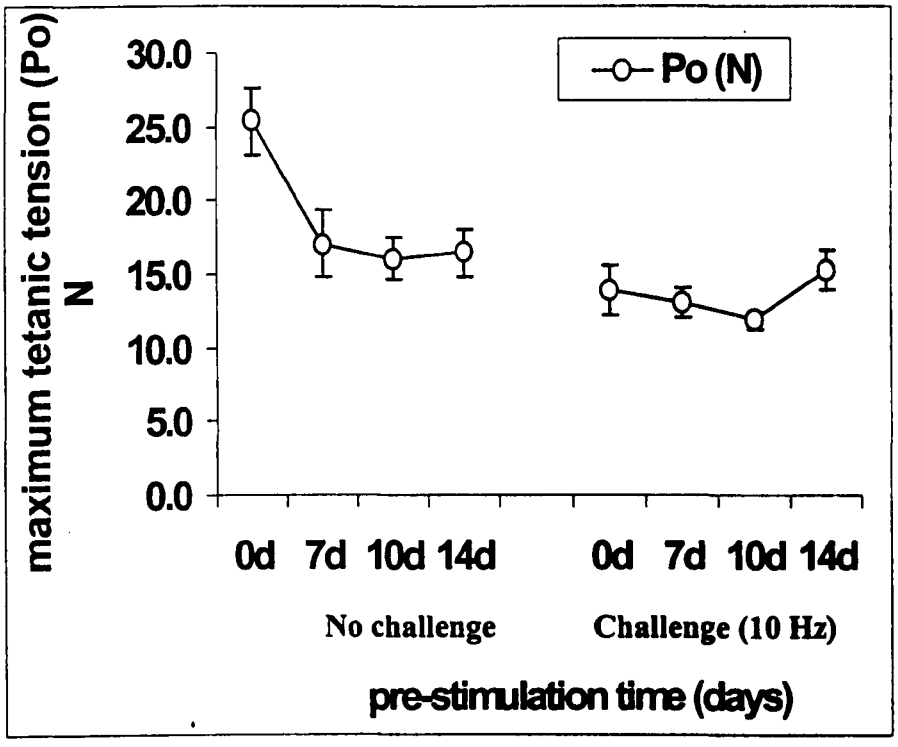

Fig. 4.1. Changes in the maximum tetanic tension (P_o), for rabbit TA after either pre-stimulation (2.5 Hz) alone for 7, 10 or 14 days or followed by stimulation at 10 Hz for 9 days. Control groups include non-stimulated fast muscles (0d-no challenge) and muscles stimulated at 10 Hz for 9 days only (0d-challenge 10Hz), (mean data points, error bars ± SEM, n=6).

4.4.2 Mass, cross sectional area (CSA) and specific tetanic tension

It has been reported that there is a correlation between the P_o and the CSA and mass of fast twitch muscle (Salmons, 1990). There were no substantive changes in muscle mass and/or CSA from control fast values for the muscle groups that had received either pre-stimulation, 7-14 days, alone or followed by the 10 Hz challenge (Table 4.1). These findings were reflected in the specific tetanic tensions calculated for each of the muscles groups, which showed no significant differences to control values, after

either pre-stimulation at 2.5 Hz for 7-14 days alone or followed by the 10 Hz challenge (Table 4.1).

Pre-stimulation time (days)	Mass (g)	CSA (g/cm^2)	Specific tetanic tension (n/m^2)
No Challenge			
0d	3.98 ± 0.16	0.5 ± 0.03	516.90 ± 46.25
7d	3.65 ± 0.14	0.5 ± 0.02	370.48 ± 43.08
10d	3.33 ± 0.35	0.4 ± 0.05	373.87 ± 26.99
14d	3.61 ± 0.24	0.5 ± 0.03	359.82 ± 29.40
Challenge 10 Hz			
0d	3.70 ± 0.17	0.5 ± 0.03	307.34 ± 40.87
7d	2.97 ± 0.16	0.4 ± 0.03	383.02 ± 35.26
10d	2.63 ± 0.31	0.3 ± 0.04	357.49 ± 26.00
14d	2.96 ± 0.28	0.4 ± 0.03	410.09 ± 24.74

Table 4.1. Changes in muscle mass, cross-sectional area (CSA) and specific tetanic tension for rabbit TA after either pre-stimulation (2.5 Hz) alone for 7, 10 or 14 days or followed by stimulation at 10 Hz for 9 days. Control groups include non-stimulated TA (fast) muscles (0d-no challenge) and muscles stimulated at 10 Hz for 9 days only (0d-challenge 10 Hz), (mean data points ± SEM, n=6).

4.4.3 Twitch to tetanus (P_t:P_o) ratio

The P_t:P_o ratio for control muscles that had received stimulation at 10 Hz for 9 days increased significantly ($P<0.001$) with respect to control non-stimulated muscles. There was a substantial increase ($P<0.01$), when compared to fast controls, in the P_t:P_o ratio after 14 days of pre-stimulation. Pre-stimulation for between 7 and 14 days

followed by the 10 Hz challenge significantly increased ($P<0.001$) the $P_t:P_o$ ratio relative to control fast ratios. There were significant differences ($P<0.05$) between the $P_t:P_o$ ratios after pre-stimulation for 7 days alone and followed by the 10 Hz challenge. More prolonged periods of pre-stimulation 10-14 days alone or followed by the 10 Hz challenge exhibited negligible differences to one another (Table 4.2).

Pre-stimulation times (days)	$P_t:P_o$ ratio
No Challenge	
0d	0.15 ± 0.02
7d	0.23 ± 0.02
10d	0.28 ± 0.02
14d	0.31 ± 0.05
Challenge 10 Hz	
0d	0.36 ± 0.02
7d	0.40 ± 0.03
10d	0.38 ± 0.02
14d	0.34 ± 0.03

Table 4.2. Changes in the twitch to tetanus ratio ($P_t:P_o$) for rabbit TA after either pre-stimulation (2.5 Hz) alone for 7, 10 or 14 days or followed by stimulation at 10 Hz for 9 days. Control groups include non-stimulated TA muscles (0d-no challenge) and muscles stimulated at 10 Hz for 9 days only (0d-challenge 10 Hz), (mean data points ± SEM, n=6).

4.5 The effect of low frequency pre-stimulation on contractile speed

4.5.1 Contraction times (C_t)

The time to contract was significantly prolonged ($P<0.001$) for those muscles that had received the 10 Hz challenge alone with respect to control fast times. The C_t showed significant increases ($P<0.05$) after prolonged periods of pre-stimulation, 14 days, with respect to control fast values. In contrast pre-stimulation for 7-14 days, followed by the 10 Hz challenge showed substantive slowing of the C_t ($P<0.01$) in comparison with the control fast C_t. There were no significant changes in the time to contract with pre-stimulation, 7-14 days, followed by the 10 Hz challenge compared with stimulation at 10 Hz for 9 days alone (Figure 4.2).

4.5.2 Relaxation times (R_t)

There was significant slowing of the R_t ($P<0.001$) following 10 Hz stimulation for 9 days with respect to control fast R_t. Longer periods of pre-stimulation, 14 days, showed substantive increases in the R_t ($P<0.05$) with respect to control fast times. 10 days of pre-stimulation followed by the 10 Hz challenge significantly increased the R_t ($P<0.01$) while 7 and 14 days of pre-stimulation prior to the challenging pattern did not significantly increase the R_t above control fast values. Pre-stimulation for 7 and 14 days followed by the 10 Hz challenge showed progressive decreases in the R_t ($P<0.05$ and $P<0.01$ respectively) compared with the prolonged R_t recorded after stimulation at 10 Hz for 9 days (Figure 4.2).

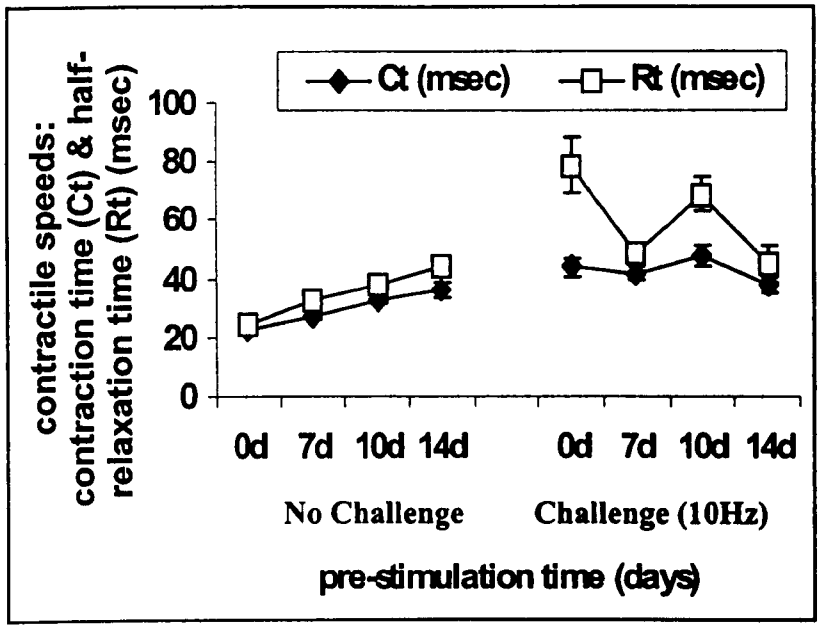

Fig. 4.2 Changes in the contraction (C_t) and relaxation (R_t) times for rabbit TA after either pre-stimulation (2.5 Hz) for 7, 10 or 14 days alone or followed by stimulation at 10 Hz for 9 days (10 Hz challenge). Control groups include non-stimulated TA (fast) muscles (0d-no challenge) and muscles stimulated at 10 Hz for 9 days only (0d-challenge 10Hz), (mean data points, error bars ± SEM, n=6).

4.6 The effect of low frequency pre-stimulation on myosin light chain (MLC) isoform composition and maximum velocity of shortening (V_{max})

4.6.1 SDS polyacrylamide gel electrophoresis (SDS-PAGE) of MLC

Pre-stimulation at 2.5 Hz for between 7 and 14 days alone or followed by the 10 Hz challenge and 10 Hz stimulation for 9 days alone did not demonstrate any change from the fast MLC isoform composition (MLC1f, 2f and 3f) identified for the control TA (fast) muscle (Figure 4.3).

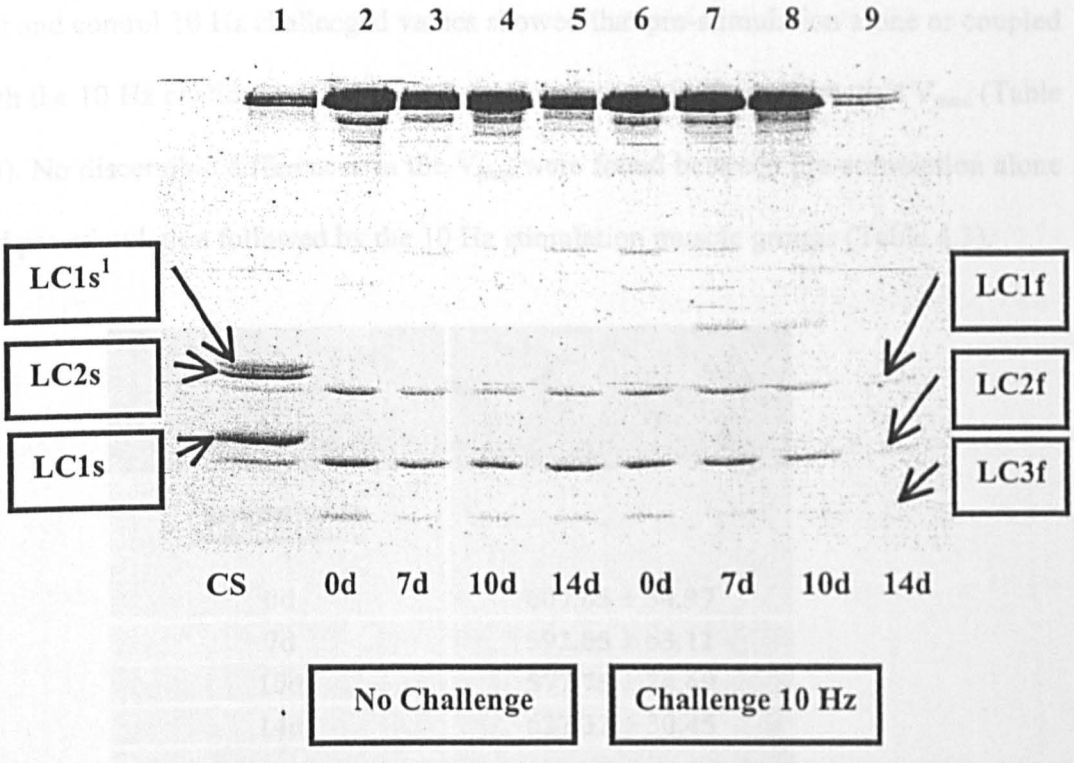

Fig. 4.3 A polyacrylamide gel of MLC expression for rabbit TA after either pre-stimulation at 2.5 Hz for 7-14 days alone or followed by stimulation at 10 Hz for 9 days. *Lane 1*, control soleus (CS; slow); *lane 2*, control non-stimulated TA muscle (0d; fast); *lanes 3, 4 and 5*, represent TA that has been pre-stimulated (2.5) for 7, 10 and 14 days respectively, with no 10 Hz challenge (7, 10, 14d; no challenge); *lane 6*, represent TA that has been stimulated at 10 Hz for 9 days (0d; 10 Hz challenge); *lanes 7, 8 and 9*, represent TA that has been pre-stimulated for 7, 10 and 14 days respectively followed by the 10 Hz challenge (7, 10 and 14 d; 10 Hz challenge).

4.6.2 Maximum velocity of shortening (V_{max})

It has been suggested that the MLC may play a role in determining the speed of shortening (**Lowey *et al.*, 1993; Sweeney *et al.*, 1993**). Comparisons between control

fast and control 10 Hz challenged values showed that pre-stimulation alone or coupled with the 10 Hz challenge did show substantial changes in their respective V_{max} (Table 4.3). No discernible differences in the V_{max} were found between pre-stimulation alone and pre-stimulation followed by the 10 Hz stimulation muscle groups (Table 4.3).

Pre-stimulation time (days)	V_{max} (mm/sec)
No Challenge	
0d	600.65 ± 34.97
7d	592.05 ± 63.11
10d	577.75 ± 24.69
14d	627.32 ± 30.45
Challenge 10 Hz	
0d	570.25 ± 36.87
7d	492.07 ± 50.76
10d	510.82 ± 30.97
14d	541.58 ± 27.21

Table 4.3. Changes in the maximum speed of velocity (V_{max}) for rabbit TA pre-stimulated (2.5 Hz) for 7, 10 or 14 days alone or followed by the challenging 10 Hz regime. Control groups include non-stimulated TA (fast) muscles (0d-no challenge) and muscles stimulated at 10 Hz for 9 days only (0d-challenge 10 Hz), (mean data points ± SEM, n=6).

4.7 The effect of low frequency pre-stimulation on fatigue resistance

The fatigue index (FI) showed a small increase, which did not appear to reach significance, after stimulation at 10 Hz for 9 days compared with fast control FI. Within the pre-stimulation alone group the resistance to muscle fatigue increased significantly for muscles that received 14 days pre-stimulation ($P<0.01$) compared with control fast muscles. Pre-stimulation for 7 days followed by the 10 Hz challenge showed substantive increases ($P<0.05$) in fatigue resistance with respect to control fast FI. While pre-stimulation 7-14 days followed by the 10 Hz challenge did not exhibit significant differences in fatigue resistance when compared with stimulation at 10 Hz for 9 days alone, (Figure 4.4).

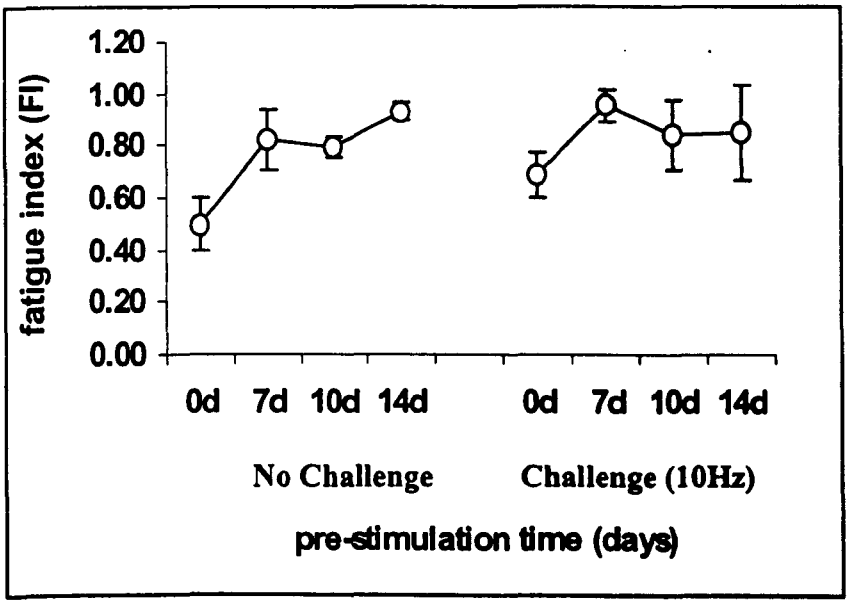

Fig. 4.4. Changes in the fatigue index (FI) for rabbit TA after either pre-stimulation (2.5 Hz) alone for 7, 10 or 14 days or followed by stimulation at 10 Hz for 9 days. Control groups include non-stimulated TA (fast) muscles (0d-no challenge) and muscles stimulated at 10 Hz for 9 days only (0d-challenge 10 Hz), (mean data points, error bars ± SEM, n=6).

4.8 Discussion

Maximal forces were significantly decreased after stimulation at 10 Hz for 9 days with pre-stimulation for between 7 and 14 days showing negligible attenuation of the 10 Hz challenge induced force depressions. Increasing duration's of pre-stimulation at 2.5 Hz alone evoked significant decreases in P_o, which appeared to be marginally less than the decline in force resulting from the two stage, 2.5 and 10 Hz, stimulation regime. These decreases in maximal force do not appear to be related to changes in CSA or muscle mass, which showed no significant changes for any of the experimental groups. This is consistent with previous studies, which have reported that stimulation at 2.5 Hz for 14 days did not induce substantive loss of muscle mass. Comparisons with stimulation at 10 Hz for the same time period, 14 days, showed that this higher stimulation frequency induced larger losses of bulk, although the losses incurred did not appear to be significant **(Jarvis *et al.*, 1996)**.

Significant increases in the time to contract and relax after stimulation at 10 Hz for 9 days illustrates that this potentially damaging 10 Hz regime alters Ca^{2+} kinetics. The SR Ca^{2+} ATPase facilitates regulation of the contraction-relaxation cycle in muscle. Previously it has been reported that stimulation of rabbit TA at 10 Hz for 10 days significantly (50%) decreased the catalytic activity of the SR Ca^{2+} ATPase. Changes in the expression of the fast and slow Ca^{2+} ATPase isoforms occurred over a longer time course than changes in the catalytic activity of the enzyme. Therefore slowing of the R_t after 10 days of stimulation were attributed to decreases in the activity and not the expression of the Ca^{2+} ATPase **(Hicks *et al.*, 1997)**.

It is reasonable to suggest that one of the main contributing factors to the increase in contraction and relaxation times after stimulation at 10 Hz for 9 days may be the decrease in the specific activity of SR Ca^{2+} ATPase activity. It has been proposed that the decreases in the catalytic activity of this enzyme with increased contractile activity may be attributed to increases in metabolic by-product accumulation within the myofibre. Ultimately this may cause membrane or structural damage to the enzyme and disrupt the normal functioning of the SR Ca^{2+} ATPase **(Zhu & Nosek, 1991).**

Jarvis *et al.*, 1996 reported that prolonged stimulation of fast twitch muscles at 2.5 Hz increased C_t to a much smaller degree than stimulation at 10 Hz **(Jarvis *et al.*, 1996).** This study showed that the longest period of pre-stimulation tested, 14 days, significantly increased (slowed) the C_t with respect to control fast values. However in comparison with the prolonged C_t recorded after the 10 Hz challenge alone the time to contract and relax had decreased (faster), although the increases in C_t did not appear to reach significance, after the two stimulation regime (2.5 Hz followed by 10 Hz). This suggests that pre-stimulation at lower frequencies may attenuate alterations in Ca^{2+} trafficking to and from the SR induced at higher stimulation frequencies (10 Hz). Korge *et al.*, 1994 demonstrated that a cellular fraction of creatine kinase (CK) remained bound to SR vesicles isolated from rabbit fast twitch. This bound CK was found to support Ca^{2+} pump function, via ATP-regenerating systems (CK and glycolytic enzymes), by maintaining ADP and ATP concentrations in the vicinity of the enzyme at normal levels. They proposed that there is functional coupling between SR Ca^{2+} ATPase and membrane bound CK **(Korge *et al.*, 1994).** Functional coupling between locally bound CK and myofibrillar ATPase has also been demonstrated

(Wallimann *et al.*, 1992). Pre-stimulation may induce moderate yet progressive increases in ATP regenerating systems which may prevent the complete disruption of Ca^{2+} pumping to and from the SR upon stimulation at higher and more metabolically demanding frequencies. In addition pre-stimulation may decrease or facilitate the more efficient removal of metabolic by-products resulting from 10 Hz stimulation, which may protect the SR Ca^{2+} ATPase protein. No significant changes in capillarization were found between muscles that had received pre-stimulation alone or followed by the 10 Hz challenge. This may argue against the proposal that the efficient removal of metabolic by-products after low frequency pre-stimulation may be responsible for the subsequent protection of the Ca^{2+} ATPase protein during higher frequency stimulation regimes.

Alterations to Ca^{2+} kinetics may ultimately evoke a prolonged Ca^{2+} transient which may explain the increases in the twitch to tetanus ratios recorded after the pre-stimulation alone or followed by the 10 Hz challenge. There were comparable increases in the twitch to tetanus ratio following the potentially damaging 10 Hz stimulation alone or when pre-stimulation for 7-14 days preceded the 10 Hz stimulation. This supports the hypothesis that pre-stimulation may attenuate 10 Hz stimulation induced decreases in SR Ca^{2+} ATPase activity.

Comparison of the pre-stimulated alone with the pre-stimulated followed by 10 Hz challenge groups showed that differences in C_t between these groups were incurred up to 10 days and differences in the R_t were only incurred at 10 days. This suggests that

prolonged periods of pre-stimulation, 10 days or more may act to preserve the rate of contraction when challenged with a higher frequency of stimulation. The relaxation rate-pre-stimulation relationship appears to be more complex. The time to relax showed negligible differences after 7 and 14 days but increased significantly after 10 days of pre-stimulation followed by the 10 Hz stimulation when compared with the pre-stimulation (7-14 days) alone muscles. This relative increase after 10 days was recorded for all of the 6 TA muscles employed in the physiological measurements and cannot be attributed to one or more of the stimulated muscles showing exaggerated R_t. Therefore it would appear that 10 days of pre-stimulation coupled with 10 Hz stimulation induced a more significant alteration of Ca^{2+} trafficking into the SR than either 7 or 14 days of pre-stimulation followed by the 10 Hz challenge. This suggests that the two stage stimulation regime employed in this study may induce phasic changes in the re-uptake of Ca^{2+} into the SR which may be dependent on the pre-stimulation time.

Decreases in the maximal force and changes in the contractile speed do not appear to be related to changes in the MLC composition. Pre-stimulation for between 7 and 14 days alone or followed by the 10 Hz challenge and 10 Hz stimulation alone did not induce changes in MLC isoform expression but continued to express the fast MLC isoforms (LC1f, LC2f and LC3f). This is not an unexpected finding as previous work has demonstrated that stimulation at 2.5 Hz for up to 12 weeks did not evoke any significant transformation from fast to slow myosin expression (**Jarvis *et al.*, 1996**). Stimulation at 10 Hz has been shown to induce the expression of slow myosin

isoforms after 2 weeks with the complete transition to a slow composition taking up to 6 weeks (**Brown *et al.*, 1983**).

The speed of shortening reflected the continued expression of fast MLC with no significant differences in V_{max} identified either within or between any of the experimental and control groups. It has been reported that the ATPase activity, thus myosin heavy chain (MHC) isoform expression is proportional to the speed of shortening (**Bárány, 1967**). Fibre type composition, determined by histochemical staining of the myofibrillar ATPase, was in agreement with the data on the speed of shortening. Fibre typing did not differ significantly from control fast populations, where the majority of fibre types were 2A and 2D with type 2D predominating, after either pre-stimulation alone of followed by the 10 Hz challenge.

Fatigue is the failure to maintain force output (**Edman & Lou, 1990**) and may be due to changes in E-C coupling and/or Ca^{2+} kinetics (**Fitts, 1994**).

Long periods of pre-stimulation, 14 days, alone and short periods of pre-stimulation, 7 days, followed by 10 Hz stimulation appeared to significantly decrease the muscles susceptibility to force fatigue. At these time points the contractile speeds of the respective muscles were approaching one another which suggests that Ca^{2+} kinetics may be facilitating the increased resistance to force fatigue.

Pre-stimulation alone or followed by the 10 Hz challenge did not change the proportions of type 2D, fatigue susceptible, or 2A, fatigue resistant, fibres from control TA fast fibre populations. However pre-stimulation followed by 10 Hz stimulation did significantly increase the proportions of the fatigue resistant type 1

fibres and pre-stimulation alone increased, although it did not appear to reach significance, the type 1 fibre populations with respect to control fast TA type 1 fibre populations. These increases, albeit small, in the fatigue resistant type 1 fibres may be in part responsible for the increased fatigue resistance.

Previous reports have identified that changes in the susceptibility to fatigue may be detected a few days after the onset of low frequency stimulation, at a stage when capillary density may be beginning to show an increase. Thus it was proposed that increased capillarization may facilitate an increased resistance to fatigue **(Hudlicka *et al.*, 1997; Degens & Veerkamp, 1994)**. In this study no significant increases in capillary density were identified for any of the experimental groups with respect to each other and control fast and 10 Hz stimulated TA muscles. Therefore it would appear that increased fatigue resistance at the aforementioned times might not be attributed to enhanced capillarization.

Chapter 5

The effects of stimulation on length-force characteristics at the proximal and distal tendons of the *extensor digitorium longus* (EDL) muscle, and at the distal tendon of *tibialis anterior* (TA) and *extensor hallicus longus* (EHL) muscles within a rat model.

5.1 Introduction

EDL, TA and EHL muscles are located within the anterior tibial compartment of the hind limb where they act as dorsiflexors of the ankle, EDL acts across two joints while TA and EHL act across one. The heterogeneous fibre type composition and blood supplies of these fast-twitch muscles are closely related. **(Lexell *et al.*, 1994; Lexell *et al.*, 1993; Lexell *et al.*, 1992).**

One major difference between EDL and TA muscles is their architecture. The EDL is comprised of fibres in pennate arrangements while the TA is made up of fibres in parallel arrays. A pennate muscle consists of fibres, which are relatively short compared to the length of the muscle and have angles with respect to the muscles' line of pull. In contrast, a parallel muscle is comprised of fibres' that have lengths similar to the length of the muscle, and are organised along the line of pull of the muscle **(Spector *et al.*, 1980).** Thus changes in EDL muscle length are attributable to a combination of fibre, aponeurosis and angle changes while changes in TA muscle length are due to fibre length changes **(Lieber, 1992).**

There are anatomical differences between the proximal and distal ends of EDL. The proximal portion of EDL has one aponeurosis to which all its spanning muscle fibres attach under a modest angle of pennation. At the distal end there are four separate

aponeuroses, which distinguishes four segments, II, III, IV and V, of the EDL, each of which are attached to a long tendon **(Huijing, 1999)**.

Sarcomere force depends on the amount of filament (myosin and actin) overlap. The optimum muscle length is defined as the muscle length at which maximal force is attained. Sarcomeres are arranged in series and exhibit heterogeneity causing decreases in force at lengths over and above optimum lengths **(Sugi & Tsuchiya, 1988)**. It has been demonstrated that briefly stretching a resting fibre by up to twice its resting length does not alter its potential to generate maximum tetanic force **(Bruton *et al.*, 1998; Goldstein *et al.*, 1991)**.

The force producing capabilities of fast-twitch muscles depend on properties that change in time during sustained contractions **(Meijer *et al.*, 1997)**. Isometric stimulation may induce fatigue in fast-twitch muscles. Fatigue is the failure to maintain force output **(Edman & Lou, 1990)** and may be attributable to disturbances in, transmission of the action potential, excitation-contraction coupling, ion transport systems, ultra-structure, and cell metabolism **(Fitts *et al*, 1994)**.

There are two distinct modes of force transmission within skeletal muscle namely myotendinous and myofascial force transmission. Myotendinous (longitudinal) force transmission involves the tensile transmission of force from sarcomere to sarcomere followed by shear transmission onto the collagen fibres of the aponeurosis or tendon at the myotendinous junction (MTJ). The MTJ is a region of the cell membrane at the end of the muscle fibres where the myofibrils terminate **(Monti et al., 1999; Huijing,**

1999). In contrast, myofascial (lateral) transmission involves the shear transmission of force from the sarcomeres, via transsarcolemma connections and the basal lamina, to the sarcolemma along the length of the myofibre and onto the endomysial structures. The connective tissue in muscle is comprised of three anatomical types namely endomysium, envelops each of the muscle fibres, perimysium, covers bundles of muscle fibres or fascicles, and epimysium, covers the entire surface of the muscle belly. While the connective tissue of the muscle is organised into three distinct levels they are continuous with each other and with the aponeurosis and the muscle tendons **(Huijing, 1999)**. Lateral force transmission is assisted by proteins including vinculin (costameres) and dystrophin (dystrophin associated complex) **(Monti *et al.*, 1999)**.

There is a modest volume of literature on myofascial force transmission however recent studies have highlighted the complexity of this mode of force transmission in skeletal muscle. Huijing *et al.*, 1998 reported that tenotomy of three (II, III, IV) of the four distal EDL tendons decreased but did not attenuate myotendinous force transmission at the distal tendon. Forces exerted at the proximal EDL tendon remained unchanged. In addition damage to the connective tissue between distal EDL tendons V (intact) and IV (severed) along the direction of the muscle fibres for a certain length resulted in a decrease in the forces exerted at the distal tendon. The extent of this decrease was dependent on the length of the interface between tendons IV and V that had been damaged. This led to the proposal that forces may be transmitted intra-muscularly, in a lateral direction, via the continuous endomysium-perimysium

infrastructure from the severed to the intact distal tendons of the EDL muscle **(Huijing *et al.*, 1998)**.

Subsequent experiments where the EDL muscle was subjected to isometric contractions at a number of proximal EDL tendon lengths have shown that the maximal forces exerted at the proximal tendon were greater than those at the distal tendon. This proximal-distal difference in EDL force (Fprox-Fdist) has been shown to be dependent on proximal EDL tendon length. Furthermore the Fprox-dist was not evident upon isolation of EDL from other muscles in the anterior tibial compartment. The abolition of Fprox-dist was attributed to changes in the proximal EDL force. Isolation of the muscle demonstrated a general decrease of sarcomere lengths over the muscle length range tested. This suggests that the connection of the EDL muscle belly to surrounding structures within the tibial compartment may be instructive for its muscle characteristics. The length dependent disparity between proximal and distal EDL forces under *in vivo* conditions has lead to the suggestion that myofascial force transmission may facilitate extra-muscular transmission of force onto the connective tissue of the anterior compartment **(Huijing & Baan, 2000)**.

In addition, it has been proposed that the Fprox-dist, or part of, may be transmitted to the TA-EHL muscle complex i.e. inter-muscular force transmission **(Huijing & Baan, 2000)**. It has been demonstrated that forces exerted at the EDL and TA-EHL tendons may be effected by the muscle tendon lengths of both muscles. Huijing 1999 reported that when EDL proximal tendons were kept at between optimum and slack length, EDL forces increased at low TA lengths (low TA forces) and remained constant at high TA lengths (high TA forces). Furthermore when the proximal EDL tendon length

was kept at above optimum length, the EDL forces increased at lower TA lengths (low TA forces) and decreased at TA lengths above optimum length (high TA forces). This suggests that there are interactions between these neighbouring muscles *in vivo* and they appear to be a function of both their lengths **(Huijing, 1999)**.

5.2 Methods

This part of my research employed a rat model (n=5) where the distal and proximal tendons of EDL, and the distal tendons of TA and EHL were dissected free. The distal tendons of TA and EHL were tied to each other (TA-EHL), thus these two muscles were mechanically coupled. The four freed distal tendons of the EDL were tied to one another (mechanically coupled) and the proximal EDL tendon was tied alone. All of the freed muscle tendon groups were attached to respective force transducers. The EDL, TA and EHL muscles were stimulated (30 Hz) maximally and simultaneously, via the common peroneal nerve, for 3 hr.

Prior to commencing the stimulation regime, isometric tetanic forces exerted at the proximal and distal EDL tendons and at the distal TA-EHL tendons were measured for 10 proximal EDL tendon lengths. The starting proximal EDL length corresponded to the lowest length at which proximal EDL force approached zero. The proximal EDL tendon was lengthened (1mm increments) in between contractions by moving the proximal EDL force transducer to new target positions. Distal EDL tendons were kept at reference positions and the distal TA-EHL tendon complex was kept at low lengths during the entirety of the experiment. After 3 hr of isometric stimulation (30 Hz) a second series of length force measurements, under the aforementioned conditions, were recorded. The muscle groups were then allowed to 'rest' (cessation of

stimulation) for 10 min, after which time, a third and final series of force length measurements, under the conditions previously described, were performed.

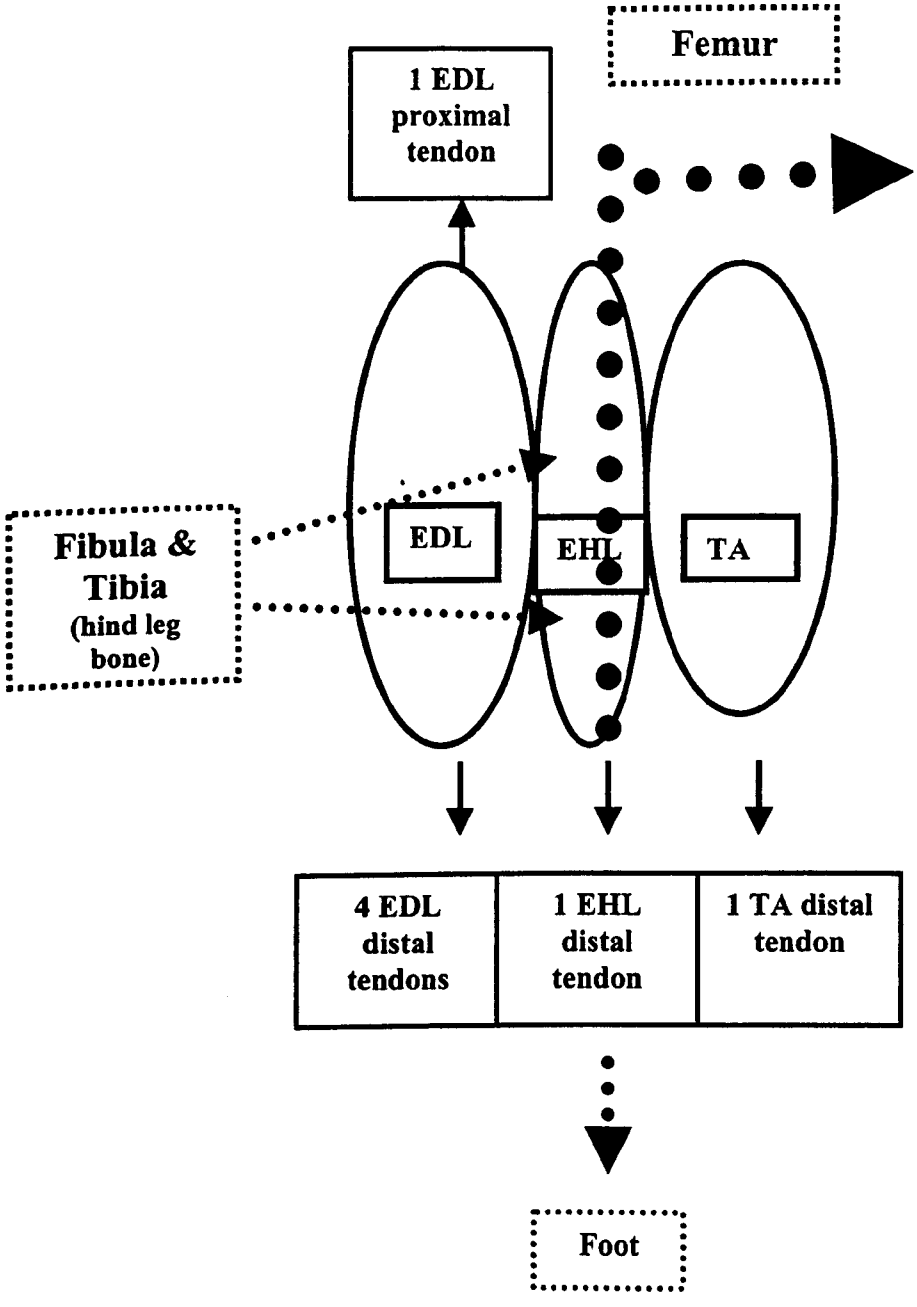

Fig.5.1. Schematic illustration of the rat biceps muscles (anterior tibial compartment) of the left hind limb employed in this study.

I employed one way analysis of variance (ANOVA) on repeated measures to determine the statistical significance of changes in the length-force data before and after stimulation and after the 'rest' period. When significant effects were found significant differences between the experimental muscles were identified using multiple comparison post hoc tests, namely Tukey post tests. Any differences at $P<0.05$ were considered significant. All results are expressed as mean ± SEM.

This piece of work had two main objectives. The first concern was to elucidate the effect of proximal EDL tendon length on forces exerted at the proximal and distal tendons of EDL muscle, and at the distal tendons of TA and EHL muscles, before and after the fatiguing stimulation regime. A second aim was to determine whether, upon its completion, cessation of stimulation for 10 min afforded significant recovery of the forces and the force-length relationships at the aforementioned EDL and TA-EHL tendons.

5.3 Results

5.4 Length-force characteristics at the proximal and distal tendons of EDL

5.4.1 Before stimulation

Prior to the onset of the stimulation regime the maximal forces exerted at the proximal tendon were greater, although they did not appear to reach significance, than the maximal forces exerted at the distal EDL tendon, 1.3 N and 1.2 N, respectively. However, distal force was greater than proximal force at low proximal EDL tendon

lengths (0-3mm). Proximal and distal forces attained equality at a 'cross-over length' of 3.5 mm and proximal force increased and overtook distal force at lengths above this 'cross-over length' (4-9mm), (Figure 5.1). The difference between proximal and distal EDL forces (Fprox-dist) increased significantly ($P<0.05$) at low proximal EDL tendon lengths but did not show significant changes at higher proximal EDL tendon lengths (Figure 5.4).

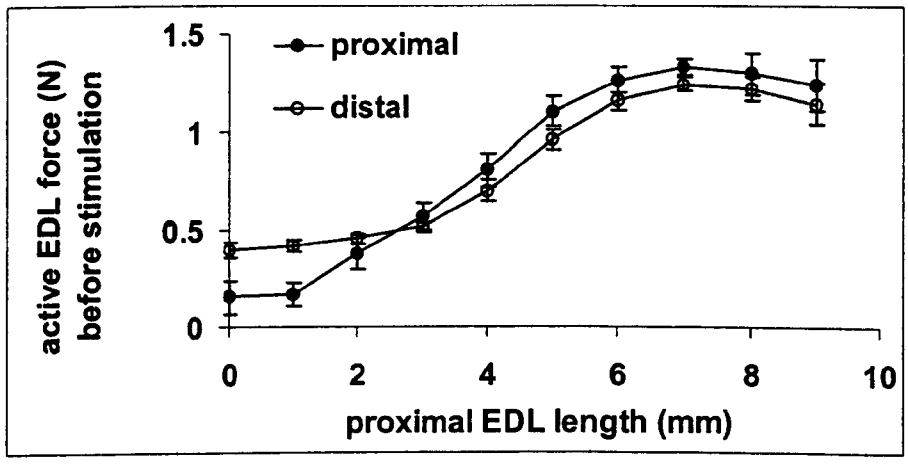

Fig.5.2 The length-force curves at the proximal and distal tendons of rat EDL before commencing the stimulation regime (mean data points, error bars ± SEM (n=5)).

5.4.2 After stimulation

After completion of the stimulation regime, there were significant reductions in both the proximal and distal peak forces, at 41% and 39% respectively, compared with maximal forces recorded before the stimulation regime ($P<0.001$). The length-force characteristics exhibited profound changes including (1) Peak proximo-distal forces were recorded at above-optimum proximal EDL tendon lengths, (2) Distal forces were greater than proximal forces over a higher proximal EDL tendon length range (0-

5mm) and the 'cross-over length' (6.5mm) was significantly extended ($P<0.05$) and (3) The proximal tendon slack length was shifted to higher lengths (0-3 mm), (Figure 5.2). The Fprox-dist did not show substantial increases with proximal EDL tendon lengthening i.e. from low to high proximal EDL lengths, after stimulation (Figure 5.4). This stimulation regime decreased the forces exerted at the proximal and distal tendons and re-arranged the length-force relationship at the aforementioned EDL tendons.

5.4.3 After 'rest'

Following 10 min of 'rest' (stimulation was stopped) there was recovery, although it did not appear to reach significance, of proximal and distal optimum forces to those values which had been recorded before the onset of stimulation. In addition, the length-force relationship was not restored to its initial status. Recovery exhibited a shift in the optimum length (1mm to the right) and the proximal slack length remained elevated (0-3mm). The distal force continued to exceed the proximal force over an extended length range (0-5mm), the 'cross-over length' (5.5mm) remained significantly higher ($P<0.05$), and the proximal force continued to overtake the distal force at higher lengths (5-9mm), (Figure 5.3). The 'rested' Fprox-dist increased significantly ($P<0.05$) with high proximal EDL tendon lengthening but did not show substantive increases at lower proximal lengths (Figure 5.4).

Cessation of the regime for a short period did not facilitate the complete recovery of forces exerted at the proximal and distal EDL tendon nor did it allow for restoration of the length-force relationship between the two ends of the EDL muscle.

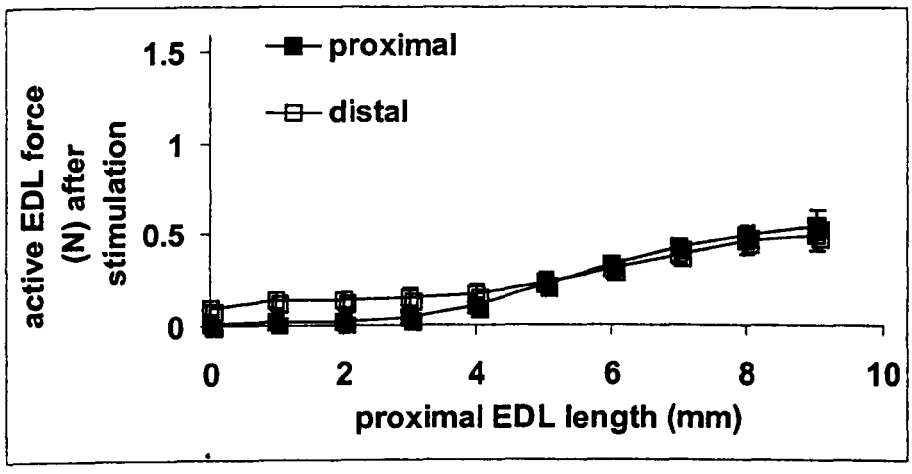

Fig.5.3 The length-force curves at the proximal and distal tendons of rat EDL after completion of the stimulation regime (mean data points, error bars ± SEM (n=5)).

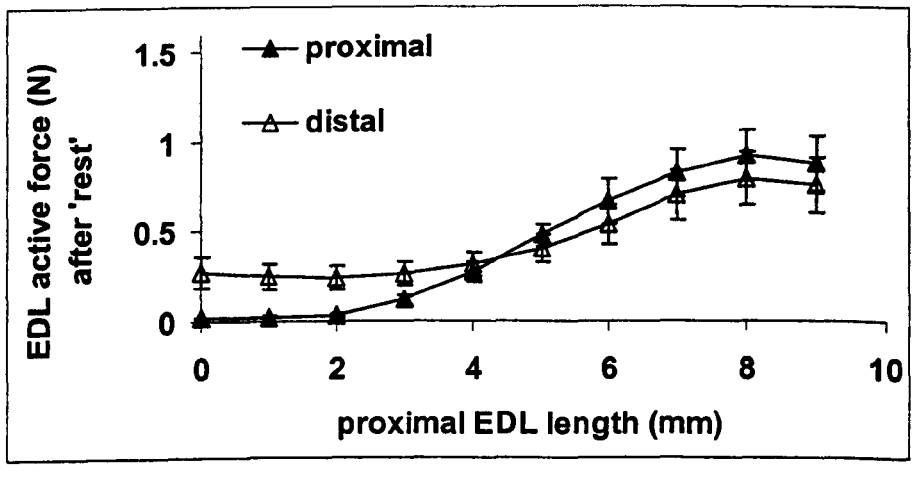

Fig. 5.4 The length-force curves at the proximal and distal tendons of rat EDL after cessation of stimulation 'rest' for a 10 min period (mean data points, error bars ± SEM (n=5)).

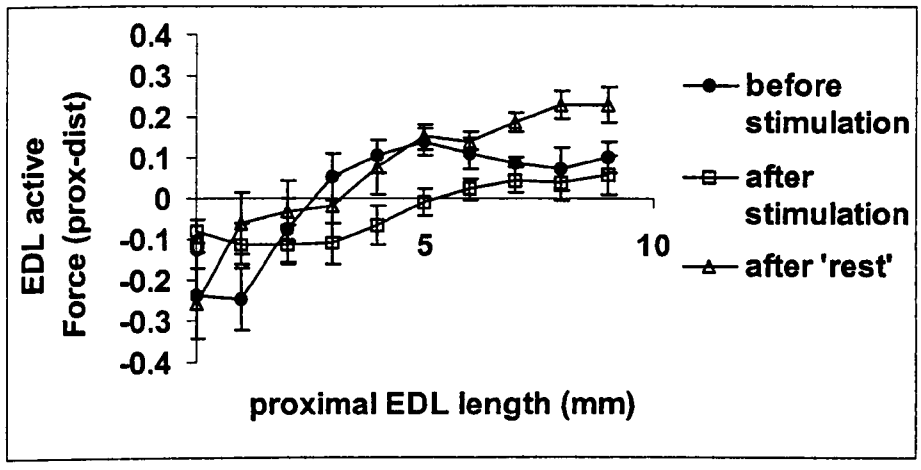

Fig.5.5 The length-force curves for the difference between proximal and distal EDL forces (Fprox-dist) before and after the stimulation regime and after the 10 min 'rest' period (mean data points, error bars ± SEM (n=5)).

5.5 Length-force characteristics at the distal tendon of the TA-EHL muscle complex

5.5.1 Before stimulation

Before commencement of regime the distal TA-EHL force peaked (0.4 N) at a low proximal EDL tendon length (4mm) with no significant changes in force with increased proximal EDL lengthening (4-10 mm), (Figure 5.5).

Before stimulation proximal EDL tendon lengthening to high lengths did not affect forces exerted at the distal TA-EHL tendon.

5.5.2 After stimulation

Upon completion of the stimulation regime, the distal TA-EHL forces were significantly decreased ($P<0.05$) at lower proximal EDL lengths but increased, albeit without reaching significance, with respect to the peak forces recorded before stimulation (0.4N) at higher proximal EDL lengths (Figure 5.5).

After stimulation forces exerted at the distal TA-EHL tendon increased with increasing proximal EDL lengthening over the entire proximal EDL length range tested.

5.5.3 After 'rest'

After the 10 min 'rest' period, forces exerted at the distal TA-EHL tendon were significantly increased with respect to before ($P<0.05$) and after stimulation ($P<0.05$) peak distal TA-EHL forces. However, proximal EDL tendon lengthening did not appear to have any significant effect on the distal TA-EHL force (Figure 5.5).

Cessation of the stimulation regime facilitated the recovery and elevation of peak TA-EHL forces and abolished the proximal EDL lengthening effects recorded immediately after completion of the stimulation regime.

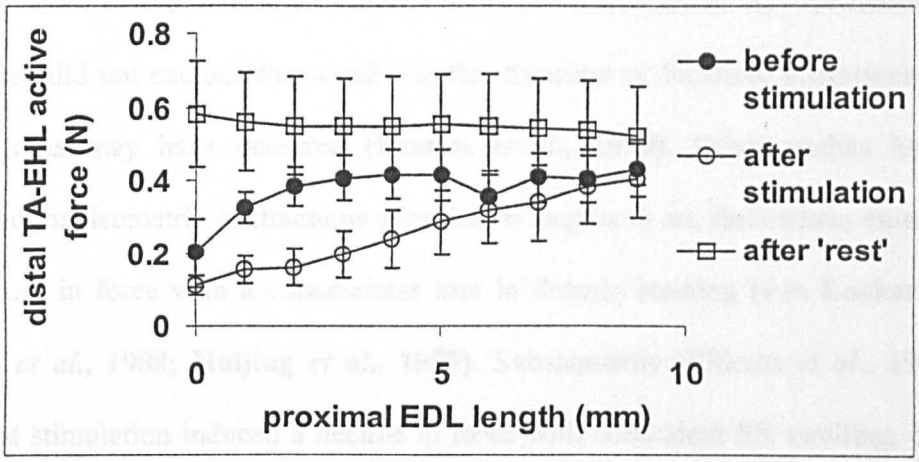

Fig.5.6 The length-force curves at the distal tendon of the rat TA-EHL muscle complex before and after stimulation and after the 10 min 'rest' period (mean data points, error bars ± SEM (n=5)).

5.6 Discussion

The maximal forces exerted at the proximal and distal EDL tendons were depressed after continuous isometric stimulation (30 Hz) for 3 hr, these decreases may be attributable to stimulation-induced muscle fatigue. The induction of force fatigue in stimulated EDL and TA-EHL muscles may not be due to fibre degeneration as preliminary staining of transverse sections (10 μm), from proximal and distal regions of EDL and TA-EHL, with H&E showed no histological damage in the before or after stimulated muscles or in the rested muscles. However, the technique (H&E) employed to assess damage is a gross morphological stain and cannot identify 'early' damage i.e. Z-line streaming and loss of cytoskeletal proteins. 'Early' damage may have been present and instructive in the induction of force fatigue during this stimulation protocol. It has been suggested that force deficits induced under isometric conditions may not result from damaged sarcomeres. Bruton *et al.*, 1998 reported that after a

series of isometric contractions the sarcolemma, as a whole, showed no disturbances, however, they did not exclude the possibility that transient or localised alterations in the sarcolemma may have occurred **(Bruton *et al.*, 1998)**. Other studies have demonstrated that isometric contractions at optimum lengths in rat, fast-twitch, muscle induced a loss in force with a concomitant loss in desmin staining **(van Lookeren Campagne *et al.*, 1988; Huijing *et al.*, 1989)**. Subsequently Willems *et al.*, 1999 reported that stimulation induced a decline in force with coincident SR swelling, but no loss of desmin staining, in peripheral fibres of rat, fast-twitch, muscle. This would suggest that the role of cytoskeletal proteins in the initial stages of stimulation-induced damage remains tentative. It was hypothesized that the swelling of the SR, due to an ionic imbalance between the myoplasm and the SR, may cause disorientation of the fine architecture of the triads and impair E-C coupling and Ca^{2+} homeostasis thus precipitating force fatigue in the muscle fibres **(Willems *et al.*, 1999)**. There is growing support for the hypothesis that elevated intra-cellular Ca^{2+} levels may induce progressive reductions in force by impairing E-C coupling at the triad junction. However the mechanism, mechanical or metabolic, through which stimulation- may induce (a) disruption of Ca^{2+} homeostasis and (b) the subsequent disruption of E-C coupling has not been elucidated **(Bruton *et al.*, 1998; Fitts, 1994)**. Furthermore whether the action potentials are propagated along the fibres but not propagated into the T-tubules (E-C coupling) in the presence of force fatigue has to be determined **(Bruton *et al.*, 1998)**.

Upon completion of the stimulation regime, a 10 min 'rest' period showed partial recovery of proximal and distal EDL forces. Many studies have demonstrated metabolic recovery in the presence of force fatigue. This suggests that high-energy metabolites are not the primary factors in either the persistence of or the recovery from force fatigue **(Hicks *et al.*, 1997; Bruton *et al.*, 1998; Mayne *et al.*, 1991)**. The partial recovery of proximal and distal EDL forces observed in this study may be attributable to the fact that while a large proportion of proximal and distal sarcomeres experienced force-fatigue they may not have incurred irreversible 'early' damage. Thus the short rest period may have restored E-C coupling and/or ionic charges. It is conceivable that these parameters could be restored very rapidly to their physiological norm, thus facilitating the partial recovery from stimulation-induced force fatigue in the EDL and TA-EHL muscles.

The fatiguing protocol employed in this study disrupted the length-force relationship between the proximal and distal ends of the EDL muscle. In the presence of force fatigue the distal exceeded the proximal forces over a higher proximal EDL tendon length range, and the 'cross-over length' and the proximal EDL slack length shifted to higher lengths. A short 'rest' period allowed for the partial recovery of optimum forces, albeit at a shifted optimum length (1mm), at both ends of EDL but did not restore the pre-fatigue length-force characteristics, which continued to display stimulation-induced alterations. The optimum length remained shifted to the right, the distal force continued to exceed proximal force over a higher proximal EDL tendon length range, and the 'cross-over length' and the proximal EDL slack length remained

at extended lengths. These results suggest that some elastic component(s) of the EDL muscle might have been conditioned during the fatiguing protocol. It has been reported that the collagen fibril network, which comprises the endomysium, is re-oriented from a circumferential to longitudinal direction with muscle lengthening **(Purslow & Duance, 1991; Purslow & Trotter, 1994; Rowe, 1981)**. It is conceivable that the intramuscular connective tissue may have been conditioned or re-oriented during the isometric stimulation protocol. As the intra-muscular connective tissue is continuous with the extra-muscular connective tissue it may be that any changes incurred by one will be incurred by the other and vice versa. It is reasonable to suppose that stimulation-induced changes in the intra- and/or extra-muscular connective tissue could potentially alter the stiffness of the myofascial and/or myotendinous transmission routes thus altering the length-force characteristics recorded at the distal and proximal tendons of the EDL muscle. More generally these results may suggest that stimulation-induced changes of the biochemical components involved in sarcomere force production, for example, Ca^{2+} homeostasis, cell metabolism and E-C coupling, are more rapidly reversed than the biomechanical changes incurred by the muscle.

Passive lengthening of the proximal EDL tendon, from low to high lengths, demonstrated that greater optimal forces were consistently exerted at the proximal tendon with lower forces recorded at the distal tendon of EDL in the absence (before stimulation) and presence of (after stimulation), and recovery from (rest period) stimulation-induced fatigue. Similar length-dependent disparities between proximal

and distal forces have been reported for non-fatigued EDL **(Huijing, 1999; Huijing & Baan, 2000)**. This work has added to the complexity of the proximal-distal length-force relationship, as my results indicate that stimulation-induced force fatigue may abolish length dependent differences in the Fprox-dist in the EDL muscle. Furthermore following a short 'rest' period the length dependency of the Fprox-dist is restored without the concomitant recovery of the length-force relationships at either end of the muscle. This suggests that force-fatigue effects force transmission in both the longitudinal and lateral direction at both ends of the EDL muscle. It has been proposed that this disparity between forces recorded at the EDL tendons of origin and insertion may be due to extra-muscular myofascial force transmission from the EDL muscle to the connective tissue in the surrounding anterior compartment **(Huijing, 1999; Huijing & Baan, 2000)**. In addition there may be inter-muscular force transmission from the proximal and distal regions of EDL to other muscles in the compartment **(Huijing & Baan, 2000)**.

It has been reported that for non-stimulated rat biceps muscles lengthening of the proximal EDL tendon from low to high lengths did not change the forces recorded at the distal TA-EHL tendon with the TA-EHL complex kept at a low muscle tendon length **(Huijing & Baan, 2000)**. In this study isometric stimulation of the EDL and TA-EHL appears to have altered the interaction between EDL proximal tendon lengths and distal TA-EHL forces. Before and after the stimulation regime the TA-EHL complex exhibited comparable peak forces albeit the affects of proximal EDL lengthening on these forces was different. Before stimulation the forces exerted at the

distal TA-EHL tendon peaked at below optimum proximal EDL tendon lengths while after stimulation peak distal TA-EHL forces were recorded at above optimum EDL lengths. It appears that TA-EHL force fatigue may be abolished with lengthening of the proximal EDL tendon. Following the short 'rest' period the TA-EHL muscle complex exhibited significantly higher peak distal forces at both low and high proximal EDL tendon lengths. In fact lengthening of the proximal portion of the EDL muscle appeared to have no significant affect on distal TA-EHL forces, which remained elevated, above before and after stimulation peak forces, over the entire proximal EDL tendon length range tested. It may be that this fatiguing stimulation regime facilitates myofascial force transmission from the EDL muscle to the TA-EHL muscle complex. The short 'rest' period, which does not restore the EDL length-force characteristics to their original state, appears to change the interaction between proximal EDL tendon length and TA-EHL forces so that proximal EDL lengthening does not effect the elevated distal TA-EHL force. While this data illustrates the complexity of the relationship between proximal EDL tendon length and distal TA-EHL forces it does not provide conclusive evidence of inter-muscular myofascial force transmission between these two muscles.

Chronic low frequency neuromuscular stimulation reversibly increases the fatigue resistance of fast twitch skeletal muscle **(Salmons & Sréter, 1976; Salmons & Henrikkson, 1981; Jarvis, 1993)**. This conditioning process involves changes in metabolism, myosin isoform content, Ca^{2+} transport kinetics, capillary density and mitochondrial volume **(Pette & Vrbová, 1992)**.

The stimulation protocols employed to condition skeletal may also damage it. The primary factors or pathways responsible for stimulation-induced damage have not been elucidated but probably include excessive mechanical stress and/or metabolic overload **(Mc Ardle & Jackson, 1994)**. It has been proposed that the primary factor in this process may be the disparity between the amount of work imposed upon the muscle during stimulation and the rate of ATP production, leading to the loss of Ca^{2+} homeostasis, an increase in free radical reactions and initiation of the damage process **(Jones *et al.*, 1997)**.

Initial experiments by Jones *et al.*, 1997 tested whether a stimulation pattern that causes minimal damage might protect the muscle from the challenge of a more demanding regime. They demonstrated that pre-stimulation with a minimally damaging regime (2.5 Hz for 7-14 days) protected the muscle against a subsequent, potentially damaging challenge (10 Hz for 9 days) **(Jones *et al.*, 1997)**.

In this study rabbit TA muscles were pre-stimulated at 2.5 Hz for 7, 10 and 14 days, either alone or followed by stimulation at 10 Hz for 9 days. Transverse muscle sections were treated with the H&E stain to assess the morphological state of the experimental muscles. It was established that stimulation at 10 Hz alone incurred significant incidences of fibre degeneration. Pre-stimulation at the lower frequency of 2.5 Hz prior to stimulation at the higher frequency of 10 Hz showed significant attenuation of the morphological abnormalities recorded after stimulation at 10 Hz alone. Pre-stimulation at 2.5 Hz alone, for all the times tested, or coupled with the damaging 10 Hz challenge evoked comparably low incidences of damage.

These results demonstrate that progressive yet moderate metabolic challenges evoked with 2.5 Hz stimulation can be accommodated by skeletal muscle and prevent the induction of damage when more metabolically demanding challenges at higher stimulation frequencies are imposed on skeletal muscle.

The objective nature of and the extensive amount of literature on the MPO assay made it an attractive marker of neutrophil content i.e. inflammation in response to muscle damage (**Tang *et al.*, 1998, Bradley *et al.*, 1982**). However my results suggested that MPO activities may increase with stimulation duration and may not, as would be expected, decrease with decreasing volumes of histological damage, as identified with H&E staining. Subsequently I hypothesised that neutrophil mobilisation in response to stimulation-induced damage may culminate in time-dependent degranulation of the displaced neutrophil population. Practically these results suggest that immunological

assays should be routinely employed with the MPO assays to accurately quantitate the neutrophil and MPO content of muscle samples.

Muscles cryostat sections were stained histochemically (myofibrillar ATPase with acid pre-incubation) to demonstrate capillaries. Capillary density in muscles pre-stimulated at 2.5 Hz for 7, 10 or 14 days respectively was not significantly higher than controls. Capillarization was not significantly effected by fibre degeneration or its protection.

The fibre type composition of the experimental muscles was demonstrated using the ATPase reaction with alkaline pre-incubation. The fast 2D and 2A fibre populations did not show substantive changes from control TA fast fibre populations after either pre-stimulation alone or followed by the 10 Hz challenge. However, muscles pre-stimulated for 14 days followed by 10 Hz stimulation showed a significantly higher percentage of type 1 fibres than controls.

These results suggest that stimulation-induced protection is not wholly dependent on fibre type transformation from fast glycolytic to oxidative metabolism. Furthermore fibre degeneration or its prevention under the stimulation regimes employed did not exhibit fibre type specificity.

Stimulation at 10 Hz for 9 days evoked significant decreases in maximum tetanic tension (P_o). The force deficits resulting from stimulation at 10 Hz did not show substantive changes when pre-stimulation preceded the 10 Hz challenge. Stimulation-

induced force depressions did not appear to be related to changes in cross-sectional area or muscle mass, which showed no significant changes for any of the experimental groups.

Prolonged contraction and relaxation times were recorded after stimulation at 10 Hz for 9 days which suggests that Ca^{2+} transport kinetics, more specifically the activity of the SR Ca^{2+} ATPase activity, may be disrupted with the damaging 10 Hz pattern. Pre-stimulation alone preserved fast contraction and relaxation times and pre-stimulation prior to the 10 Hz challenge prevented the significant slowing of the relaxation time recorded after the 10 Hz pattern alone. These results suggest that Ca^{2+} trafficking to the SR in all fibres, irrespective of type, participating in contractile activity may be involved in the pre-stimulation-induced protective effect.

The decreases in P_o and changes in the contractile times do not appear to be a consequence of changes in the expression of myosin light chain (MLC) isoforms which did not deviate from the fast LC1f, LC2f and LC3f pattern of expression for any of the experimental groups. This result was reflected in the absence of any significant changes in the maximum velocity of shortening (V_{max}) for all of the experimental groups, which in turn was substantiated by the aforementioned persistence of fast 2D and 2A fibre populations after either pre-stimulation alone or followed by the 10 Hz pattern. The increases, albeit small in type 1 fatigue resistant fibres may in part explain the increased resistance to force fatigue after either prolonged periods of pre-stimulation alone or short periods of pre-stimulation followed by the 10 Hz pattern.

Two distinct modes of force transmission have been identified in skeletal muscle, myotendinous (longitudinal) and myofascial (lateral) force transmission **(Monti *et al.*, 1999; Huijing *et al.*, 1999; Street, 1983)**. It has been demonstrated that there is a length dependent disparity between forces exerted at the proximal and distal tendons of rat EDL muscle under *in vivo* conditions **(Huijing & Baan, 2000)**. It has not been established whether these length dependent differences between proximal and distal EDL forces may facilitate extra-muscular (to surrounding structures in the tibial compartment) and/or inter-muscular (to neighbouring muscles in the tibial compartment) myofascial force transmission. However it has been demonstrated that forces exerted at rat EDL and TA-EHL tendons may be effected by the muscle tendons lengths of both muscles **(Huijing, 1999)**.

In this study rat EDL, TA and EHL muscles were subjected to stimulation at 30 Hz for 3 hours. Before commencing the regime, after completion of the regime and after cessation of stimulation for 10 min ('rest') isometric tetanic forces exerted at the proximal and distal EDL tendons and at the distal TA-EHL tendons were measured for 10 proximal EDL tendon lengths.

Isometric stimulation at 30 Hz for 3 hours significantly decreased the maximal forces exerted at the proximal and distal EDL tendons and altered the length-force relationship between either end of the EDL muscle. These force depressions may be attributable to the induction of force fatigue, the causative factors of which did not appear to be the presence of fibre degeneration. However it must be borne in mind that

the histological stain (H&E) used to assess the morphology of the fibres cannot identify 'early damaging events i.e. loss of cytoskeletal proteins, which may be instructive in initiating stimulation-induced force fatigue.

Upon completion of the stimulation regime cessation of stimulation for 10 min evoked partial recovery of the proximal and distal forces but did not restore the length-force characteristics to their pre-fatigue state which continued to exhibit stimulation-induced alterations at either end of the EDL muscle.

Passive lengthening of the proximal EDL tendon induced disparities between maximal proximal and distal EDL forces with the magnitude of the disparity dependent on the fatigue status of the muscle.

This fatiguing regime altered the interaction between EDL proximal tendon lengths and distal TA-EHL forces. Comparable peak TA-EHL forces were recorded before and after stimulation, however before stimulation peak forces were attained at low while after stimulation peak forces were recorded at high proximal EDL tendon lengths.

Distal TA-EHL forces were significantly higher after the 'rest' period and these elevated forces were attained over the entire proximal EDL tendon length range tested i.e. low and high lengths.

It would appear that in the absence and presence of and recovery from force fatigue there is a relationship between proximal EDL tendon length and distal TA-EHL forces. Whether there is inter-muscular force transmission between these two muscles remains unresolved.

Subbing glass slides

Reagents

Subbing solution

0.1% (w/v) gelatine (BDH)

0.01% (w/v) potassium chromium sulphate (BDH)

Made up to a final volume of 200 ml (distilled water) and gently heated to dissolve.

Protocol

Prior to subbing the glass slides, they were cleaned using absolute alcohol and air dried at room temperature. Clean slides were then dipped into the subbing solution and dried overnight at room temperature.

Damage: Haematoxylin and eosin (H&E) stain.

Reagents

Haematoxylin Solution (Ehrlich's)

1% (w/v) haematoxylin (Difco)

100 ml absolute alcohol

100 ml glycerin (Sigma)

Made up to a final volume of 100ml (distilled water) and gently heated to dissolve. Cooled and filtered before used.

Eosin solution

1% aqueous solution

Alcohol solution 1

50% (v/v) absolute alcohol

Alcohol solution 2

70% (v/v) absolute alcohol

Alcohol solution 3

90% (v/v) absolute alcohol

Alcohol solution 4

100% (v/v) absolute alcohol

Protocol

Frozen cryostat sections were left at room temperature for 2-3 min to thaw. Slides were dipped quickly in tap water and incubated in haematoxylin solution for 5 min. Samples were gently washed in running tap water for approximately 1 min and then

incubated in eosin solution for 2 min. Slides were again quickly dipped in water. They were then incubated in alcohol solution 1 for 1 min, alcohol solution 2 for 2 min, alcohol solution 3 for 1 min and alcohol solution 4 for 2 min. Incubation in alcohol solution 4 was repeated twice. Incubation through graded alcohols progressively removed excess stain. Slides were incubated twice in xylene for 2 min, to dehydrate the samples. Sections were immediately mounted in DPX and left to dry at room temperature over night.

Result

Haematoxylin stained the sarcolemma nuclei dark blue-black. Eosin stained the sarcoplasm of the muscle fibres dark pink and the fibres of the connective tissue a paler pink.

Fibre type: Tunell and Hart stain (1977) with an alkali pre-incubation

Reagents

Pre-incubation solution (pH 7.25)

3.7% (v/v) formaldehyde

15% (w/v) $CaCl_2$

100 mM glycine

pH to 7.25.

ATP-incubating solution (pH 9.4)

100 mM 2-amino-2-methyl-1-propanol

50 mM KCl

18 mM $CaCl_2$ (added last to avoid precipitation)

2.7 mM ATP

Prepare fresh, pH to 9.4

$CaCl_2$ wash solution

1% (w/v) $CaCl_2$

Alkaline wash solution (pH 9.4)

100 mM 2-amino-2 methyl-1-propanol

Prepare fresh, pH to 9.4

Rinse solution (pH 7.8)

100 mM Tris

18 mM $CaCl_2$

pH to 7.8

Cobalt chloride solution

2% (w/v) cobalt chloride

Ammonium sulphide solution

0.5% (w/v) ammonium sulphide

Alcohol solution 1

50% (v/v) absolute alcohol

Alcohol solution 2

70% (v/v) absolute alcohol

Alcohol solution 3

90% (v/v) absolute alcohol

Alcohol solution 4

100% (v/v) absolute alcohol

Protocol

Frozen cryostat sections were left at room temperature for 2-3 min to thaw. Slides were incubated in pre-incubation solution for 7.5 min at room temperature. Slides were quickly rinsed in distilled water five times and then incubated twice in rinse solution for 1 min. Slides were incubated in ATP-incubating solution for 50 min at 37°C. Sections were rinsed in $CaCl_2$ wash solution three times for 30 sec. Slides were immersed in cobalt chloride solution for 3 min. Sections were rapidly rinsed in distilled water and then washed four times in alkali wash solution for 30 sec. Slides were immersed in ammonium sulphide solution for 3 min. Slides were washed in running tap water for 2 min. Slides were then brought through graded alcohol

solutions 1-4 once for 1 min periods. Slides were immersed twice in xylene for 2 min. Sections were mounted in DPX

Result

Type 1 fibres = white-pale staining, staining with lightest intensity

Type 2A fibres = a light grey staining, staining with intermediate intensity

Type 2B fibres = a black staining, staining with darkest intensity

Capillary density: Tunell and Hart stain (1977) with acid pre-incubation

Reagents

Acid pre-incubation solution (pH 3.8)

18 mM $CaCl_2$

3% (v/v) acetic acid

pH to 3.8

ATP-incubating solution (pH 9.4)

100 mM 2-amino-2-methyl-1-propanol

50 mM KCl

18 mM $CaCl_2$ (added last to avoid precipitation)

2.7 mM ATP

Prepare fresh, pH to 9.4

Rinse solution (pH 7.8)

100 mM Tris

18 mM $CaCl_2$

pH to 7.8

Protocol

Frozen cryostat sections were left at room temperature for a 2-3 min to thaw. Slides were incubated in acid pre-incubating solution for 10 mins at room temperature. Sections were washed twice in rinse solution for 1 min. Slides were incubated in ATP

incubating solution for 1 hour at 37°C. Slides were processed as previously described in Appendix 3 from the stage of incubation in ATP incubating solution.

Results

Capillaries were stained black and lay outside the sarcolemma of the muscle fibres. Fast and slow muscle fibres showed a negligible intensity of staining.

Myeloperoxidase (MPO) assay

Reagents

Solution 1 (pH 5.0)

0.05 M citrate phosphate buffer

pH to 5.0

Solution 2 (pH 5.5)

0.1 M sodium acetate

pH to 5.5

Solution 3

0.01 M 2,2'-azino-bis-diammonium salt

0.05 M citrate phosphate buffer pH 5.0

0.003 % (v/v) hydrogen peroxide

Protocol

50 mg of serial transverse muscle sections (20 μm) were cut using the cryostat (Bright Instrument Co. Ltd.). The cross-sectional area (number of squares / 20 μm) was used to estimate the number of transverse sections needed to give 50 mg of muscle. Muscle weight was approximated using this methodology to make the comparison between the MPO activity (marker of neutrophil content) and the H&E staining (percentage volume of damage tissue) more reliable.

Muscle (50 mg) was suspended in solution 1 and placed on ice. The resulting solution was homogenized using a hand held homogenizer for 1 min on ice. The muscle

homogenate was sonicated three times for 10 sec intervals. The homogenate was pipetted after each bout of sonication. The homogenate was centrifuged at 2,000 g for 25 min at room temperature. The resulting supernatant was diluted 1 in 10 in solution 1. 50 µl of the diluted muscle samples and 50 µl of solution 2 were pipetted into a 96-well Immulon II microtiter plate. 100 µl samples of standard purified human MPO (Sigma) were diluted across one lane of the microtiter plate in solution 2. 100 µl of solution 3 was added to each well immediately prior to reading the plates. The plates were allowed to develop at room temperature over 30 min during which time the optical density at 405 nm was measured with a microplate reader (Molecular Devices, UK) every 2 min. This allowed the most concentrated standard to reach peak absorbance values. It is important that the standards (purified human MPO) are within the range of the MPO concentration of the muscle samples being assayed. Each sample was assayed in duplicate wells. Background values were obtained by adding solution 3 alone to duplicate wells on the microtiter plate, negative controls were also included.

MPO activities in the samples were calculated from their relative change in absorbance and calibrated against a standard curve based on human MPO. Results were corrected for the weight of individual muscle samples and expressed as units of activity per gram (U/g).

Myosin purification

Reagents

1M Na phosphate buffer (pH 6.6)

1.5 M Na_2HPO_4 (base)

1 M $Na_2H_2PO_4$ (acid)

pH to 6.6

0.2 M ATP solution (pH 7.0)

0.2 M ATP dissolved in 0.1 M phosphate buffer

pH to 7.0, store at –20°C

Extraction buffer

0.3 M NaCl

0.1 NaH_2PO_4

50 mM Na_2HPO_4

10 mM $Na_4P_2O_4$

1 mM $MgCl_2$

10 mM EDTA

0.01% β-mercaptoethanol

Made up fresh and stored on ice

High salt buffer

0.5 M NaCl

1 M Na phosphate buffer, pH 6.6

Protocol

All steps in this protocol were performed on ice or at 4°C. Frozen muscle samples were pulverised using a pestle and mortar pre-cooled with liquid nitrogen. Pulverised tissue was incubated in four volumes of chilled extraction buffer for 30 min on ice. The solution was centrifuged at 10,000 rpm for 10 min at 4°C. The actomyosin in the supernatant was precipitated by the addition of 10 volumes of ice-cold water over 2 hours. The suspension was centrifuged at 12,000 rpm for 15 min at 4°C and the pellet was collected. The pellet was re-suspended in 0.01M sodium phosphate buffer, pH 6.6, containing 0.45 M NaCl and stirred on ice for 15 min. To dissociate actin from myosin, 18 mM $MgCl_2$ and 9 mM ATP were added and stirred for a further 30 min on ice. Myosin and actin were precipitated out at levels of 30, 40 and 55% saturated ammonium sulphate. The resulting suspensions were spun down at 12,000 rpm for 10 min at 4°C and the pellets were re-suspended in high salt buffer. All samples were dialysed against high salt buffer over night at 4°C. The dialysis membrane (Fisons UK) had a diameter of 6 mm and a molecular weight cut off of 12-14,000 Daltons. It was pre-treated by boiling for 10 minutes in 1 mM EDTA, 0.48 M $NaHCO_3$, rinsed with distilled water and boiled for further 10 min in 1 mM EDTA alone. The following day the myosin was divided between several eppendorfs. A small aliquot was removed for a protein assay and SDS was added to the remainder at a concentration of 0.5% for the light chain analysis.

SDS polyacrylamide gel electrophoresis (SDS-PAGE) of myosin light chain (MLC) isoforms

Reagents

4X separating gel buffer

1.5 M Tris-HCl, pH 8.8

0.4% (w/v) SDS

4X stacking gel buffer

0.5 M Tris-HCl, pH 6.8

0.4% (w/v) SDS

10X electrophoresis buffer

0.25 M Tris

1.92 M glycine

1% (w/v) SDS

3X dissociating buffer

0.18 M Tris-HCl, pH 6.8

3% (w/v) SDS

30% (w/v) glycerol

15% (w/v) β-mercaptoethanol

0.01% (w/v) bromophenol blue

30% (w/v) acrylamide, filtered

1% (w/v) methylene bis-acrylamide, filtered

tetramethylethylene diamine (TEMED)

10% (w/v) ammonium persulphate (AMPS), freshly prepared

Protocol

Separating gel

30% acrylamide	16.6 ml
1% BIS	4.0 ml
4X separating gel buffer	10.0 ml
H_2O	9.28 ml
10% AMPS	0.11 ml
TEMED	0.011 ml

Added and mixed in the above order

Stacking gel

30% acrylamide	1.67 ml
1% BIS	1.3 ml
4X stacking gel buffer	2.5 ml
H_2O	4.5 ml
10% AMPS	0.03 ml
TEMED	0.005 ml

Added and mixed in the above order

Gels 1.5 mm thick were set in the Protean II system (Biorad Laboratories Ltd., Hemel Hempstead). 10 cm of separating gel was poured avoiding bubbles and covered with 1 ml of water. The gel was allowed set, 1 ml of water drained off and the top of the

separating gel was washed with water. 2 cm of stacking gel was added and a 15-well comb inserted. After the stacking gel had set the comb was removed, the gel was washed with distilled water and clamped into the Protean II apparatus.

Myosin samples were mixed 2:1 (v/v) with dissociating buffer, and heated in a boiling water bath for 3-4 min. Samples were added to the wells in volumes that gave approximately equal protein concentrations. Gels were run in 1X electrophoresis buffer at a current of 30-40 mA until the bromophenol blue front had reached the bottom of the gel.

Staining polyacrylamide gels

Gels were stained for 1 hour in 0.25% Coomassie Blue R250 dye (Sigma Cat. No. B 8647) (w/v) in de-stain solution (methanol: water: glacial acetic acid, 5:5:1) at room temperature with gently rocking. The dye was eluted from the gel with 2-3 changes of de-stain over a period of 24 hours at room temperature with rocking. Gels were viewed on a light box and stored in plastic boxes with de-stain solution or water.

Acker, M. A., Hammond, R., Mannion, J. D., Salmons, S. & Stephenson, L. W. (1986). An autologous biologic pump motor. *J. Thorac. Cardiovasc. Surg.* **12**, 733-746.

Aigner, S., Gohlsch, B., Hamalainen, N., Staron, R.S., Uber, A., Wehrle, U. & Pette, D. (1993). Fast myosin heavy chain diversity in skeletal muscles of the rabbit: heavy chain IId, not IIb predominates. *Eur. J. Biochem.* **211**, 367-372.

Anderson, D. R., Pochettino, A., Hammond, R. L., Hohenhaus, E., Spanta, A. D., Bridges, C. R., Jr., Lavïne, S., Bhan, R. D., Colson, M. & Stephenson, L. W. (1991). Autogenously lined skeletal muscle ventricles in circulation. Up to nine months' experience. *J. Thorac Cardiovasc. Surg.* **101**, 661-670.

Armstrong R. B., Duan C., Delp, M. D., Hayes, D. A., Glenn, G. M. & Allen, G. D. (1993). Elevations in rat sloeus muscle [Ca^{2+}] with passive stretch. *J. Appl. Physiol.* **74**, 2990-2997.

Armstrong, R. B., Ogilvie, R. W. & Schwane, J. A. (1983). Eccentric exercise induced injury to rat skeletal muscle. *J. Appl. Physiol.* **54**, 80-93.

Armstrong, R. B., Warren, G. L. & Warren, J. A. (1991). Mechanisms of exercise-induced muscle fibre injury. *Sports Med.* **12**, 184-207.

Bagge, U., Amundson, B. & Lauritzen, A. (1980). White blood cell deformability and plugging of skeletal muscle capillaries in hemorrhagic shock. *Acta. Physiol. Scand.* **108**, 159-63.

Bajd, T., Kralj, A., Turk R. & Munih, M. (1991). Control of FES walking in incomplete SCI patients. In *Basic and Applied Mycology: Perspectives for the 90's* (ed. U. Carraro & S. Salmons), pp. 319-327. Padua: Unipress.

Bär, D. P. R., Rodenburg, A. J. B., Koot, R. W. & Amelink, *H.G.J. (1994). Exercise-*induced muscle damage: recent developments. *BAM* **4**, 5-16.

Baracos, V. E. & Goldberg, A. L. (1986). Maintenance of normal length improves protein balance and energy status in isolated rat skeletal muscles. *Am. J. Physiol.* **251**, C588-C596.

Barnard, E. A., Barnard P.J., Jarvis, J.C. & Lai, J. (1986). Low-frequency chronic electrical stimulation of normal & dystrophic chicken muscle. *J. Physiol.* **376**, 377-409.

Bárány, M. (1967). ATPase activity of myosin correlated with speed of muscle shortening. *J. Gen. Physiol.* **50**, 197-218.

Belcastro, A. N. (1993). Skeletal muscle calcium-activated neutral protease (calpain) with exercise. *J. Appl. Physiol.* **73**, 1381-1386.

Belcastro, A. N., Arthur, G. D., Albisser, T. A. & Raj, D. A. (1996). Heart, liver, and skeletal muscle myeloperoxidase activity during exercise. *J. Appl. Physiol.* **80**, 1331-1335.

Belcastro, A. N., Shewchuk, L. D. & Raj, D.A. (1998). Exercise-induced muscle injury: A calpain hypothesis. *Mol. Cell. Biochem.* **179**, 135-45.

Best, T. M., Fiebig, R., Corr, D. T., Brickson, S. & Ji, L. (1999). Free radical activity, antioxidant enzyme, and glutathione changes with muscle stretch injury in rabbits. *J. Appl. Physiol.* **87**, 74-82.

Biral, D., Sandri, M. &·Jakubiec-Puka, A. (1998). The fate of dystrophin and some signs of apoptosis in the skeletal muscle work-overloaded in extension. *Basic Appl. Myol.* **8**, 205-210.

Bottinelli, R., Schiaffino, S. & Reggiani, C. (1991). Force-velocity relationship and myosin heavy chain isoform composition of skinned fibres from rat skeletal muscle. *J. Physiol.* **437**, 655.

Bozeman, P. M., Learn, D. B. & Thomas, E. L. (1990). Assay of the human leukocyte enzymes myeloperoxidase and eosinophil peroxidase. *J. Immuno. Methods* **126**, 125-133.

Bradford, M. (1976). A rapid and sensitive method for the quantitation of microgram quantities of protein utilizing the principle of protein-dye binding. *Anal. Biochem.* **72**, 248-54.

Bradley, P. P., Priebat, D. A., Christensen, R. D. & Rothstein, G. (1982). Measurement of cutaneous inflammation: estimation of neutrophil content with an enzyme marker. *J. Invest. Derma.* **78**, 206-209.

Brand, R. A., Pedersen, D. R. & Friederich, J. A. (1986). The sensitivity of muscle force predictions to changes in physiologic cross-sectional area. *J. Biomecha.* **19**, 589-93.

Brandl, C.J., Green, M.N., Korczak, B. & MacLennan, D.H. (1986). Two Ca^{2+} ATPase genes: homologies and mechanistic implications of deduced amino acid sequences. *Cell.* **44**, 597-607.

Brennan. J. E., Chao, D. S., Xia, H., Aldape, K. & Bredt, D. S. (1995). Nitric oxide synthase complexed with dystrophin and absent from skeletal muscle sarcolemma in Duchenne muscular dystrophy. *Cell* **82**, 743-52.

Briggs, N. F., Lee, F. K., Feher, J. J., Welscher, A. S., Ohlendieck, K. & Campbell, K. (1990). Ca-ATPase isozyme expression in sarcoplasmic reticulum is altered by chronic stimulation of skeletal muscle. *FEBS* **259**, 269-272.

Brooke, M.H. & Kaiser, K.K. (1970). Muscle fibre types: How many and what kind? *Arch. Neurol.* **23**, 369-379.

Brooks, S. V., Zerba, E. & Faulkner, J. A. (1995). Injury to muscle fibres after single stretches of passive and maximally stimulated muscles in mice. *J. Physiol.* **488**, 459-69.

Brown, J.M.C., Henrikkson, J. & Salmons, S. (1989). Restoration of fast muscle characteristics following cessation of chronic stimulation: physiological, histochemical and metabolic changes during fast to slow transitions. *Proc. R. Soc. Lond.* **235B**, 321-346.

Brown, M. D., Cotter, M. A., Hudlicka, O. & Vrbová, G. (1976). The effects of different patterns of muscle activity on capillary density, mechanical properties and structure of slow and fast rabbit muscles. *Pflugers Arch. 361, 241-250.*

Brown, M.D., Hudlická, O., Makki, R.F. & Weiss, J.B. (1995). Low-molecular-mass endothelial cell-stimulating angiogenic factor in relation to capillary growth induced in rat skeletal muscle by low-frequency electrical stimulation. *Int. J. Microcirc. Clin. Exp.* **15**, 111-116.

Brown, W. E., Salmons, S. & Whalen, R. G. (1983). The sequential replacement of myosin subunit isoforms during muscle type transformation induced by long term electrical stimulation. *J. Biol. Chem.* **258**, 14686-14692.

Brown, W. E., Salmons, S. & Whalen, R.G. (1985). Mechanisms underlying the asynchronous replacement of myosin light chain isoforms during stimulation-induced fiber-type transformations of skeletal muscle. *FEBS Lett.* **192**, 235-238.

Brownson, C., Little, P., Jarvis, J.C. & Salmons, S. (1992). Reciprocal changes in myosin isoform mRNAs of rabbit skeletal muscle in response to initiation and cessation of chronic stimulation. *Muscle & Nerve* **15**, 694-700.

Bruton, J. D., Lännergren, J. & Westerblad, H. (1998). Mechanisms underlying the slow recovery of force after fatigue: importance of intracellular calcium. *Acta. Physiol. Scand.* **162**, 285-93.

Buller, A.J., Eccles, J.C. & Eccles, R.M. (1960). Interactions between motoneurons and muscles in respect of the characteristic speeds of their response. *J. Physiol.* **150**, 417-439.

Burke, R.E, Levine, D.N., Tsairis, P. & Zajac, F.E. (1973). Physiological types and histochemical profiles of motor units in the cat gastrocnemius. *J. Physiol.* **234**, 723-748.

Bury, T. B. & Pirany, F. (1995). Effect of prolonged exercise on neutrophil MPO secretion. *Int. J. Sports Med.***16**, 410-2.

Bushell, A., Klenerman, L., Davies, H., Grierson, I. & Jackson, M. J. (1996). Ischemia-reperfusion-induced muscle damage. *Acta. Orthop. Scand.* **67**, 393-98.

Cadefau, J. A., Parra, J., Cusso, R., Heine, G. & Pette, D. (1993). Responses of fatiguable and fatigue-resistant fibres of rabbit muscle to low frequency. *Pfluegers Arch.* **424**, 529-37.

Chi, M. M-Y, Hintz C.S., Coyle E.F., Martin W.H., Ivy, J.L., Nemeth, P.M., Holloszy, J.O. & Lowry, O.H. (1983). Effects of detraining on enzymes of energy metabolism in individual human muscle fibres. *Am. J. Physiol. (Cell Physiol. 23)* **244**, C276-C287.

Chin, E. R., Green, H. J., Grange, F., Mercer, J. D. & O'Brien, P. J. (1995). Effects of prolonged low frequency stimulation on skeletal muscle sarcoplasmic reticulum. *Can. J. Physiol. Pharmacol.* **73**, 1154-64.

Cotter, M., Hudlicka, O., Pette, D., Staudte, H. & Vrbová, G. (1973). Changes of capillary density and enzyme pattern in fast rabbit muscles during long-term stimulation. *J. Physiol.* **230**, 34-35P.

Clarkson, P.M. & Tremblay, I. (1988). Exercise-induced muscle damage, repair, and adaptation in humans. *J. Appl. Physiol.* **65**, 1-6.

Degens H. & Veerkamp J. H. (1994). Changes in oxidative capacity and fatigue resistance in skeletal muscle. *Int. J. Biochem.* **26**, 871-878.

Dufaux, B. & Order, U. (1989). Plasma elastase-alphal-antitrypsin, neopterin, tumour necrosis factor, and soluble interleukin-2 receptor after prolonged exercise. *Int. J. Sports Med.* **10**, 434-438.

Dux, L., Green H. J. & Pette, D. (1990) Chronic low-frequency stimulation of rabbit fast-twitch muscle induces partial inactivation of the sarcoplasmic reticulum Ca^{2+}-ATPase and changes in its tryptic cleavage. *Europ. J. Biochem.* **195**, 92-100

Ebashi, S., Endo, M. & Ohtsuki, I. (1969). Control of muscle contraction. *Rev. Biophys.* **2**, 351-384.

Ebbeling, C. B. & Clarkson, P. M. (1990). Muscle adaptation prior to recovery following eccentric exercise. *Eur. J. Appl. Physiol.* **60**, 26-31.

Eccles, J.C., Eccles, R.M. & Lundberg, A. (1958). The action potentials of the alpha motoneurones supplying fast and slow muscles. *J. Physiol.* **142**, 275-291.

Edman, K. A. P. & Lou, F. (1990). Changes in force and stiffness induced by fatigue and intracellular acidification in frog muscle fibres. *J. Physiol.* **424**, 133-49.

Edwards, S. W., Nurcombe, H. L. & Hart, A. C. (1987). Oxidative inactivation of myeloperoxidase released from human neutrophils. *Biochem. J.* **245**, 925-928.

Eisenberg, B. R., Brown, J. M. C. & Salmons, S. (1984). Restoration of fast muscle characteristics following cessation of chronic stimulation. *Cell tissue Res.* **238**, 221-230.

Eisenberg, B. R. & Salmons, S. (1981). The re-organization of subcellular structure in muscle undergoing fast to slow type transformation. *Cell Tiss. Res.* **220**, 449-471.

Faulkner, J. A., Brooks, S. V. & Opiteck, J. A. (1993). Injury to skeletal muscle fibres during contractions: conditions of occurrence and prevention. *Phys. Ther.* **73**, 911-21.

Fitts, R. H. (1994). Cellular mechanisms of muscle fatigue. *Physiol. Rev.* **74**, 49-94.

Franchi, L. L., Murdoch, A., Brown, W. E., Mayne, C. N., Elliot, L. & Salmons, S. (1990). Subcellular localisation of newly incorporated myosin in rabbit fast skeletal muscle undergoing stimulation-induced type transformation. *J. Musc. Res. Cell Motil.* **11**, 227-239.

Frey, M., Thoma, H., Gruber, H., Stöhr, H. & Havel, M. (1986). The chronically stimulated psoas muscle as an energy source for artificial organs: an experimental study in sheep. In *Biomechanical cardiac. Assist. Cardiomyoplasty and muscle-powered devices.* (ed. R. C. Chiu), pp, 179-191. Mount Kisco, New York: Futura Publishing Company.

Fridèn, J. (1984). Changes in human skeletal muscle induced by long term eccentric exercise. *Cell Tissue Res.* **236**, 365-72.

Fridén, J. & Lieber, R.L. (1992). Structural and mechanical basis of exercise-induced damage. *Med. Sci. Sports Exerc.* **24**, 521-530.

Glenn, W. W. L., Hogan, J. F., Loke, J. S. O., Cieselski, T. E., Phelps, M. L. & Rowedder, R. (1984). Ventilatory support by pacing of the conditioned diaphragm in quadriplegis. *New Eng. J. Med.* **310**, 1150-1155.

Goldstein, M. A., Schroeter, J. P. & Michael, L. H. (1991). Role of the Z band in the mechanical properties of the heart. *FASEB J.* **5**, 2167-74.

Gollnink, P.D., Timson, B.F., Moore, R.L. & Reidy, M. (1981). Muscular enlargement and number of fibres in skeletal muscles of rat. *J. Appl. Physiol.* **50**, 936-943.

Gordon, A.M., Huxley, A.F. & Julian, F. J. (1966). The variation in isometric tension with sarcomere length in vertebrate muscle fibres. *J. Physiol.* **184**, 170-192.

Gorza, L. (1990). Identification of a novel type 2 fibre population in mammalian skeletal muscle by combined use of histochemical myosin ATPase and anti-myosin monoclonal antibodies. *J. Histochem. Cytochem.* **38**, 257-265.

Gray, A. B., Telford, R. D. Collins, M., Baker, M. S. & Weidemann, M. J. (1993). Granulocyte activation induced by intense interval running. *J. Leuc. Biol.* **53**, 591-597.

Green, H. J., Düsterhöft, S., Dux, L. & Pette, D. (1992). Metabolite patterns related to exhaustion, recovery, and transformation of chronically stimulated rabbit fast-twitch muscle. *Pflugers Arch.* **420**, 359-66

Green, H. J & Pette, D. (1997). Early metabolic adaptations of rabbit fast twitch muscle to chronic low frequency stimulation. *Eur. J. Appl. Physiol.* **75**, 418-24.

Guth, L. & Samaha, F. J. (1970). Procedure for histochemical demonstration of actomyosin ATPase. *Exper. Neurol.* **28**, 365-67.

Harris, K., Walker, P. M., Mickle, A. G., Harding, R., Gatley, R., Wilson, G. J., Kuzon, B., Mc Kee, N. & Romaschin, A. D. (1986). Metabolic response of skeletal muscle to ischemia. *Am. J. Physiol.* **250** (Heart Circ Physiol 19), H213-H220.

Heilig, A. & Pette, D. 1980 Changes induced in the enzyme activity pattern by electrical stimulation of fast-twitch mucle. In *Plasticity of Muscle* (ed. D. Pette), pp. 409-420. Berlin: Walter de Gruyter.

Heilmann, C. & Pette, D. (1979). Molecular transformations in sarcoplasmic reticulum of fast-twitch muscle by electro-stimulation. *Eur. J. Biochem.* **93**, 437-446.

Henriksson, J., Chi, M. M-Y., Hintz, C. S., Young, D. A., Kaiser, K. K., Salmons, S. & Lowry, O. H. (1986). Chronic Stimulation of mammalian muscle: changes in enzymes of six metabolic pathways. *Am. J. Physiol.* **251** (Cell Physiol. 20), C616-C632.

Hicks, A., Ohlendieck, K., Göpel, S. O. & Pette, D. (1997). Early functional and biochemical adaptations to low-frequency stimulation of rabbit fast-twitch muscle. *Am. J. Physiol.* **273** (Cell Physiol. 42), C297-305.

Howell, J. N., Chelboun, G. & Conaster, R. (1993). Muscle stiffness, strength loss and swelling and soreness following exercise-induced injury in humans. *J. Physiol.* **464**, 183-196.

Hudlicka, O., Tyler, K. R., Srihari, T., Heilig, A. & Pette, D. (1982). The effect of different patterns of long-term stimulation on contractile properties and myosin light chains in rabbit fast muscles. *Eur. J. Physiol.* **393**, 164-170.

Huijing, P. A. (1999a). Muscular force transmission: A unified, dual or multiple system? A review and some explorative experimental results. *Arch. Physiol. Biochem.* **107**, 292-311.

Huijing, P. A. (1999b). Muscle as a collagen fibre re-inforced composite material: Force transmission in muscle and in whole limbs. *J. Biomech.* **32**, 329-345.

Huijing, P. A. & Baan, G. C. (2000). Extra-muscular myofascial force transmission within the rat anterior tibial compartment: Proximo-distal differences in muscle force. ***In press***

Huijing, P. H., van Lookeren Campagne, A. A. & Kooper, J. F. (1989). Muscle architecture and fibre characteristics of rat gastrocnemius and semimembranous muscles during isometric contractions. *Acta. Anat. (Basel)* **135**, 46-52.

Iwahori, Y., Ishiguro, N., Shimizu, T., Kondo, S., Yabe, Y., Oshima, T., Iwata, H. & Sendo, F. (1998). Selective neutrophil depletion with monoclonal antibodies attenuates ischemia/reperfusion injury in skeletal muscle. *J. Reconstr. Microsurg.* **14**, 109-16.

Jarvis, J. C. (1993). Power production and working capacity of rabbit tibialis anterior muscles after chronic electrical stimulation at 10 Hz. *J. Physiol.* **470**, 157-169.

Jarvis, J. C. & Salmons, S. (1991). A family of neuromuscular stimulators with optical transcutaneous control. *J. Med. Eng. Technol.* **15**, 53-57.

Jarvis, J. C., Sutherland, H., Mayne, C. N., Gilroy, S. J. & Salmons S. (1996). Induction of fast-oxidative phenotype by chronic muscle stimulation: mechanical and biochemical studies. *Am. J. Physiol.* **270**, C306-C312.

Jones, J., Emmanuel, J., Sutherland, H., Jackson M. J., Jarvis J. C. & Salmons, S. (1997). Stimulation-induced skeletal muscle damage: cytoprotective effect of pre-stimulation. *Basic Appl. Myol.* **7**, 39-44.

Jones, D. A. & Round, J. M. (1994). Human muscle damage as a result of eccentric exercise or reperfusion injury: a common mechanism? *BAM* **4**, 51-58.

Jorgensen, A. O., Arnold, W., Pepper, D. R., Kahl, S. D., Mandel, F. & Campbell, K. P. (1988). A monoclonal antibody to the Ca^{2+}-ATPase of cardiac sarcoplasmic reticulum cross-reacts with slow type I but not with fast type II canine skeletal muscle fibres: An immunochemical study. *Cell Motil. Cytoskeleton* **9**, 64-174.

Komulainen, J., Takala, T. E. S., Kuipers, H. & Hesselink, M. K. C. (1998). The disruption of myofibre structures in rat skeletal muscle after forced-lengthening contractions. *Pflugers Arch – Eur. J. Physiol.* **436**, 735-741.

Korge P. & Campbell K.B. (1994) Local ATP generation is important for sarcoplasmic reticulum calcium pump function. *Am. J. Physiol.* **267** (Cell Physiol. 36), C357-C366.

Korthuis, R. J., Granger, D. N, Townsley, M. I & Taylor, A. E. (1985). The role of oxygen-derived free radicals in ischemia-induced increases in canine skeletal muscle vascular permeability. *Circ. Res.* **57**, 599-609.

Korthuis, R. J., Grisham, M. B. & Granger, D. N. (1988). Leukocyte depletion attenuates vascular injury in post-ischemic skeletal muscle. *Am. J. Physiol.* **254** (Heart Circ Physiol 23), H823-H827.

Laemmli, U. K. (1970). Cleavage of structural proteins during the assembly of the head of bacteriophage T4. *Nature (Lond.)* **227**, 680-685.

Lai, C. C. (1999). Induction of heat-shock protein 72 in rat skeletal muscle does not increase tolerance to ischemia-reperfusion injury. *Muscle Nerve* **22**, 390-3.

Leberer, E., Härtner, K. T., Brandl, C. J., Fujii, J. & Tada, M. (1989). Slow/cardiac sarcoplasmic reticulum Ca^{2+}-ATPase and phospholamban mRNAs are expressed in chronically stimulated rabbit fast-twitch muscle. *Eur. J. Biochem.* **185**, 51-54.

Leberer, E., Härtner, K. T. & Pette, D. (1987). Reversible inhibition of sarcoplasmic reticulum CA-ATPase by altered neuromuscular activity in rabbit fast twitch muscle. *Europ. J. Biochem.* **162**, 555-61.

Lehrer, R. I. & Ganz, T. (1990). Antimicrobial polypeptides of human neutrophils. *Blood* **76**, 2169-2181.

Lexell, J., Jarvis, J. C., Currie, J., Downham, D. Y. & Salmons, S. (1994). Fibre type composition of rabbit tibialis anterior and extensor digitorium longus muscles. *J. Anat.* **185**, 95-101.

Lexell, J., Jarvis, J. C., Downham, D. Y. & Salmons, S. (1992). Quantitative morphology of stimulation-induced damage in rabbit fast-twitch skeletal muscles. *Cell Tiss. Res.* **269**, 195-204.

Lexell, J., Jarvis, J. C., Downham, D. Y. & Salmons, S. (1993). Stimulation-induced damage in rabbit fast-twitch skeletal muscles: a quantitative morphological study of the influence of the influence of pattern and frequency. *Cell Tiss. Res.* **273**, 357-62.

Lexell, J. & Taylor, C. C. (1991). Fiber density: a fast and accurate way to estimate human muscle fiber areas. *Muscle Nerve* **14**, 476-477.

Lieber, R. L. (1992). Skeletal muscle structure and function: implications for rehabilitation and sport medicine. Baltimore, MD Williams and Wilkins.

Lieber, R. L. & Friden, J. (1993). Muscle damage is not a function of muscle force but active muscle strain. *J. Appl. Physiol.* **74**, 520-6.

Lowey, S., Waller, G. S. & Trybus, K.M. (1993). Skeletal muscle myosin light chains are essential for physiological speeds of shortening. *Nature* **365**, 454-456.

Lynn, R. & Morgan, D.L. (1994). Decline running produces more sarcomeres in rat vastus intermedius muscle fibres than does incline running. *J. Appl. Physiol.* **77**, 1439-44.

Maier, A. & Pette, D. (1997). The time course of glycogen depletion in single fibres of chronically stimulated rabbit fast-twitch muscle. *Pflugers Arch.* **408**, 338-342.

Mayne, C. N., Anderson, W. A., Hammond, R. L., Eisenberg, B. R., Stephenson, L. W. & Salmons, S. (1991). Correlates of fatigue resistance in canine skeletal muscle stimulated electrically for up to one year. *Am. J. Physiol.* **261** (Cell Physiol. 30), C259-C270.

Mayne, C. N., Jarvis, J. C. & Salmons, S. (1991). Dissociation between metabolite levels and force fatigue in the early stages of stimulation-induced transformation of mammalian skeletal muscle. *BAM* **1**, 63-70.

Mayne, C. N., Mokrusch, T., Jarvis, J. C., Gilroy, S. J. & Salmons S. (1993). Stimulation-induced expression of slow myosin in a fast muscle of the rat. *FEBS* **327**, 297-300.

Mayne, C. N., Sutherland, H., Jarvis, J. C., Gilroy, S. J., Craven, A. J. & Salmons, S. (1996). Induction of a fast-oxidative phenotype by chronic muscle stimulation: histochemical and metabolic studies. *Am. J. Physiol.* **270** (Cell Physiol. 39), C313-C320.

McArdle, A. & Jackson, M. J. (1994). Intracellular mechanisms involved in damage to skeletal muscle. *BAM* **1**, 43-50.

Mc Hugh, M. P., Connolly D. A. J., Eston, R. G. & Gleim G. W. (1999). Exercise-induced muscle damage and potential mechanisms for the repeated bout effect. *Sports Med.* **23**, 157-170.

Meijer, K., Grootenboer, H. F., Koopman, J. M. & Huijing, P. A. (1997). Isometric length-force curves during and after concentric contractions differ from the initial isometric length-force curve in rat muscle. *J. Appl. Biomech.* **24**, 163-7.

Monti, R. J., Roy, R. R., Hodgson, J. A. and Edgerton, V. R. (1999). Transmission of forces within mammalian skeletal muscles. *J. Biomech.* **32**, 371-380.

Morgan, D. L. (1990). New insights into the behaviuor of muscle during active lengthening. *Biophys. J.* **57**, 209-2.

Moss, R. L., Diffee, G. M. & Greaser, M. L. (1995). Contractile properties of skeletal muscle fibres in relation to myofibrillar protein isoforms. *Rev. Physiol. Biochem. Pharmacol.* **126**, 1-63.

Neufer, D. P., Ordway, G. A., Hand, G. A., Shelton, M., Richardson, J. A., Benjamin, I. J., and Williams, R. S. Continuous contractile activity induces fibre type specific expression of HSP 70 in skeletal. (1996). *Am. J. Physiol.* **271** (Cell Physiol 40), C1828-37.

Newham, D. J., Jones, D. A & Clarkson, P. M. (1987). Repeated high-force eccentric exercies: effects on muscle pain and damage. *J. Appl. Physiol.* **63**, 1381-1386.

Nosaka, K. & Clarkson, P. M. (1995). Muscle damage following repeated bouts of high force eccentric exercise. *Med. Sci. Sports Exerc.* **27**, 1263-1269.

Oakley, R. M. E. & Jarvis, J. C. (1994). Cardiomyoplasty: a critical review of experimental and clinical results. *Circulation* **90**, 2085-2090.

Ohlendieck, K., Briggs, N. F., Lee, F. K., Wechsler, A. W. & Campbell K. P. (1991). Analysis of excitation-contraction-coupling components in chronically stimulated canine skeletal muscle. *Eur. J. Biochem.* **202**, 739-47.

Ornatsky, O. I., Connor, M. K. & Hood, D. A. (1995). Expression of stress proteins and mitochondrial chaperonins in chronically stimulated skeletal muscle. *Biochem. J.* **311**, 119-123.

Papanastasiou, S., Estdale, S. E., Homer-Vanniasinkam, S. & Mathie, R. T. (1999). Protective effect of pre-conditioning and adenosine pre-treatment in experimental skeletal muscle reperfusion injury. *Br. J. Surg.* **86**, 916-22.

Patel, T. J., Cuizon, D., Mathieu-Costello, O., Friden, J. & Lieber, R. L. (1998). Increased oxidative capacity does not protect skeletal muscle fibres from eccentric contraction-induced injury. *Am. J. Physiol.* **274**, R1300-8.

Patel, T. J. & Lieber, R. L. (1997). Force transmission in skeletal muscle:From actomyosin to external tendons. *Exec. Sports Sci. Review* **25**, 321-63.

Pattison, C. W., Cumming, D. V. E., Williamson, A., Clayton Jones D., Dunn, M. J., Goldspink, G. & Yacoub, M. (1991). Aortic counterpulsation for up to 28 days with autologous latissimus dorsi in sheep. *J. Thorac. Cardiovasc. Surg.* **102**, 766-773.

Peter, J. B., Barnard, R. J., Edgerton, V. R., Gillepsie, C. A. & Stempel, K. E. (1972). Metabolic profile of three fibre types of skeletal muscle in guinea pigs and rabbit. *Biochemistry* **11**, 2627-2633.

Pette, D., Muller, W., Leisner, E. & Vrbová, G. (1976). Time dependent effects on contractile properties, fibre population, myosin light chains and enzymes of energy metabolism in intermittently and continuously stimulated fast twitch muscles of the rabbit. *Eur. J. Physiol.* **364**, 103-112.

Pette, D., Smith, M. E., Staudte, H. W. & Vrbová, G. (1973). Effects of long-term electrical stimulation on contractile and metabolic characteristics of fast rabbit muscle. *Eur. J. Physiol.* **338**, 257-272.

Pette, D. & Staron, R. S. (1990). Cellular and molecular diversities of mammalian skeletal muscle fibers. *Rev. Physiol. Biochem. Pharmacol.* **116**, 1-76.

Pette, D. & Vrbová, G. (1992). Adaptation of mammalian skeletal muscle fibres to chronic electrical stimulation. *Rev. Physiol. Biochem. Pharmacol.* **120**, 116-190.

Phan, L. H., Hickey, M. J., Niazi, Z. B. M. & Stewart, A. G. (1994). Nitric oxide synthase inhibitor, nitro-iminoethyl-L-ornithine, reduces ischemia-reperfusion injury in rabbit skeletal muscle. *Microsurgery* **15**, 703-707.

Pochettino, A., Anderson, D. R., Hammond, R. L., Spanta, A., Hohenhaus, E., Niinami, H., Huiping, L., Ruggiero, R., Hooper, T. L., Baars M., Devireddy, C. & Stephenson, L. W. (1991). Skeletal muscle ventricles: a promising treatment option for heart failure. *J. Cardiac. Surg.* **6**, 1-9.

Purslow, P. & Duance V. C. (1991). Structure and function of intramuscular connective tissue. In *Connective tissue matrix,* Vol. 2 (ed. Hukins, D. W. L.) pp 127-66. London, MacMillan Press.

Purslow, P. P. & Trotter J. A. (1994). The morphology and mechanical properties of endomysium in series-fibred muscles: variations with muscle length. *J. Mus. Res. Cell Motil.* **15**, 299-308.

Pyne, D. B. (1994). Regulation of neutrophil function during exercise. *Sports Med.* **17**, 245-258.

Radák, J., Asano, K., Inoue, M., Kizaki, T., Oh-Ishi, S., Suzuki, K., Taniguchi, N. & Ohno, H. (1995). Superoxide dismutase derivative reduces oxidative damage in skeletal muscle of rats during exhaustive exercise. *J. Appl. Physiol.* **79**, 129-135.

Raj, D. A., Booker, T. S. & Belcastro, A. N. (1998). Striated muscle calcium-stimulated cysteine protease (calpain-like) activity promotes myeloperoxidase activity with exercise. *Pflugers Arch.* **435**, 840-9.

Rayment, I., Rypniewski, W. R., Schmidt-Base, K., Smith, R., Tomchick, D. R., Benning, M. M., Winkelmann, D. A., Wesenberg, G. & Holden, H. M. (1993). Three-dimensional structure of myosin subfragment-1: a molecular motor. *Science* **261**, 50-58.

Reichmann, H. & Pette, D. (1982). A comparative study of succinate dehydrogenase activity levels in type 1, type 2A and type 2B fibres of mammalian and human muscles. *Histochem.* **74**, 27-41.

Reiser, P. J., Kline, W. O. & Vaghy P. L. (1997). Induction of neuronal type nitric oxide synthase in skeletal muscle by chronic stimulation *in vivo*. *J. Appl. Physiol.* **82**, 1250-1255.

Romanul, F. C. A. (1965). Capillary supply and metabolism of muscle fibres. *Arch. Neurol.* **12**, 497-507.

Rowe, R. W. (1981). Morphology of perimysial and endomysial connective tissue in skeletal muscle. *Tissue Cell* **13**, 681-90.

Roy, R. R., Meadows I. D., Baldwin K. M. & Edgerton, V. R. (1982). Functional significance of compensatory overloaded rat fast muscle. *J. Appl. Physiol.* **52**, 473-478.

Salmons, S. (1967). An implantable electrical stimulator. *J. Physiol.* **188**, 13-14P.

Salmons, S. 1980 The response of skeletal muscle to different patterns of use – some new developments and concepts. In *Plasticity of Muscle.* (ed. D. Pette), pp.387-399. Berlin: Walter de Gruyter.

Salmons, S. (1990). On the reversibility of stimulation-induced muscle transformation. In *The Dynamic State of Muscle Fibres* (ed. D. Pette), pp.401-414. Berlin: Walter de Gruyter.

Salmons, S., Gale, D. R. & Sréter, F. A. (1978). Ultrastructural aspects of the transformation of muscle fibre type by long term stimulation: changes in Z-discs and mitochondria. *J. Anat.* **127**, 17-31.

Salmons, S. & Henrikkson, J. (1981). The adaptive response of skeletal muscle to increased use. *Muscle Nerve* **4**, 94-105.

Salmons, S. & Jarvis, J. C. (1991). Simple optical switch for implantable devices. *Med. Biol. Engng. Comput.* **29**, 554-556.

Salmons, S. & Jarvis, J. C. (1992). Cardiac assistance from skeletal muscle: a critical appraisal of the various approaches. *Br. Heart J.* **68**, 333-338.

Salmons, S & Sréter, F. A. (1976). Significance of impulse activity in the transformation of skeletal muscle type. *Nature* **263**, 30-34.

Salmons, S. & Vrbová, G. (1969). The influence of activity on some contractile characterisitics of mammalian fast and slow muscles. *J. Physiol.* **201**, 535-549.

Sillau A. H. & Banchero N. (1977). Visualisation of capillaries in skeletal muscle by ATPase reaction. *Pflugers Arch.* **369**, 269-271.

Simonides W, S, & van Hardeveld C. (1990) An assay for sarcoplasmic reticulum Ca^{2+} ATPase activity in muscle homogenates. *Analytical Biochem.* **191**, 321-331.

Skorjanc, D., Jaschinski, F., Heine, G. & Pette, D. (1998). Sequential increases in capillarization and mitochondrial enzymes in low-frequency-stimulated rabbit. *Am. J. Physiol.* **274**, (Cell Physiol. 43), C810-18.

Smith, J. K., Grisham, M. B., Granger, D. N. & Korthuis, R. J. (1989). Free radical defense mechanisms and neutrophil infiltration in post-ischemic skeletal muscle. *Am. J. Physiol.* 256 (Heart Circ Physiol 25), H789-H793.

Smith, J. A. & Weidemann, M. J. (1990). The exercise and immunity paradox: a neuro-endocrine/cytokine hypothesis. *Med. Sci. Res.* **18**, 749-753.

Spector, S. A., Gardiner, P. F., Zernicke, R. F. Roy, R. R. & Edgerton, V. R. (1980). Muscle architecture and force velocity characteristics of cat soleus and medial gastrocnemius: implications for motor control. *J. Neurophysiol.* **44**, 951-960.

Sréter, F.A. (1969). Temperature, pH and seasonal dependence of Ca-uptake and ATPase activity of white and red muscle microsomes. *Arch. Biochem. Biophys.* **134**, 25-33.

Sréter, F. A., Romanul, F. C. A., Salmons, S. & Gergely, J. 1974 The effect of a changed pattern of activity on some biochemical characteristics of muscle. In *Exploratory Concepts in Muscular Dystrophy 11*, vol. 333 (ed. A. T. Milhorat), pp. 338-343. Amsterdam: Excerpta Medica.

Staron, R. S., Gohlsch, B. & Pette, D. (1987). Myosin Polymorphism in single fibers of chronically stimulated rabbit fast-twitch muscle. *Pflugers Arch.* **408**, 444-450.

Staron, R. S. & Johnson, P. (1993). Myosin polymorphism and differential expression in adult human skeletal muscle. *Comp. Biochem. Physiol.* **106B**, 463-475.

Sternbergh, W. C. 3rd & Adelman, B. (1992). Skeletal muscle fibre type does not predict sensitivity to post-ischemic damage. *J. Surg. Res.* **53**, 535-41.

Stoscheck, C. M. (1990). Increased uniformity in the response of the coomassie blue G protein assay to different proteins. *Anal. Biochem.* **184**, 111-116.

Street, S. F. (1983). Lateral transmission of tension in frog myofibres: a myofibrillar network and transverse cytoskeletal connections are possible transmitter. *J. Cell. Physiol.* **114**, 346-64.

Street, S. F. and Ramsey, R. W. (1965). Sarcolemma transmitter of active tension in frog skeletal muscle. *Science.* **149**, 1370-1380.

Sugi, H. & Tsuchiya, T. (1988). Stiffness changes during enhancement and deficit of isometric force by slow length changes in frog skeletal muscle fibres. *J. Physiol.* **407**, 215-29.

Sweeney L. H., Bowman B. F & Stull J. T. (1993). Myosin light chain phosphorylation in vertebrate striated muscle: regulation and function *Am. J. Physiol.* **264** (Cell Physiol. 33): C1085-95.

Talmadge, R. J. & Roy, R. R. (1993). Electrophoretic separation of rat skeletal muscle heavy chain isoforms. *J. Appl. Physiol.* **75**, 2337-2340.

Tang, A. T. G., Geraghty, P., Dascombe M. J., Jarvis J. C., Salmons, S. & Hooper T. L. (1998). Nitroglycerine reduces neutrophil activation and acute damage in latissimus dorsi muscle grafts. *Ann. Thorac. Surg.* **66**, 2015-21.

Taylor, I., Jarvis, J. C., Grainger, S. R. W., Hitchings, D. J. & Salmons, S. (1996) Development of implantable stimulators based on semicustom CMOS technology. In *Biotelemetry* XIII (ed. C. Cristalli, C.J. Amlaner & M.R. Neuman), pp. 87-92.

Trotter, J. A. (1993). Functional morphology of force transmission in skeletal muscle. A brief review. *Acta. Ana.* **146**, 205-222.

Tunell, G. L. & Hart, M. N. (1977). Simultaneous determination of skeletal muscle fiber types I, IIA and IIB by hisochemistry. *Arch. Neurol.* **34**, 171-173.

Ugolini, F. (1986). Skeletal muscle for artificial heart device: theory and in vivo experiments. In *Biochemical cardiac. assist. Cardiomyoplasty and muscle-powered devices* (ed. R. C. Chiu), pp. 193-210. Mount Kisco, New York: Futura Publishing Company.

van Lookeren Campagne, A. A. H., te Kronnie, G. & Huijing P. A. (1988). Muscle and fibre length force characteristics and filament length of rat semimembranous and gastrocnemius muscles. In: U. Carraro (ed.) *Sarcomeric and non-sarcomeric muscles: Basis and applied research prospects for the 90's*, pp525-530. Unipress Padova, Padova.

Veltink, P. J., Mulder, A. J., Franken, H. M. & van Alsté, J. A. 1991 Optimising control of functional neuromuscular stimulation. In *Basic and Applied Myology: Perspectives for the 90's* (ed. U. Carraro & S. Salmons), pp. 311-318. Padua: Unipress.

Wallimann, T., M., Wyss, D., Brdiczka K., Nicolay K. and Eppenberger, E. 1992. Intracellular compartmentation, structure and function of creatine kinase isoenzymes in tissues with high fluctuating energy demands: the 'phosphocreatine circuit' and cellular energy homeostasis. *Biochem. J.* **281**, 21-40.

Warmington S. A., Hargreaves M. & Williams D. A. (1996) A method for measuring sarcoplasmic reticulum calcium uptake in skeletal muscle using Fura-2. *Cell Calcium*, **20**, 73-82

Warren, G. L., Hayes, D. A., Lowe, D. A., Prior B. M. & Armstrong R. B. (1993). Materials fatigue initiates contraction-induced injury in rat soleus muscle. *J. Physiol. (Lond.)* **464**, 477-489.

Willems, M. E. T., Huijing, P. A. & Fridén, J. (1999). Swelling of sarcoplasmic reticulum in the periphery of muscle fibres after isometric contractions in rat semimembranous lateralis msucle. *Arch. Physiol. Scand.* **165**, 347-356.

Williams, N. S, Hallan R. I., Koeze, *D. H.* & Watkins, E. S. (1989). Construction of a neorectrum and a neoanal sphincter following previous proctolectomy. *Br. J. Surg.* **76**, 1191-1194.

Woitaske, M. D. & Mc Carter, R. J. (1998). Effects of fibre type on ischemia-reperfusion injury in mouse skeletal muscle. *Plast. Reconstr. Surg.* **102**, 2052-63.

Wood, S. A., Morgan, D. L. & Proske, U. (1993). Effects of repeated eccentric contractions on structure and mechanical properties of toad satorius muscle. *Am. J. Physiol.* **265**, C792-800.

Zhu, Y. and Nosek, T. M. (1991). Intracellular milieu changes associated with hypoxia impair sarcoplasmic reticulum Ca^{2+} transport in cardiac muscle. *Am. J. Physiol.* **261**, H620-H626.